



**Hydraulics Research**  
Wallingford

PERFORMANCE OF AERATORS FOR DAM SPILLWAYS

By R W P May and A P Deamer

Report SR 198  
March 1989

**Registered Office: Hydraulics Research Limited,  
Wallingford, Oxfordshire OX10 8BA.  
Telephone: 0491 35381. Telex: 848552**

This report describes work funded by the Department of the Environment under Research Contract PECD 7/6/46, It is published on behalf of the Department of the Environment, but any opinions expressed in this report are not necessarily those of the funding Department. The work was carried out in the River Engineering Department of Hydraulics Research, Wallingford headed by Dr W R White. The nominated project officers were Dr R P Thorogood for DOE and Dr W R White for HR.

© Crown copyright 1989

Published by permission of the Controller of Her Majesty's Stationery Office

## ABSTRACT

This report describes laboratory tests on the performance of spillway aerators carried out as stage 2 of a research contract funded by the Department of the Environment. In stage 1, a comprehensive review was made of the available literature on cavitation and aeration in hydraulic structures; results of the review were presented in an earlier Hydraulics Research Report No SR 79.

On the basis of this review it was decided to carry out a systematic experimental study of ramp aerators which are used to prevent cavitation damage on dam spillways by entraining air into the high velocity flows. A flume was specially built for the study; the test section is 4m long and the width can be varied up to a maximum of 0.3m. The flume can be set at angles between horizontal and 45°, and the pump has a flow capacity of 0.2m<sup>3</sup>/s and can produce velocities of up to 15m/s.

Initial tests were carried out with a nitrogen gas injection system in order to study the convection and diffusion of gas in turbulent flows. Measurements of velocity profiles and gas concentration profiles were made downstream of the injection point for a range of flow depths and velocities.

An air supply system was installed in the flume for the tests on the aeration ramps. This enabled the flow over a ramp to create a low-pressure air cavity which drew in air naturally from the atmosphere. A large number of tests was carried out in order to determine the effect on the air demand of the following factors : water velocity; water depth; height of aeration ramp; slope of aeration ramp; slope of channel; and head loss characteristics of air supply system. Results were analysed both in dimensional and non-dimensional form and compared with formulae from other studies.

The experiments were designed to provide data for a proposed numerical model of cavitation and aeration in dam spillways. The model would be developed from an existing computer program (SWAN) for spillway flows, and would identify the risks of cavitation damage and facilitate the design of suitable aeration systems. Descriptions are included of the existing SWAN program (produced by Binnie & Partners) and of a proposed convection-diffusion model of two-phase flows.



## SYMBOLS

$A_a$	Cross-sectional area of air ducts at outlet
$a$	Constant in Equation (34)
$B$	Width of channel
$C$	Local air concentration
$\bar{C}$	Depth-averaged air concentration
$c$	Speed of sound in air
$c_1, c_2$ etc	Constants
$d$	Depth of flow measured normal to channel invert
$d_c$	Depth of flow at vena contracta
$d_v$	Mean size of voids
$E$	Euler number (Equation (37))
$e$	Constant in Equation (38)
$F$	Modified Froude number (Equation (18))
$F_k$	Critical Froude number at start of air entrainment
$F_r$	Froude number (Equation (20))
$g$	Acceleration due to gravity
$h$	Height of ramp measured vertically
$h_1$	Height of ramp measured normal to channel invert
$i$	Energy gradient of flow
$J$	Head loss parameter for air-supply system (Equation (9))
$k$	Air entrainment coefficient (Equation (15))
$k_s$	Nikuradse equivalent sand roughness
$L_c$	Length of air cavity
$L_{cm}$	Value of $L_c$ measured from tip of ramp to centre of mass of reattaching jet
$L_r$	Length of ramp measured parallel to channel invert
$m$	Coefficient in Equation (34)
$N_v$	Number of voids in sampling period
$n$	Manning roughness coefficient
$p$	Pressure
$\Delta p$	Pressure difference below atmospheric
$Q_a$	Volumetric flow rate of air
$q$	Volumetric flow rate of water per unit width of channel
$q_a$	Volumetric flow rate of air per unit width of channel
$R$	Hydraulic radius (= area/wetted perimeter)
$Re$	Reynolds number
$r$	Vertical rise velocity of bubble
$s$	Height of offset in channel floor, measured vertically
$s_1$	Height of offset in channel floor, measured normal to invert
$T$	Temperature
$T_c$	Time probe in conducting liquid
$T_v$	Time probe in voids
$t$	Time
$u$	Mean velocity parallel to x-axis
$V$	Mean velocity of water
$V_a$	Mean velocity of air
$V_d$	Velocity of water at downstream end of air cavity
$V_k$	Effective minimum velocity of water for air entrainment (Equation (38))

$V_r$	Root-mean-square velocity fluctuation
$v$	Mean velocity parallel to y-axis
$W_e$	Weber number
$w$	Overall step height
$X_u$	Parameter defined by Equation (26)
$x$	Distance measured along channel
$y$	Distance measured normal to channel
$\alpha$	Energy coefficient
$\beta$	Air demand ratio ( $= q_a/q$ )
$\epsilon_x$	Coefficient of turbulent diffusion for air in water in x-direction
$\epsilon_y$	Coefficient of turbulent diffusion for air in water in y-direction
$\theta$	Angle of channel to horizontal
$\lambda$	Darcy-Weisbach friction factor
$\nu$	Kinematic viscosity of water
$\nu_a$	Kinematic viscosity of air
$\rho$	Density of water
$\rho_a$	Density of air
$\sigma$	Surface tension for air-water interface
$\phi$	Angle of ramp relative to channel

## CONTENTS

	Page
1 INTRODUCTION	1
2 DIMENSIONAL ANALYSIS	4
3 PREVIOUS STUDIES	10
4 EXPERIMENTAL ARRANGEMENT	17
4.1 Flume	17
4.2 Air supply system	20
4.3 Aeration ramps	21
4.4 Measuring equipment	23
5 TESTS WITH GAS INJECTION SYSTEM	27
6 TESTS WITH AERATION RAMPS	31
7 ANALYSIS AND DISCUSSION	35
8 CONCLUSIONS	38
9 ACKNOWLEDGEMENTS	40
10 REFERENCES	41

## TABLES

1	Test data for aerator no. 1
2	Test data for aerator no. 3
3	Test data for aerator no. 7
4	Test data for aerator no. 9
5	Data analysis for aerator no. 1
6	Data analysis for aerator no. 3
7	Data analysis for aerator no. 7
8	Data analysis for aerator no. 9

## FIGURES

1	Geometry of aeration system
2	Layout of high-velocity flume
3	Air supply system
4	Measured and predicted velocity profiles at $x = 0.195\text{m}$
5	Measured and predicted velocity profiles at $x = 0.5\text{m}$
6	Measured and predicted velocity profiles at $x = 1.0\text{m}$
7	Measured and predicted velocity profiles at $x = 1.5\text{m}$
8	Measured and predicted velocity profiles at $x = 2.0\text{m}$
9	Gas concentration profiles at $x = 0.08\text{m}$ , $0.195\text{m}$ , $0.5\text{m}$ and $0.75\text{m}$
10	Transverse variation in gas concentration profiles at $x = 0.08\text{m}$

CONTENTS (CONT'D)

FIGURES (CONT'D)

11-36 Air demand versus velocity

Flume slope	Air valve setting	Figure No			
		Aerator No			
		1	3	7	9
15.5°	0	11	18	24	31
15.5°	2	12	19	25	32
15.5°	3	13	20	26	33
15.5°	4	14	21	27	34
45.3°	0	15	22	28	35
45.3°	3	16	-	29	-
45.3°	4	17	23	30	36

37 Head loss characteristics for air supply : valve setting 0

38 Head loss characteristics for air supply : valve setting 2

39 Head loss characteristics for air supply : valve setting 3

40 Head loss characteristics for air supply : valve setting 4

41-66 Air demand ratio versus Froude number

Flume slope	Air valve setting	Figure No			
		Aerator No			
		1	3	7	9
15.5°	0	41	48	54	61
15.5°	2	42	49	55	62
15.5°	3	43	50	56	63
15.5°	4	44	51	57	64
45.3°	0	45	52	58	65
45.3°	3	46	-	59	-
45.3°	4	47	53	60	66

APPENDICES

A Numerical convection - diffusion model

B Numerical model of cavitation and aeration

## 1 INTRODUCTION

Cavitation in hydraulic structures is usually associated with high-velocity flows. If the pressure within flowing water drops close to the vapour pressure of the water, cavities will form in the flow and be carried along by it. Regions of low pressure can typically be caused by a general increase in flow velocity (e.g at contractions in closed conduits), by flow separation at sharp edges (e.g joints, slots, surface irregularities), or by velocity fluctuations due to high turbulence. The cavities are normally occupied by a mixture of water vapour and air, and will expand in size if they remain in an area of low enough pressure. When the cavities move into an area of increasing pressure, they can collapse violently and generate very high velocities and pressure impulses in the fluid; pressures as high as 15,000 atmospheres have been recorded by Lesleighter (1983).

If cavities collapse up against a solid boundary, they are capable of damaging materials as hard as stainless steel. In the case of concrete, cavitation attacks the sand-cement component and loosens the aggregate, which is then plucked out by the flow. A surface damaged by cavitation usually presents a pitted appearance, and concrete exposed to severe cavitation can sometimes be eroded to depths of several metres. Cavitation is therefore capable of causing serious damage or even failure in tunnels and spillways carrying high-velocity flows. As a result, the worldwide trend towards the construction of larger dams with higher heads has led to an increased awareness of the dangers posed by cavitation.

In 1985 the Construction Industry Directorate of the Department of the Environment (DOE) commissioned Hydraulics Research (HR) to carry out a research project on cavitation damage in major civil

engineering works. It was foreseen that the study would be mainly experimental, and that it would be necessary to build a new test facility for the work. However, before embarking on major capital expenditure, it was decided that the available literature on cavitation should be reviewed in order to identify in which area new research would be most beneficial. The literature on cavitation is large so it was decided to extend the scope of the review and produce a document which would be of use not only to researchers but also to engineers designing hydraulic structures. The review was published in 1987 as Hydraulics Research Report SR 79, and includes sections on the mechanism of cavitation, the factors governing its occurrence in various types of hydraulic structure, the resistance of different materials, the use of air entrainment to prevent damage, and the problems of modelling and instrumentation.

The review identified two main options for the experimental part of the research study; these were to study at reduced scale either:

1. the occurrence of cavitation at features of hydraulic structures such as transitions, slots and surface irregularities;

or

2. the performance of systems for entraining air into high-velocity flows in order to prevent cavitation damage.

The first option required the use of a vacuum test rig because, in order to reproduce cavitation correctly at reduced scale, it is necessary to lower the ambient pressure below atmospheric. Such a test rig would have been very expensive to build and maintain. New

research on the cavitation potential of slots and surface irregularities could have extended the results of previous studies and helped to resolve certain discrepancies, but the benefit might well not have been large in relation to the expenditure involved.

The second option of studying aeration systems was considered to offer greater benefits for the design of high-head structures, and required a simpler test rig that could be built within the available budget.

The presence of a sufficient quantity of undissolved air in water has been shown to prevent cavitation damage by cushioning the collapse of the cavities. Many high-head spillways and tunnels are now being built with aeration devices which can consist of ramps, slots or offsets (singly or in combination) set in the walls and invert of the channels. Water flowing past such a device separates and produces a low-pressure zone, to which air can be drawn naturally from the atmosphere through a suitable arrangement of ducts or slots.

Model studies of aerators have previously been carried out for specific schemes but the designs have varied considerably. The literature review showed that it is not yet possible to generalise the results from these studies or predict how the air demand will be affected by changes in geometry and flow characteristics. It was therefore recommended that the experimental part of the DOE-funded project should be a study to identify and quantify in a systematic manner the factors governing the performance of aerators. This recommendation was accepted, and a special rig for testing aerators at high velocities and steep channel slopes was therefore designed and built at HR. The results of the experiments carried out with the test rig are the subject of this report.

The data on the performance of aerators obtained from this study are seen as forming an important part of a proposed numerical model of flow on dam spillways. The planned model will determine the flow profile and boundary layer development along a spillway of specified geometry, identify sections of the channel where there is a risk of cavitation and assist in the design of a suitable aeration system for preventing cavitation damage. Further details of this model are given in an Appendix to this report.

## 2 DIMENSIONAL ANALYSIS

The geometry of a typical aeration system for a surface spillway is shown diagrammatically in Figure 1; a list of symbols is given at the beginning of this report.

An aerator located in the invert of a channel usually consists of a plain ramp ( $s_1 = 0$  in Figure 1), a plain offset ( $h_1 = 0$ ) or a combination of the two. In a well-designed aerator, water passing over the ramp or offset separates and forms a stable cavity from which air is entrained and carried downstream by the flow. This air cavity is distinct from the vapour cavities responsible for cavitation damage. Maintenance of the cavity requires a continuous supply of air and the pressure inside it is usually only slightly below atmospheric; vapour cavities are essentially holes in the liquid which form spontaneously when the local pressure is close to its vapour pressure.

Air for an aerator in the invert of a channel can be supplied naturally from the atmosphere by means of a system of ducts having outlets which may be in the base of the side walls, in the downstream face of the ramp/offset or in a slot in the bottom of the channel. The need for ducts can sometimes be avoided by using

by using wall slots (with or without side deflectors) which allow air to be drawn down from the surface to the invert of the channel. Figure 1 shows an example of a duct supplying outlets in the downstream face of the offset and an example of a wall offset with a side deflector.

The performance of an aeration system may be expected to depend upon some or all of the following factors:

Geometry of aerator

height of ramp	$h, h_1$
angle of ramp to channel	$\theta$
height of offset	$s, s_1$
geometry of slots or deflectors at side walls	-

Geometry of channel

angle of channel to horizontal	$\theta$
width of channel	$B$
hydraulic resistance, e.g Manning or Nikuradse	$n$
sand roughness	$k_s$

Characteristics of air supply system

cross-sectional area of ducts at outlet	$A_a$
velocity of air at outlet	$V_a$
head loss parameter of system	$J$
density of air	$\rho_a$
kinematic viscosity of air	$\nu_a$
speed of sound in air	$c$

Flow conditions approaching aerator

depth of flow	$d$
mean velocity	$V$
root-mean-square turbulent velocity fluctuation	$V_r$

vertical velocity profile	-
density of water	$\rho$
kinematic viscosity of water	$\nu$
surface tension (air/water)	$\sigma$
acceleration due to gravity	$g$

If it is assumed that the above parameters are fixed (i.e independent), then the dependent parameters of principal interest are:

Dependent parameters

flow rate of entrained air per unit width of channel	$q_a$
pressure in cavity relative to atmosphere (positive if lower than atmospheric)	$\Delta p$
length of air cavity	$L_c$

Dimensional analysis can be useful in identifying relationships between different factors, but it is important to realise its limitations in complex problems such as the present one. The variables can be grouped in many different ways, and it is usually difficult to establish which combination is most relevant to the problem. If there are many non-dimensional groupings, it can be difficult to devise tests which identify the influence of each one in isolation. As an example, consider the three parameters which have been found to be significant in many problems of fluid motion: the Froude number  $F_r$  which describes the relative importance of inertial and gravitational forces

$$F_r = \frac{V}{(g L)^{1/2}} \quad (1)$$

the Reynolds number  $R_e$  which relates inertial and viscous forces

$$R_e = \frac{VL}{\nu} \quad (2)$$

and the Weber number  $W_e$  which compares forces due to inertia and surface tension

$$W_e = \frac{V (\rho L)^{1/2}}{\sigma} \quad (3)$$

Combining these definitions it can be shown that

$$W_e = \left( \frac{g^{1/6} \nu^{2/3} \rho^{1/2}}{\sigma^{1/2}} \right) F_r^{1/3} R_e^{2/3} \quad (4)$$

Previous investigators have attempted to identify the influence of Weber number on the performance of aerators but have always used air and water in their tests. Equation (4) shows that if the values of  $g$ ,  $\nu$ ,  $\rho$  and  $\sigma$  are not altered, it is impossible to vary  $W_e$  without at the same time altering  $F_r$  and/or  $R_e$ . Therefore, in order to establish the effect of surface tension, it is necessary to carry out tests with fluids of different properties.

Consideration of the process of entrainment of entrainment resulting from flow over an air cavity suggests that the air demand per unit width of channel will depend primarily upon the following parameters

$$q_a = \text{fn} (V, L_c, \nu, \sigma, \rho, \rho_a, d, V_r, k_s) \quad (5)$$

$$\frac{q_a}{V L_c} = \text{fn} \left( \frac{V L_c}{\nu}, \frac{V(\rho L_c)^{1/2}}{\sigma^{1/2}}, \frac{\rho_a}{\rho}, \frac{d}{L_c}, \frac{V_r}{V}, \frac{k_s}{d} \right) \quad (6)$$

The first two terms on the right-hand side are types of Reynolds number and Weber number respectively; the ratio  $V_r/V$  describes the influence of turbulence in the flow and  $k_s/d$  defines the shape of the vertical velocity profile upstream of the aerator (if the flow is fully developed and rough turbulent).

The length of the air cavity  $L_c$  appears to have an important role, but it is itself dependent upon the following main factors

$$L_c = \text{fn} (V, g, d, \theta, \phi, h_1, s_1, \rho, \rho_a, \Delta p, V_a, V_r, \nu, \sigma) \quad (7)$$

In non-dimensional form the relationship can be written as

$$\frac{L_c}{d} = \text{fn} \left( \frac{V}{(gd)^{1/2}}, \theta, \phi, \sigma, \frac{h_1}{d}, \frac{s_1}{h}, \frac{\rho_a}{\rho}, \frac{\Delta p}{\rho V^2}, \frac{V_a}{V}, \frac{V_r}{V}, \frac{Vd}{\nu}, \frac{V(\rho d)^{1/2}}{\sigma^{1/2}} \right) \quad (8)$$

The last two terms on the right-hand side are types of Reynolds number and Weber number but with different length parameters from those in Equation (6).

An independent relationship between the air demand and the pressure in the cavity is provided by the head-loss characteristics of the air supply system which can be described by

$$q_a = J \frac{A_a}{B} \left( \frac{\Delta p}{\rho_a} \right)^{1/2} \quad (9)$$

where  $A_a$  is the cross-sectional outlet area of the ducts supplying air to width  $B$  of channel and  $J$  is a non-dimensional coefficient which depends upon the following factors

$$J = \text{fn} \left( \frac{V_a A_a^{1/2}}{V_a}, \frac{V_a}{c}, \text{shape of the supply system} \right) \quad (10)$$

The first term on the right-hand side is a type of Reynolds for air flow in the supply system, and the second relates to the Mach number which governs compressibility effects.

The above formulations illustrate the complex inter-relationships which exist between the dependent parameters  $q_a$ ,  $L_c$  and  $\Delta p$ , and show that the performance of an aerator is affected by the characteristics of its air supply system. If the head loss in the system is increased, the pressure in the cavity decreases further below atmospheric (i.e.  $\Delta p$  increases); this increases the curvature of the flow over the cavity and shortens its length  $L_c$ ; this in turn reduces the rate of air entrainment  $q_a$  into the flow. It is also apparent from the analysis that different definitions of Reynolds number and Weber number may be appropriate for different aspects of the entrainment process.

When analysing data from tests on aerators, it is simpler to adopt an external view of the problem and consider the dependent quantities as separate functions of the independent variables, i.e

$$\left( \frac{q_a}{Vd} \right), \left( \frac{L_c}{d} \right), \left( \frac{\Delta p}{\rho V^2} \right) = \text{fn} \left( \frac{V}{(gd)^{1/2}}, \theta, \phi, \frac{h_1}{d}, \frac{s_1}{h}, \frac{\rho_a}{\rho}, J, \frac{Bh_1}{A_a}, R_e, W_e, \frac{V_r}{V}, \frac{k_s}{d} \right) \quad (11)$$

The quantity  $(Bh_1/A_a)$  is needed to allow for the effect of the term  $V_a/V$  in Equation (8). The list of

factors is not complete, but it is hoped that the most important ones have been included. Appropriate definitions for  $R_e$  and  $W_e$  cannot be identified without more detailed study.

The mean volumetric air concentration  $\bar{C}$  produced by an aerator is defined as

$$\bar{C} = \frac{\beta}{1 + \beta} \quad (12)$$

where

$$\beta = \frac{q_a}{q} = \frac{q_a}{V_d} \quad (13)$$

is one of the non-dimensional parameters obtained in Equation (11). At low concentrations  $\bar{C} \approx \beta$ , but at higher ones it is necessary to distinguish between the two definitions.

### 3 PREVIOUS STUDIES

Two important studies on the performance of spillway aerators were carried out independently in China and Brazil, and interestingly came to similar conclusions. Pan et al (1980) made a theoretical and experimental study of ramp aerators and found that the air demand was given by

$$q_a = 0.022 V_d L_{60} \quad (14)$$

where  $V_d$  is the flow velocity at the end of the cavity (not upstream of the aerator), and the length of the cavity  $L_{60}$  is the distance from the downstream end of the aerator to the point on the floor of the channel where the air concentration decreases to 60%. A method of predicting the cavity length was developed based on a theoretical solution but with correction factors to allow for energy losses and air resistance.

Pinto et al (1982) obtained prototype measurements of air demand for ramp aerators on the Foz do Areia Dam (Brazil). Results from a 1:50 scale model of the aerators were used to obtain corresponding values of the cavity length  $L_c$ , and estimates of the depth and velocity of flow were determined by calculation. Analysis showed that the air demand was given by

$$q_a = k V L_c \quad (15)$$

which can also be written as

$$\beta = k \frac{L_c}{d} \quad (16)$$

where  $\beta$  is defined in Equations (12) and (13). It was found that  $k = 0.033$  for air supplied laterally from both sides of the 70.6m wide channel and  $k = 0.023$  for air supplied from only one side. Equations (14) and (15) are similar in form and are consistent with the functional Equation (6) obtained from dimensional analysis. Further model tests carried out by Pinto & Neidert (1983) showed that the value of  $k$  varied with the Froude number, the size of the aerator in relation to the depth of flow, and the pressure in the cavity; however, for a particular installation the value of  $k$  remained approximately constant over a relatively wide range of discharges.

Several researchers have adopted Equation (15) as a basis for analysing laboratory or field data on the performance of aerators. Marcano & Castillejo (1984) obtained field data from Guri Dam (Venezuela), and found that a 0.10m high ramp in conjunction with a 2.0m deep groove and offset had a value of  $k = 0.011$  and a plain 0.75m high ramp had a value of  $k = 0.073$ . Wood (1985) analysed the data for the Foz do Areia spillway given by Pinto et al and produced the formula

$$k = 0.0079 (F - F_k) \quad (17)$$

where the modified Froude number of the flow is

$$F = \frac{V}{(gd)^{1/2}} \quad (18)$$

and the critical value at which air entrainment starts is given by

$$F_k = 4.3 \left[ 1 + 4.7 \left( \frac{\Delta p}{\rho g d} \right) \left( \frac{h}{d} \right) \right] \quad (19)$$

The value of  $F_k$  is therefore dependent upon the pressure in the air cavity ( $\Delta p$ ) and the height of the ramp in relation to the depth of flow; note that  $h$  is the vertical height of the ramp while  $h_1$  in Equation (7) is the height measured normal to the channel.  $F$  in Equation (1) is termed a modified Froude number because the "true" Froude number  $F_r$ , based on the concept of minimum energy and the speed of wave propagation, is given (for a rectangular channel) by

$$F_r = \frac{\alpha^{1/2} V}{(gd \cos \theta)^{1/2}} \quad (20)$$

where  $\alpha$  is the energy coefficient (= 1 if the velocity distribution in the channel is uniform) and  $\theta$  is the angle of the channel to the horizontal.

Bretschneider (1986) tested models of slot-type aerators to determine the critical flow velocity for the start of air entrainment. The results were described by an equation which, for water at 20°C, is equivalent to a value of the critical Froude number of

$$F_k = 5.8 \quad (21)$$

Ervine (1989) evaluated prototype data for aeration ramps at Foz do Areia, Tarbela, Emborcacao, Colbun and McPhee dams, and obtained the relation

$$k = 0.75 (\lambda/8)^{\frac{1}{2}} \quad (22)$$

where  $\lambda$  is the Darcy-Weisbach friction factor for the spillway channel defined by

$$\lambda = \frac{8g Ri}{v^2} \quad (23)$$

Here  $i$  is the energy gradient of the flow and  $R$  is the hydraulic radius.

Rutschmann (1988) carried out laboratory tests on five shapes of aerator in a 120mm wide flume inclined at an angle of  $\theta = 34.5^\circ$ . The geometries of the ramps and offsets were as follows (see Figure 1 for definitions of dimensions):

No	$h_1$ (mm)	$L_r$ (mm)	$\theta$ (deg)	$s$ (mm)
1A	13.5	135	5.7	-
1B	17.55	135	7.4	-
1C	9.45	135	4.0	-
1D	13.5	135	5.7	54
1E	13.5	135	5.7	27

Various correlations were considered to describe the measured relationship between air demand, flow conditions and geometry of aerator. The recommended equations were

$$\beta = 0.0372 \left( \frac{L_{cm}}{d} \right) - 0.2660 \quad (24)$$

$$\beta = 0.0493 \left( \frac{L_{cm}}{d} \right) - 0.0061 F^2 - 0.0859 \quad (25)$$

in which  $L_{cm}$  is the length of the air cavity measured from the downstream end of the aerator to the point where the centre of mass of the water jet reattaches to the invert of the channel. Equation (24) strictly applies only when the pressure in the air cavity  $\Delta p = 0$ ; however it appears to give reasonable estimates of air demand (within about 20%) for cases where  $\Delta p > 0$  provided the cavity length (measured or calculated) takes account of the effect of the sub-atmospheric pressure. Equation (25) was obtained using data for tests where  $\Delta p > 0$  and so should only be used for arrangements that are reasonably similar to those studied. The two equations were found to be in fair agreement with results from two other studies. Laboratory tests (in New Zealand) were carried out in a 250mm wide flume inclined at an angle of  $\theta = 51.3^\circ$ ; the dimensions of the aerators were as follows

No	$h_1$ (mm)	$L_r$ (mm)	$\theta$ (deg)	$s$ (mm)
2A	39	300	7.4	30
2B	39	300	7.4	15
2C	39	300	7.4	-
2D	30	300	5.7	30
2E	30	300	5.7	15
2F	30	300	5.7	-
2G	23	300	4.4	30
2H	23	300	4.4	15
2I	23	300	4.4	-

The second study was carried out on a small prototype aerator (at Zmutt in Switzerland) installed in part of

a 0.80m wide chute having a slope angle of  $\theta = 34.5^\circ$ . The dimensions of the aerator were

No	$h_1$ (mm)	$L_r$ (mm)	$\emptyset$ (deg)	s (mm)
3	1500	150	5.7	-

Rutschmann also considered the characteristics of air supply systems. If air ducts are located only at the side walls of a spillway, the pressure in the cavity is not uniform across the width of the channel but it is closer to atmospheric at the centre-line. This needs to be taken into account when estimating the air demand of a prototype system from measurements of a sectional model of the aerator.

Aerators are also used to provide cavitation protection downstream of gates in high-head tunnels. Most studies have correlated the air demand with the Froude number of the flow in the vena contracta just downstream of the gate. However, Rabben et al (1983) related the air demand to the cavity length produced by a floor offset located downstream of a gate and obtained the equation

$$\beta = 0.032 \left( \frac{L_c}{d_c} \right) - 0.066 \quad (24)$$

where  $d_c$  is the depth of flow at the vena contracta. The equation is valid for  $L_c/d_c \leq 20$ ; beyond this limit the jet breaks up and the air cavity is no longer sealed.

The various formulae for air demand considered so far require knowledge of the length of the air cavity. Estimates of this length for prototype aerators can be obtained from measurement in models or from

theoretical calculations. Most theoretical methods assume that the fluid is inviscid and irrotational, and that the flow has a uniform velocity distribution upstream of the aerator. Numerical solutions have been obtained using finite element or boundary integral techniques; see for example Wei & De Fazio (1982), De Fazio & Wei (1983) and Yen et al (1984). Analytical solutions with certain simplifying assumptions have also been produced. Schwarz & Nutt (1963) determined the trajectory of a jet subject to a pressure difference between upper and lower surfaces but assumed that the thickness of the jet was small. Pan et al (1980) allowed for the effect of jet thickness but did not take account of a possible pressure difference; correction factors for energy losses and air resistance were determined by comparing the theoretical solution with experimental measurements. Shi et al (1983) analysed results of laboratory tests on ramp aerators and produced the following empirical formula for predicting the length of the air cavity

$$\frac{L_c}{d} = 0.155 + 2.961 X_u - 1.674 X_u^{-1} \quad (25)$$

where

$$X_u = \frac{(h_1/d)^{1/2}}{\cos\theta \cos\phi} F \quad (26)$$

where F is given by Equation (18). It should be noted that so far no measurements of cavity length for large prototype aerators have yet been made due to the obvious practical difficulties. In cases where prototype air demands have been related to cavity lengths, these lengths have been obtained from model measurements or have been calculated theoretically.

Formulae for air demand which do not require knowledge of the cavity length have also been produced. Pan & Shao (1984) analysed data for aerators with ramp or slots (but not offsets) in terms of the parameter  $X_u$  in Equation (26) and obtained the relation

$$\beta = - 0.0678 + 0.0982 X_u - 0.0039 X_u^2, \text{ for } X_u > 1 \quad (27)$$

Bruschin (1985) used data from the Foz do Areia Dam and from a model of Piedra del Aguila Dam (Argentina) and produced the formula

$$\beta = 0.0334 F \left(\frac{w}{d}\right)^{\frac{1}{2}} \quad (28)$$

where  $w$  is the overall step height of a ramp and/or offset. Neither Equation (27) or (28) takes account of the pressure in the air cavity and the characteristics of the air supply system. Rutschmann (1988) analysed laboratory results for the aerators types 1A to 1E listed previously and obtained the result

$$\beta = 0.1135 F + 0.3820 \left(\frac{w}{d}\right)^{1.5} + 15.51 \tan \theta - 0.9029 \quad (29)$$

This result applies for a channel slope of  $\theta = 34.5^\circ$  and specifically assumes that the cavity pressure  $\Delta p = 0$ .

## 4 EXPERIMENTAL ARRANGEMENT

### 4.1 Flume

Following the decision to carry out laboratory research on the performance of spillway aerators (see Section 1), a specification was drawn up for a suitable test rig. The dimensions and flow capacity of the rig were chosen so that it could be used for

testing sectional model of prototype aerators at scales between 1 : 10 and 1 : 20 and would be capable of reproducing prototype unit discharges of up to 100 m<sup>3</sup>/s/m (based on Froudian scaling). It was also considered important that higher flow velocities than used in previous studies should be available so that the influence of scale effects on air entrainment could be investigated more thoroughly.

The principal requirements for the test rig were:

- 1) unit discharges up to 1 m<sup>3</sup>/s/m;
- 2) flow velocities up to 15 m/s;
- 3) variable slope between horizontal and 1V : 1H.

Two alternative types of test rig were considered. The first was a long flume in which the model aerator would be located in the downstream section where the flow had reached uniform depth. The second type was a short flume in which the aerator would be placed at the upstream end and the required depth and velocity of flow would be produced by an adjustable gate. The first option had the advantage that the vertical velocity distribution over the aerator would be more representative of prototype conditions because the boundary layer would be fully developed. However, calculations showed that the length of flume needed to produce a fully-developed boundary layer at high flow velocities was excessive. This would have made the flume very expensive and precluded it from being tilted to the high slopes required. For this reason it was decided to adopt the second option.

The layout of the test rig is shown in Figure 2. The design is innovative and its key features are the mounting of part of the supply pipework on the

underside of the flume and the use of a swivel pipe joint to provide the pivot at the downstream end of the flume. The major advantage of the design is that no changes in the inlet arrangements are needed as the slope of the flume is altered.

In order to cater for the high flow velocities required, it was necessary to purchase a new pump specially for the project. The pump has a nominal rating of  $0.16 \text{ m}^3/\text{s}$  at a head of 20m, but at lower heads it has proved capable of providing a flow of about  $0.21 \text{ m}^3/\text{s}$ . The pump draws from an open sump and the discharge is measured by an acoustic flow meter which is non-intrusive and therefore does not produce any additional head loss. Tappings were also installed on the inside and outside of a radial bend so that the pressure difference between them could be used as an alternative method of measuring the discharge. After the swivel joint, the flow is conveyed to the top end of the flume by a length of 200mm diameter uPVC pipe. The pipe is followed by a circular-to-rectangular transition and then a  $180^\circ$  degree rectangular elbow of width 300mm. The elbow is connected to a 1.2m long pressure box from which the flow discharges into the 4m long open section of the flume; at a flow velocity of 15 m/s the pressure in the box is of the order of 11.5m head of water. The required depth of flow in the flume is achieved by adjusting a movable block vertically inside the pressure box; the upstream edge of the block is protected by a fixed wedge in order to streamline the flow when the block is lowered. The size of the block enables a maximum flow depth of 140mm to be obtained. A streamlined block was chosen instead of a simpler vertical lift gate in order to prevent the formation of a vena contracta downstream; such a vena contracta would have produced undesirable vertical curvature of the flow at the position where it was planned to locate the aeration device.

The 4m long open section of the flume discharges freely into the sump from which the flow is drawn by the pump. One side of the flume is made up of perspex panels stiffened by steel frames; the floor and other side wall are of plywood. Provision was made for the plywood side wall to be movable so that the width of the flume could be varied up to a maximum of 300mm; reducing the width allows higher unit discharges to be obtained in the test rig. For the tests described in this report, the width was kept constant at 300mm.

The slope of the flume is altered by temporarily supporting the top end from a movable gantry. The twin support arms are then unpinned and the flume raised or lowered to its new position by means of the gantry; the pins are then replaced and the gantry removed. A restraining wire keeps the support arms in place during this operation.

#### 4.2 Air supply system

Provision was made in the flume for the installation of aerators a short distance downstream from the end of the pressure box. A removable panel measuring 300 mm long x 300 mm wide was set into the floor of the flume, and beneath this was attached an aeration box with a length of inlet pipe. The arrangement is shown in Figure 3. The aeration box and inlet pipe were located in the gap between the flume and the water supply pipe (see Figure 2), so the whole system moves as one unit when the flume is rotated about its pivot point.

Air entrained by the aerator is drawn via a bellmouth into the 102mm diameter inlet pipe. The flow rate is measured by means of a Dall tube located part way along the pipe. The Dall tube is similar in principle to a venturi meter, and consists of a specially shaped constriction in the pipe which gives rise to a

pressure difference that is related to the rate of flow. Although the Dall tube is considerably shorter than an equivalent British Standard venturi meter, the head loss that it produces is not significantly greater. The specification for the Dall tube required that at an air flow rate of  $0.1 \text{ m}^3/\text{s}$  (at standard atmospheric temperature and pressure) it should give a pressure difference equivalent to 0.5m head of water with an overall head loss not exceeding 0.05m head of water.

The head loss characteristics of the air supply system can be altered by adjusting a butterfly valve installed in the inlet pipe. Air from this pipe enters the aeration box to which the aerator in the flume is connected. The principal function of the box is to collect any water escaping from the flume by way of the aerator and prevent it from affecting the performance of the air supply system. Even when an aerator is operating efficiently, a drainage system is needed because water droplets will always tend to collect in the bottom of the air cavity. In the test rig, the aeration box is therefore provided with a drain valve, the opening of which is adjusted so as to maintain a small depth of water in the box; this stops air entering the box by means of the drain valve and also prevents water flowing down the air inlet pipe.

#### 4.3 Aeration ramps

Ramps in the inverts of spillway channels are one of the most effective ways of entraining air into high-velocity flows. It was therefore decided that the test programme should principally investigate the factors affecting the performance of floor ramps (without offsets). In order to carry out the study systematically, a family of nine ramps was made having the following dimensions (see Figures 1 and 3):

Ramp No	Height ( $h_1$ ) (mm)	Length ( $L_r$ ) (mm)	$h_1/L_r$	$\theta$ deg
1	8	50	0.16	9.1°
2	8	67	0.12	6.8°
3	8	100	0.08	4.6°
4	12	75	0.16	9.1°
5	12	100	0.12	6.8°
6	12	150	0.08	4.6°
7	16	100	0.16	9.1°
8	16	133	0.12	6.8°
9	16	200	0.08	4.6°

The dimensions were carefully chosen so that comparative tests could be made to determine the effect of ramp height and ramp slope separately. Thus, for example, ramps 1, 2 and 3 are of equal height but have different shapes; conversely ramps 1, 4 and 7 have the same shape but different sizes.

The nine ramps were formed as parts of nine different 300mm wide x 262mm long panels which were fitted in the floor of the flume above the aeration box (see Figure 3). When installed, the downstream ends of the ramps are all at the same distance from the start of the flume; therefore the positions of the upstream ends of the ramps vary slightly according to their lengths.

The objective of the installation was to allow air to be supplied to the aerator uniformly across the width of the flume. Air from the aeration box therefore flows through a full-width opening in the top of the box; the length of the opening was made equal to half the length  $L_r$  of the ramp in order to maintain geometric similarity between the nine ramps. The air then enters the flume via the transverse gap between

the tip of the ramp and the floor of the flume. The width of this gap is slightly less than the width of the flume due to the provision of thin supports for the steel portion of the ramp. The height of the gap is also less than the height of the ramp by the 3.1mm thickness of the steel plate. Within these practical limitations, however, the design does result in an approximately constant relationship between the exit area of the air supply system and the product of the width and height of the ramp. Therefore, in the present tests, the factor  $(Bh_1/A_a)$  (see Equation (11)) does not vary significantly; this makes it easier to identify separately the effects which changes in the flow conditions and ramp geometry have on the air demand.

Three small diameter pressure tapings were installed in the 38mm wide panel immediately downstream of the ramp in order to measure pressures in the air cavity. It was found that water droplets collecting in the cavity tended to fill the tapping tubes, so it proved necessary to raise the tops of the tapings approximately 1mm above the floor level.

#### 4.4 Measuring equipment

Characteristics of high-velocity flows are difficult to measure accurately because of the effects of turbulence and air entrained in the water.

In the present study, the depth of flow just upstream of the aerator was controlled by moving the wooden block inside the pressure box (see 4.3). Water levels along the flume were measured by means of a manually-operated point gauge mounted on rails fixed to the tops of the side walls. The high flow turbulence inevitably caused the measurements of the water surface to be approximate and somewhat subjective.

Water velocities within the flow were determined by means of a pitot-static tube with an external diameter of 3mm connected to a water manometer. Due to the experimental arrangement, it proved more convenient to use only the total head reading and to determine the static pressure at the position of the tube independently. The calibration of pitot tubes can be affected by the presence of air in the water. Vischer et al (1982) found that they could be used satisfactorily for air concentrations up to 10%. Corrections can be calculated (see Lakshmana Rao & Kobus) assuming that a two-phase flow behaves as an incompressible mixture, but uncertainties exist about how its mean density and velocity should be defined. Cain & Wood (1981) showed that the presence of air in water can reduce the speed of sound in a mixture to the order of 20 m/s. Compressibility effects may, therefore, need to be taken into account when determining correction factors for pitot tubes used in high-velocity two-phase flows. In the present study, measurements with the pitot tube were made only under conditions where the air or gas concentrations were small or zero.

The pressure difference across the Dall tube, which was used to determine the rate of air flow in the supply system (see 4.3), was measured using a water manometer. In order to reduce fluctuations in the manometer it proved necessary to put small-bore restrictions in the tapping tubes. Mean pressures in the air cavity downstream of the aeration ramp were measured by another water manometer having large diameter stilling wells that helped to damp out the fluctuations.

Point measurements of air concentration within the flow were made using a void-fraction meter obtained for a previous DoE research contract at HRL. The

instrument was developed by White & Hay (1975) at the University of Nottingham, and works by recording the proportionate lengths of time that a probe is in and out of a conducting liquid; the liquid need not necessarily be water and the gas within the voids need not be air. The tip of the probe is a fine conducting wire or needle which is insulated from the main body of the probe, which must also be immersed. When the tip is wetted, a conducting path exists between it and the body of the probe. When the tip enters a void, it becomes unwetted and the resistance in the electrical circuit increases; likewise at the end of the void, the tip becomes wetted again and the electrical resistance decreases. Previous instruments of this type have used the change in mean resistance as a measure of the bubble concentration, but the calibration is difficult to establish and subject to changes in the conductivity of the liquid. White & Hay adopted a different approach in which differentiators and comparators in the electrical circuit are used to measure the rate of change of the signal produced by the tip. In this way it is possible to identify the start and end of each bubble that causes the tip to become unwetted. The circuitry thus enables the instrument to behave as a simple on/off switch, "on" when the tip is in a conducting liquid and "off" when it is in a non-conducting void; the absolute conductivity of the liquid does not need to be measured so there is no need to calibrate the instrument in normal use. The concentration is determined by integrating the signal using a Schmitt trigger to find the total times,  $T_c$  and  $T_v$ , that the tip has been in the conducting fluid and in the non-conducting voids. The average concentration of voids is given by

$$C = \frac{T_v}{T_c + T_v} \quad (30)$$

It is implicitly assumed here (as with other instruments of this type) that the voids move at the same velocity  $V$  as the water. The trigger also counts the number  $N_v$  of voids registered by the instrument during the sampling period, and from this it is possible to calculate the mean size  $d_v$  of the voids from

$$d_v = \frac{VT_v}{N_v} \quad (31)$$

The tip of the probe needs to be made as small as practically possible because this determines the minimum size of bubble that the instrument is able to register; smaller bubbles will not insulate the tip from the body of the probe. The probe provided with the instrument by Nottingham University had a tapered glass tip from the end of which projected a short length of fine wire. This design proved fragile, and new probes were therefore made at HR using fine needles coated, except at the tip, with a non-conducting paint. The length of the exposed conducting tip was approximately 0.25mm.

The Nottingham instrument is able to generate a synthetic saw-tooth signal, and this is used periodically to check the counting circuit associated with the Schmitt trigger; no other calibration is needed. However, an independent test of the

instrument was carried out by measuring local air concentrations in a water jet with a velocity of 3.3 m/s. The mean air concentration in the jet was known independently to be 20%; integrating point values obtained from the void-fraction meter gave a calculated mean concentration of 18.9%. This result indicates that the meter operates satisfactorily and has good accuracy.

## 5 TESTS WITH GAS INJECTION SYSTEM

Construction of the flume was completed before detailed design of the air supply system began. It was therefore decided to carry out flow tests with a temporary gas injection system while the permanent arrangement for the aerators (see 4.2 and 4.3) was being built. The purpose of these preliminary tests was to study, in a controlled fashion, the way in which gas diffuses into a liquid as it is carried downstream from the point of injection. The convection-diffusion process is an important factor influencing the required spacing for spillway aerators; a proposed numerical model of this process is described in Appendix A.

In order to produce a simple injection system, it was decided to use nitrogen gas supplied from pressurised cylinders. The behaviour of nitrogen in a turbulent flow will be very similar to that of air because the buoyancy forces acting on bubbles of equal size will be almost identical. Fortunately, the void-fraction meter needed for the measurements works equally well with nitrogen or air.

The aim was to inject gas in a thin layer into the flowing water at the upstream end of the flume. To achieve a uniform distribution of gas across the width of the flume, a very thin streamlined box was produced

from two metal plates measuring 500mm x 300mm in plan and separated by a gap of 2mm. The downstream edge of the box was not sealed, thereby producing a transverse slot 300mm wide and 2mm high. The injection box was mounted in the flume beneath the movable block (see Figure 2) so that the transverse slot was at a height of 11mm above the floor and located at the downstream end of the pressure box. Nitrogen was supplied under controlled pressure to either side of the box and thus injected downstream into the flow.

In order to study the diffusion of the injected gas, measurements of the vertical distributions of water velocity and gas concentration were made at points along the centreline of the flume for a range of discharges and flow depths. The slope of the flume was kept constant at an angle of  $\theta = 15.5^\circ$  to the horizontal.

Flow velocities were measured using a pitot-static tube with the injection box in position but with no gas being supplied. Vertical profiles were obtained on the flume centreline at distances of 0.08m, 0.195m, 0.5m, 1.0m and 2.0m downstream of the transverse slot; at each section measurements were made at 5mm or 10mm vertical intervals from the floor of the flume. A total of 28 velocity profiles was recorded for unit discharges between 0.067 and 0.67 m<sup>3</sup>/s/m; a representative sample of the results is shown in Figures 4 to 8 for a flow rate of 0.33 m<sup>3</sup>/s/m and a gate opening of 0.081m. Although the injection system was made as streamlined as possible, it was impossible to avoid some disturbance to the flow in its immediate vicinity. This is the reason for the kink in the velocity profile at a distance of 1m from the injection slot. Further downstream the disturbance disappears, and the vertical distribution becomes more uniform.

As explained in Section 4.1, it was appreciated that the flume would not be long enough to allow the development of a boundary layer through the full depth of flow. It is therefore interesting to compare the measured velocity profiles with those which would theoretically occur if the flows were at uniform depth.

For rough turbulent flow with a fully-developed boundary layer, the local velocity  $u$  at a height  $y$  above the bed is related to the mean velocity  $V$  and flow depth  $d$  by the velocity defect law

$$\frac{u}{V} = 1 + \{2 \log_{10} (y/d) + 0.886\} \sqrt{\lambda} \quad (32)$$

where  $\lambda$  is the Darcy-Weisbach friction factor. For flow at uniform depth in a channel of slope  $i = \sin \theta$ , the value of  $\lambda$  can be determined directly from Equation (23). Theoretical vertical velocity profiles of  $u/V$  versus  $y/d$  calculated using Equation (32) are compared with some of the experimental measurements in Figures 4 to 8. In general it can be seen that the actual velocity gradients near to the bed of the channel are steeper than predicted theoretically; this is consistent with the boundary layer in the flume being only partially developed. The theoretical solution also does not take account of the effect of the air-water interface at the surface, which in practice causes the maximum velocity to occur below the surface.

Measurements of vertical profiles of gas concentration were made at intervals along the centreline of the flume for a range of discharges and flow depths. Each test was repeated at two different gas injection rates, corresponding to supply pressures of 1 bar and 3 bars above atmospheric. The volume of the nitrogen

cylinders and the characteristics of the supply system limited the mean gas concentrations which could be achieved to a maximum of about 5% to 10%, depending on the flow rate in the flume. It was therefore necessary to carry out the concentration measurements within about 0.75m of the injection slot because further downstream the values became too small to be recorded accurately.

The change in distribution of gas as it is carried downstream by the flow is illustrated in Figure 9. This shows profiles on the centreline of the flume at distances of 0.08m, 0.195m, 0.5m and 0.75m downstream from the injection slot, for a gas supply pressure of 3 bars; the water flow rate of 0.2 m<sup>3</sup>/s/m and the gate opening of 0.081m were the same as for the velocity profiles in Figures 4 to 8. As expected, the results indicate that the gas diffuses vertically as it is carried downstream by the flow and that the point of maximum concentration moves upwards away from the bed. Development of a numerical convection-diffusion model (see Appendix A) will enable the data to be analysed more fully and provide information about turbulent diffusion coefficients.

Study of results such as those in Figure 9 indicated that the distribution of gas across the width of the flow might not have been fully uniform. Comparative measurements were therefore made at various positions across the flume. Figure 10 shows profiles recorded 0.08m downstream from the injection slot at points 1/3, 1/2 and 2/3 across the width of the flume for a water flow rate of 0.1 m<sup>3</sup>/s/m, a gate opening of 105mm and a gas supply pressure of 3 bars. The maximum concentration on the centreline appears to be lower than at the 1/3 and 2/3 width points. This may have been due to the design of the gas injection box because the connections between the two supply pipes

and the box had to be made at the sides of the flume in order to minimise the disruption of the flow; flow rates from the slot may therefore have been higher near the sides of the flume than in the centre. Alternatively, since the void meter was moved vertically in 5mm steps and the initial jet thickness was only 2mm, it is possible that the measurements on the centreline may not have recorded the maximum value of the gas concentration.

## 6 TESTS WITH AERATION RAMPS

The test programme was designed to investigate the effect on air demand of the various non-dimensional quantities identified in Equation (11). Some of the parameters on the right-hand side of this equation were fixed or could not be varied easily. If Equation (11) is expressed in terms of the independent parameters that were capable of being varied, then it reduces to

$$\beta = \frac{q_a}{q} = f n_1 \left( F, \frac{h_1}{d}, \phi, \theta, J \right) \quad (33)$$

The absence of  $R_e$  and  $W_e$  from Equation (33) does not imply that their influence on the amount of air entrainment is not significant. Large changes in  $R_e$  and  $W_e$  of one or two orders of magnitude between model and prototype can certainly introduce major scale effects. However, in the present experiments, the variations in their values were probably too small to have been significant when comparing the results of one test with another. Also, as explained in Section 2, it is not yet certain what definitions of  $R_e$  and  $W_e$  are most relevant to the air entrainment process. However, a full listing of the experimental data is given in this report so that values can be calculated when required.

The test rig enables each of the five variables on the right-hand side of Equation (33) to be altered independently. As the number of values for each variable is increased, the total number of combinations to be tested rises very rapidly (eg 2 values per variable requires 32 tests, 3 values require 243 tests and so on). In order to limit the test programme to reasonable proportions, it was therefore not possible to study all the aerators and flume slopes that were available. The number and range of values chosen for each variable were as follows:

<u>Variable</u>	<u>Number</u>	<u>Range</u>
Froude number (F)	up to 8	2 - 9
Relative depth ( $h_1/d$ )	5	3.3 - 13.7
Ramp angle ( $\emptyset$ )	2	4.6°, 9.1°
Flume angle ( $\emptyset$ )	2	15.5°, 45.3°
Air supply parameter (J)	4 valve settings	-

Not all possible combinations of the above variables were studied. The experiments were carried out using four of the ramp aerators, numbers 1, 3, 7 and 9 (see Section 4.3). Each aerator was normally tested at three different flow depths, two flume slopes and four settings of the butterfly valve in the air supply system. The velocities at each flow depth were chosen so as to give approximately integer values of Froude number with a maximum range of  $F = 2$  to 9; in certain cases the combinations of depth and velocity were limited by the available discharge capacity of the pump. Although the test rig functioned satisfactorily

in most respects, it proved difficult to prevent water leaking from joints in the pressure box; for this reason it was decided in the present tests to restrict flow velocities to a maximum of about 6.5 m/s. As described in Section 4.1, the pump is capable of producing considerably higher velocities; modifications to the construction of the pressure box will enable the full potential of the test rig to be exploited. In the present tests the width of the flume was kept constant at 0.3m.

A full listing of the test data for the four aerators is given in Tables 1 to 4. The measurements include the water discharge per unit width ( $q$ ), the flow depth normal to the flume invert ( $d$ ), the rate of air flow per unit width ( $q_a$ ) to the aerator as measured by the Dall tube, the pressure ( $\Delta p$ ) below atmospheric in the air cavity (in head of water), the setting of the air valve, the ambient temperature and pressure of the air, and the water temperature. Each value of flow depth given is the thickness of the water jet at its exit from the pressure box (0.47m upstream from the lip of the aerator). Valve setting 0 corresponds to the butterfly valve in the air supply system being fully open, setting 2 to the valve being two turns closed and so on.

The data are first plotted in dimensional form in order to demonstrate the main trends of the results. Figures 11-36 show how the air demand  $q_a$  varies with the flow velocity  $V$  and water depth  $d$  for a given aerator, flume slope and air valve setting. The best-fit straight lines in the Figures are included in order to assist comparisons between different sets of results; power-law or other types of equation may fit the data better than linear equations. The results are analysed and discussed in Section 7.

The relationships between the pressure in the air cavity ( $\Delta p$ ) and the total air demand ( $Q_a$ ) are shown in Figures 37 to 40 for each of the four settings of the butterfly valve in the air inlet pipe. Despite a certain amount of scatter, it can be seen that the head-loss characteristic is affected by the valve setting and the height of the ramp aerator but not by the slope of the ramp. This is to be expected because the exit area  $A_a$  of the air supply system is determined by the width and height of the ramp (see Figure 3). Each set of data was analysed in terms of the equation:

$$Q_a = a (\Delta p)^m \quad (34)$$

Typical values of the exponent  $m$  were found to be in the range  $m = 0.47 - 0.54$  so it was decided to assume a value of  $m = 0.5$  for convenience. This is also consistent with Equation (9) which was used in the dimensional analysis in Section 2 and which can be written

$$Q_a = J A (\Delta p / \rho_a)^{1/2} \quad (35)$$

The curves drawn in Figures 37 to 40 are best-fit plots of Equation (35) for each valve setting and ramp height; the corresponding values of  $J$  for the curves were calculated assuming:

$$A_a = B h_1 \quad (36)$$

and are shown on the Figures. A few experimental points that were clearly erroneous were omitted from the Figures and the calculations of  $J$ , but the complete set of data is given in Tables 1 to 8.

The measurements of air demand shown in Figures 11 to 36 are replotted in equivalent non-dimensional form in

Figures 41 to 66 and values are listed in Tables 5 to 8. Each Figure shows how the air demand ratio  $\beta$  varies with Froude number  $F$  (Equation 18) for different values of the relative flow depth  $d/h_1$ . The pressure  $\Delta p$  in the air cavity is expressed in non-dimensional form as the Euler number

$$E = \frac{\Delta p}{\rho V^2} \quad (37)$$

The results are analysed and discussed in Section 7.

## 7 ANALYSIS AND DISCUSSION

Study of the data on air demand shown in Figures 11 to 36 indicates that (for a given aerator, channel slope and air valve setting) there is an approximately linear relationship between the rate of air entrainment ( $q_a$ ) and the flow velocity  $V$ . Extrapolation of the data in each Figure also suggests that air entrainment ceases below a minimum velocity which varies between about 1.5m/s and 3.5m/s depending on conditions.

Due to the difficulty of making measurements in high-velocity flows, there is a certain amount of scatter in the results. However, comparisons between the Figures enable the following conclusions to be drawn about how each of the factors that was studied influences air demand (assuming all the other factors to be unchanged):

- (1) increasing the flow velocity increases  $q_a$ ;
- (2) increasing the height of the ramp while keeping the slope constant increases  $q_a$
- (3) increasing the slope of the ramp while keeping the height constant increases  $q_a$ ;

- (4) increasing the head loss in the air supply system decreases  $q_a$ ;
- (5) increasing the slope of the channel increases  $q_a$ ;
- (6) increasing the water depth first causes  $q_a$  to increase to a maximum and then to decrease.

The effects of these factors can mostly be explained in terms of Equation (15) which suggest that  $q_a$  depends linearly on the flow velocity and the length of the air cavity. Changes such as increasing the height or slope of the aeration ramp or steepening the channel will all tend to increase the cavity length and thereby increase the amount of air entrainment. Similarly, increasing the head loss in the air supply system will reduce the pressure in the cavity further below atmospheric; this causes the flow above the cavity to become more sharply curved and thus reduces its length. The effect of varying the flow depth (item 6 above) is more complex. Generally, increasing the depth will tend to suppress the air cavity and so reduce the length of cavity and hence the air demand. However, this argument does not explain why the air demand initially increases to a maximum when the flow depth is small. At small flow depths, the thickness of the water jet may become insufficient to keep the air cavity fully sealed and this could act to reduce the efficiency of the air entrainment process. The air demand also depends upon the amount of turbulence in the water and this may vary with the flow depth.

The air demand data are plotted in non-dimensional form in Figures 41 to 66. Before comparing the plots, it is worthwhile considering what shape the curves might be expected to take. Figures 11 to 36 indicate that (for a given aerator, channel slope and air valve setting) the rate of air flow is given approximately by

$$q_a = e (V - V_k) \quad (38)$$

where  $e$  and  $V_k$  are dimensional constants which vary slightly with the depth of flow. If this equation is expressed in terms of the non-dimensional parameters  $\beta$  and  $F$  (Equations (13), (18) and (33)), it becomes

$$\beta = \frac{e}{d} \left[ 1 - \frac{V_k}{F (gd)^{1/2}} \right] \quad (39)$$

This corresponds to a curve that is convex downwards and asymptotic to a value of  $\beta = e/d$  as  $F \rightarrow \infty$ . Increasing the depth of flow  $d$  should reduce the value of  $\beta$  (assuming that  $e$  and  $V_k$  are nearly constant).

Study of Figures 41 to 66 shows that, as expected, the data generally follow the trend predicted by Equation (39). The effect of flow depth is more marked than it was in Figures 11 to 36, but the anomaly noted in item (6) above is removed; increasing the relative flow depth  $d/h_1$  causes the air demand ratio  $\beta$  to decrease steadily. However, it is interesting to note that there is often little difference between values of  $\beta$  for the two larger relative flow depths. This suggests that it may be possible to define a limiting envelope to the data in each of the Figures 41 to 66; each limiting curve would represent the maximum entrainment efficiency possible with that particular aerator and air supply system.

The measured air demands can be compared with values predicted by Equations (27), (28) and (29) in Section 3. For a given aerator, channel slope and relative flow depth ( $d/h_1$ ), the three equations have the following forms

$$\text{Pan \& Shao (1984)} \quad \beta = c_1 F - c_2 F^2 - c_3 \quad (40)$$

$$\text{Bruschin (1985)} \quad \beta = c_4 F \quad (41)$$

$$\text{Rutschmann (1985)} \quad \beta = c_5 F + c_6 \quad (42)$$

The first two equations do not take account of the head-loss characteristics of the air supply system; the third equation is based only on data for a channel slope of  $\theta = 34.5^\circ$  and pressure in the air cavity equal to atmospheric (ie  $\Delta p = 0$ ). Of the three equations, Pan & Shao's is the most flexible because of the inclusion of the quadratic term in  $F^2$ . With a suitable choice of coefficients, it is capable of fitting data such as those in Figures 41 to 66 where the start of air entrainment ( $\beta = 0$ ) occurs at a positive value of  $F$  and where the curve of  $\beta$  becomes flatter as  $F$  increases.

Rutschmann's Equation (29) does not give sensible values of  $\beta$  when applied to the types of aerator tested in the present study. This appears to be because the term  $15.51 \tan \phi$  considerably overestimates the effect of the ramp angle  $\phi$ . Pan & Shao's Equation (27) and Bruschin's Equation (28) both give estimates of  $\beta$  that are of the correct order of magnitude. Pan & Shao's equation, however, is superior because it fits the shape of the data better and because it takes account of the ramp angle  $\phi$  and the channel slope  $\theta$  as well as the relative flow depth  $d/h_1$ . Further analysis of the present data is needed in order to optimise the values of the coefficients in Equation (27) and include for the head-loss characteristics of the air supply system.

## 8 CONCLUSIONS

Laboratory experiments were carried out to investigate the factors determining the amount of air entrained by water flowing over ramp aerators. Measurements of air demand were made using four designs of aerator at two channel slopes for a range of flow velocities and depths and with different head-loss characteristics in the air supply system. The tests showed that the value of the air demand ratio  $\beta$  (Equation (13)) is increased by increasing:

- (1) the Froude number  $F$  of the flow ( $F$ )
- (2) the height of the ramp ( $h_1$ )
- (3) the slope of the ramp ( $\phi$ )
- (4) the slope of the channel ( $\theta$ )

and by decreasing:

- (5) the relative flow depth ( $d/h_1$ )
- (6) the head loss parameter ( $J$ ) of the air supply system

Air entrainment begins at a positive value of  $F$ , and the curve of  $\beta$  versus  $F$  becomes flatter as  $F$  increases.

Preliminary comparison of the results with available formulae suggests that Equation (27) due to Pan & Shao (1984) may provide a suitable framework for further analysis of the data. An advantage of this equation is that it does not require information about the length of the air cavity, which in some other prediction methods has to be calculated or measured independently. However, the equation needs to be developed in order to take into account the head-loss characteristics of the air supply system.

Model tests of aerators can be subject to scale effects which may cause them to underestimate the air demand in prototype installations. It is recommended that some of the present tests be repeated at higher flow velocities and discharges in order to investigate how laboratory data can be reliably extrapolated to full-scale conditions.

Development of a numerical model for dam spillways that can predict the risks of cavitation damage and assist in the design of aeration systems is recommended. A suitable basis for such a model is the

SWAN program (produced by Binnie & Partners) which determines the development of flow along a spillway, including the growth of the boundary layer and the occurrence of self-aeration at the free surface; simple checks on the risks of cavitation damage are made. Information from the Stage 1 literature review and the present Stage 2 experiments could be added to improve the predictions of cavitation damage and enable the model to be used for the design of spillway aeration systems.

## 9 ACKNOWLEDGEMENTS

The experimental measurements were carried out by Mr I C Meadowcroft, Miss K Monks and Mr A P Deamer. The data were analysed and presented by Mr I R Willoughby. The project was carried out under the supervision of Mr J A Perkins and Mr R W P May in the River Engineering Department headed by Dr W R White.

10 REFERENCES

Ackers P & Priestley S J (1985). Self-aerated flow down a chute spillway. 2nd Intern Conf on Hydraulics of Floods and Flood Control, BHRA, Cambridge, England, pp1-16.

Bretschneider H (1986). The beginning of air entrainment at bottom grooves. Sounnderdruck aus Wasserwirtschaft, Heft 5, Franckh-Kosmos, Stuttgart (in German).

Bruschin J (1985). Hydraulic modelling at the Piedra del Aguila dam. Water Power & Dam Construction, Vol 37, January, pp24-28.

Cain P & Wood I R (1981). Instrumentation for aerated flow on spillways. Proc ASCE, Jnl Hydr Div, Vol 107, HY11, November, pp1407-1424.

De Fazio F G & Wei C Y (1983). Design of aeration devices on hydraulic structures. Proc Conf on Frontiers in Hydraulic Engineering, ASCE, Cambridge, USA, pp426-431.

Ervine D A (1989). Cavitation, aeration and pressure fluctuations. Seminar on Spillways, Scottish Hydraulics Study Group, Glasgow, Scotland, March.

Lakshmana Rao N S & Kobus H E. Characteristics of self-aerated free-surface flows. Water and Waste Water : Current research and practice, Vol 10, Erich Schmidt Verlag.

Lesleighter E J (1983). Cavitation in high-head gated outlets - prototype measurements and model simulation. Proc XXth IAHR Congress, Moscow, Vol 3, pp495-503.

Marcano A & Castillejo N (1984). Model-prototype comparison of aeration devices of Guri dam spillway. Symp on Scale Effects in Modelling Hydraulic Structures, IAHR/DVWK, Esslingen, FR Germany, September, Paper 4.6.

May R W P (1987). Cavitation in hydraulic structures: occurrence and prevention. Hydraulics Research, Wallingford, Report SR 79, March.

Pan S-B et al (1980). The self-aeration capacity of the water jet over the aeration ramp. Jnl Hydr Engng (Beijing), No 5, pp13-22 (in Chinese).

Pan S & Shao Y (1984). Scale effects in modelling air demand by a ramp slot. Symp on Scale Effects in Modelling Hydraulic Structures, IAHR/DVWK, Esslingen, FR Germany, September, Paper 4.7.

Pinto N L de S et al (1982). Aeration at high velocity flows. Water Power & Dam Construction, Vol 34, (Part 1) February, pp34-38; (Part 2) March, pp42-44.

Pinto N L de S & Neidert S H (1983). Evaluating entrained air flow through aerators. Water Power & Dam Construction, Vol 35, August, pp40-42.

Rutschmann P (1988). Belüftungseinbauten in Schussrinnen. Mitteilungen der Versuchsanstalt für Wasserbau, Hydrologie und Glaziologie, ETH, Zürich (in German).

Schwarz H I & Nutt L P (1963). Protected nappes subject to tranverse pressure. Proc ASCE, Jnl Hydr Div, Vol 89, HY4, July, Part 1, pp97-104.

Shi Q et al (1983). Experimental investigation of flow aeration to prevent cavitation erosion by a deflector. Jnl Hydr Engng (Beijing), No 3, ppl-13 (in Chinese).

Wei C Y & De Fazio F G (1982). Simulation of free jet trajectories for the design of aeration devices on hydraulic structures. 4th Intern Conf on Finite Elements in Water Resources, DFG/ISCME/IAHR, Hannover, pp17/45-54.

White P R S & Hay N (1975). A portable air concentration meter. Proc XVIth IAHR Congress, São Paulo, Vol 3, pp541-548.

Wood I R (1985). Air water flows. Proc XXIst IAHR Congress, Melbourne, Vol 6, pp18-29.

Yen C L et al (1984). Flow characteristics around an aeration device in tunnel spillway. Proc 4th IAHR Congress, Asian & Pacific Division, Chiang Mai, Thailand, pp669-684.



**TABLES.**



TABLE 1 TEST DATA FOR AERATOR NO. 1

FLUME SLOPE DEGREES	NOMINAL DEPTH d MM	VALVE SETTING	WATER FLOW L/S	AIR DEMAND L/S	SUB-NAPPE PRESSURE MM WATER	AIR TEMP C	AIR PRESSURE MM Hg	WATER TEMP C
45.3	110.0	4	136.9	9.2	9.0	12.2	764.0	17.5
45.3	110.0	4	205.3	26.4	41.6	14.7	758.3	15.7
45.3	110.0	4	205.3	21.1	54.3	12.2	764.0	17.5
45.3	110.0	4	103.1	3.9	1.3	12.2	759.2	18.5
45.3	110.0	4	103.1	3.9	1.3	14.7	758.3	15.7
45.3	110.0	4	171.6	16.8	30.6	12.2	759.2	18.5
45.3	110.0	4	136.9	8.8	4.9	14.7	758.3	15.7
45.3	110.0	4	171.6	16.9	18.7	14.7	758.3	15.7
45.3	110.0	3	171.6	19.9	16.0	14.7	758.3	15.7
45.3	110.0	3	171.6	18.9	28.7	12.2	759.2	18.5
45.3	110.0	3	205.3	25.1	49.8	12.2	764.0	17.5
45.3	110.0	3	205.3	32.5	32.2	14.7	758.3	15.7
45.3	110.0	0	205.3	36.8	28.8	14.7	758.3	15.7
45.3	110.0	0	103.1	5.8	1.0	14.7	758.3	15.7
45.3	110.0	0	205.3	24.8	48.9	12.2	764.0	17.5
45.3	110.0	0	69.0	0.0	0.0	14.7	758.3	15.7
45.3	110.0	0	171.6	19.3	27.4	12.2	759.2	18.5
45.3	110.0	0	205.3	27.3	50.7	12.2	764.0	17.5
45.3	110.0	0	171.6	17.9	28.0	12.2	759.2	18.5
45.3	110.0	0	171.6	21.2	12.9	14.7	758.3	15.7
45.3	110.0	0	136.9	10.3	7.5	12.2	764.0	17.5
45.3	110.0	0	103.1	4.4	1.4	12.2	759.2	18.5
45.3	110.0	0	171.6	21.8	13.0	14.7	758.3	15.7
45.3	110.0	0	136.9	12.0	2.9	14.7	758.3	15.7
45.3	110.0	0	103.1	3.6	1.4	12.2	759.2	18.5
45.3	110.0	0	205.3	33.6	28.4	14.7	758.3	15.7
45.3	110.0	0	68.4	1.7	0.2	12.2	759.2	18.5
45.3	80.0	4	149.1	24.0	41.5	12.8	760.3	19.3
45.3	80.0	3	149.1	33.0	34.3	12.8	760.3	19.3
45.3	80.0	0	149.1	33.2	32.6	12.8	760.3	19.3
45.3	80.0	0	149.1	37.8	31.0	12.8	760.3	19.3
45.3	73.5	4	131.2	21.3	50.0	12.2	759.2	18.5
45.3	73.5	4	93.7	13.3	20.0	12.2	759.2	18.5
45.3	73.5	4	75.0	8.4	8.1	12.2	759.2	24.6
45.3	73.5	4	112.5	18.3	36.3	12.2	759.2	18.5
45.3	73.5	3	131.2	24.9	49.4	12.2	759.2	18.5
45.3	73.5	3	112.5	21.2	35.6	12.2	759.2	18.5
45.3	73.5	0	112.5	22.0	33.4	12.2	759.2	18.5
45.3	73.5	0	131.2	26.7	50.7	12.2	759.2	18.5
45.3	73.5	0	131.2	26.3	49.6	12.2	759.2	18.5
45.3	73.5	0	112.5	22.3	34.3	12.2	759.2	18.5
45.3	73.5	0	93.7	15.9	18.2	12.2	759.2	18.5
45.3	73.5	0	75.0	9.9	6.7	12.2	759.2	24.6
45.3	73.5	0	131.2	27.3	52.4	12.2	759.2	18.5
45.3	73.5	0	56.2	6.5	2.7	13.3	759.2	20.4
45.3	53.5	4	81.6	15.7	28.1	13.3	759.2	20.4
45.3	53.5	4	92.8	15.7	28.1	13.3	759.2	20.4
45.3	53.5	3	81.6	15.0	21.6	13.3	759.2	20.4
45.3	53.5	3	92.8	17.5	26.9	13.3	759.2	20.4
45.3	53.5	0	81.6	17.5	22.1	13.3	759.2	20.4
45.3	53.5	0	46.9	7.6	4.6	13.3	759.2	20.4
45.3	53.5	0	58.1	10.3	9.4	13.3	759.2	20.4
45.3	53.5	0	92.8	19.1	27.1	13.3	759.2	20.4
45.3	53.5	0	81.6	16.2	21.3	13.3	759.2	20.4
45.3	53.5	0	105.0	20.8	33.3	13.3	759.2	20.4
45.3	53.5	0	69.4	13.0	14.5	13.3	759.2	20.4
45.3	53.5	0	92.8	19.3	28.2	13.3	759.2	20.4

TABLE 1 Cont.

FLUME SLOPE DEGREES	NOMINAL DEPTH d MM	VALVE SETTING	WATER FLOW L/S	AIR DEMAND L/S	SUB-NAPPE PRESSURE MM WATER	AIR TEMP C	AIR PRESSURE MM Hg	WATER TEMP C
15.5	110.0	4	136.9	6.7	2.6	11.7	770.0	16.0
15.5	110.0	4	205.3	15.8	27.4	11.7	770.0	17.5
15.5	110.0	4	171.6	7.7	6.3	11.7	770.0	16.0
15.5	110.0	3	171.6	8.3	5.4	11.7	770.0	16.0
15.5	110.0	3	205.3	16.4	24.1	11.7	770.0	17.5
15.5	110.0	3	136.9	9.4	2.6	11.7	770.0	16.0
15.5	110.0	2	171.6	8.7	5.4	11.7	770.0	16.0
15.5	110.0	2	205.3	16.5	23.6	11.7	770.0	17.5
15.5	110.0	0	205.3	18.2	24.5	11.7	770.0	17.5
15.5	110.0	0	103.0	0.0	0.0	11.7	770.0	16.0
15.5	110.0	0	136.9	11.2	3.2	11.7	770.0	16.0
15.5	110.0	0	171.6	8.6	5.1	11.7	770.0	16.0
15.5	73.5	4	75.0	4.0	1.8	13.3	763.0	14.5
15.5	73.5	4	112.5	15.0	25.7	13.9	769.0	13.3
15.5	73.5	4	131.2	18.9	48.4	13.9	769.0	13.3
15.5	73.5	4	150.0	24.3	53.4	11.7	770.0	16.0
15.5	73.5	4	131.2	19.3	48.8	14.7	769.0	10.3
15.5	73.5	4	93.7	8.8	8.7	13.3	763.0	14.5
15.5	73.5	4	112.5	14.0	23.8	13.9	769.0	14.5
15.5	73.5	3	112.5	15.2	21.4	13.9	769.0	14.5
15.5	73.5	3	131.2	20.4	46.6	14.7	769.0	10.3
15.5	73.5	3	150.0	27.0	44.9	11.7	770.0	16.0
15.5	73.5	2	150.0	27.9	44.8	11.7	770.0	18.3
15.5	73.5	2	131.2	20.2	46.7	14.7	769.0	10.3
15.5	73.5	2	93.7	9.4	6.9	13.3	763.0	14.5
15.5	73.5	2	112.5	15.7	20.9	13.9	769.0	14.5
15.5	73.5	0	75.0	6.0	2.2	13.3	763.0	14.5
15.5	73.5	0	150.0	28.3	44.0	11.7	770.0	18.3
15.5	73.5	0	131.2	23.3	40.5	13.9	769.0	13.3
15.5	73.5	0	112.5	16.6	23.8	13.9	769.0	13.3
15.5	73.5	0	112.5	15.8	21.2	13.9	769.0	14.5
15.5	73.5	0	150.0	28.4	39.9	11.7	770.0	16.0
15.5	73.5	0	93.7	11.1	7.1	13.3	763.0	14.5
15.5	73.5	0	131.2	20.6	47.3	14.7	769.0	10.3
15.5	73.5	0	131.2	19.6	48.2	14.7	769.0	10.3
15.5	53.5	4	92.8	14.3	24.7	13.3	763.0	14.5
15.5	53.5	4	105.0	17.5	33.7	13.3	763.0	14.5
15.5	53.5	4	81.6	12.4	17.9	13.3	763.0	17.3
15.5	53.5	4	69.4	8.7	9.5	13.3	763.0	17.3
15.5	53.5	3	105.0	20.2	32.6	13.3	763.0	14.5
15.5	53.5	3	92.8	16.5	23.5	13.3	763.0	14.5
15.5	53.5	3	69.4	9.8	8.9	13.3	763.0	17.3
15.5	53.5	3	81.6	13.6	17.1	13.3	763.0	17.3
15.5	53.5	2	81.6	14.1	16.7	13.3	763.0	17.3
15.5	53.5	2	92.8	17.2	23.0	13.3	763.0	14.5
15.5	53.5	2	105.0	21.5	33.1	13.3	763.0	14.5
15.5	53.5	0	81.6	14.5	16.5	13.3	763.0	17.3
15.5	53.5	0	92.8	17.5	22.9	13.3	763.0	14.5
15.5	53.5	0	69.4	10.0	8.3	13.3	763.0	17.3
15.5	53.5	0	105.0	21.6	32.5	13.3	763.0	14.5

TABLE 2 TEST DATA FOR AERATOR NO. 3

FLUME SLOPE DEGREES	NOMINAL DEPTH d MM	VALVE SETTING	WATER FLOW L/S	AIR DEMAND L/S	SUB-NAPPE PRESSURE MM WATER	AIR TEMP C	AIR PRESSURE MM Hg	WATER TEMP C
45.3	110.0	4	136.9	4.8	3.3	12.9	756.2	18.7
45.3	110.0	4	103.1	6.6	2.9	12.9	756.2	18.7
45.3	110.0	4	171.6	11.7	15.2	12.9	756.2	18.7
45.3	110.0	3	171.6	12.9	12.9	12.9	756.2	18.7
45.3	110.0	0	171.6	13.8	12.4	12.9	756.2	18.7
45.3	110.0	0	136.9	6.6	2.4	12.2	764.0	17.5
45.3	110.0	0	68.4	7.6	1.6	12.9	756.2	18.7
45.3	110.0	0	205.3	20.7	31.0	12.9	756.2	18.7
45.3	110.0	0	136.9	4.9	2.3	12.9	756.2	18.7
45.3	110.0	0	205.3	21.6	33.3	12.9	756.2	18.7
45.3	110.0	0	205.3	21.4	31.2	12.9	756.2	18.7
45.3	110.0	0	171.6	14.1	12.2	12.9	756.2	18.7
45.3	110.0	0	103.1	10.9	4.4	12.9	756.2	18.7
45.3	73.5	4	93.7	10.4	11.6	12.9	756.2	18.7
45.3	73.5	4	131.2	17.7	33.6	12.9	756.2	18.7
45.3	73.5	4	112.5	14.9	10.8	12.9	756.2	18.7
45.3	73.5	3	112.5	17.5	10.8	12.9	756.2	18.7
45.3	73.5	3	131.2	19.8	34.8	12.9	756.2	18.7
45.3	73.5	0	131.2	21.0	33.1	12.9	756.2	18.7
45.3	73.5	0	112.5	17.6	11.2	12.9	756.2	18.7
45.3	73.5	0	93.7	12.1	9.6	12.9	756.2	18.7
45.3	73.5	0	112.5	17.6	20.9	12.9	756.2	18.7
45.3	73.5	0	131.2	21.5	35.5	12.9	756.2	18.7
45.3	73.5	0	75.0	6.4	2.7	12.9	756.2	18.7
45.3	73.5	0	56.0	0.0	0.0	12.9	756.2	18.7
45.3	53.5	4	69.4	10.5	11.7	13.3	748.2	13.4
45.3	53.5	4	92.8	14.3	21.9	13.3	748.2	13.4
45.3	53.5	4	81.6	12.0	16.1	13.3	748.2	13.4
45.3	53.5	0	92.8	18.1	22.1	13.3	748.2	13.4
45.3	53.5	0	69.4	12.6	10.2	13.3	748.2	13.4
45.3	53.5	0	81.6	15.4	15.8	13.3	748.2	13.4
45.3	53.5	0	58.1	9.6	5.7	13.3	748.2	13.4
45.3	53.5	0	46.9	5.4	2.2	13.3	748.2	13.4
15.5	53.5	4	69.4	4.3	2.5	12.5	773.5	16.3
15.5	110.0	0	171.6	4.9	1.8	11.9	774.5	18.9
15.5	73.5	0	131.2	13.6	17.2	12.5	773.5	16.3
15.5	110.0	4	171.6	2.2	0.8	12.5	773.5	20.5
15.5	73.5	0	131.2	13.5	16.9	12.5	773.5	18.7
15.5	53.5	2	105.0	14.2	17.7	12.5	778.5	13.3
15.5	73.5	3	112.5	9.8	8.0	11.9	774.5	18.9
15.5	73.5	4	112.5	8.2	10.8	12.5	773.5	18.7
15.5	73.5	3	150.0	17.3	31.0	12.5	773.5	18.5
15.5	53.5	3	81.6	8.3	7.6	12.5	778.5	15.5
15.5	53.5	3	105.0	13.9	18.2	12.5	778.5	13.3
15.5	53.5	4	81.6	7.9	8.5	12.5	778.5	15.5
15.5	73.5	2	150.0	17.7	29.9	12.5	773.5	18.5
15.5	110.0	3	171.6	4.8	1.6	11.9	774.5	18.9
15.5	53.5	2	92.8	11.4	12.3	12.5	778.5	15.5
15.5	73.5	4	112.5	9.5	9.8	11.9	774.5	18.9
15.5	53.5	0	69.4	4.8	2.2	12.5	778.5	18.4
15.5	110.0	2	205.3	10.5	8.9	11.7	770.0	16.0
15.5	73.5	0	150.0	18.1	30.0	12.5	773.5	18.5
15.5	73.5	3	112.5	8.7	9.5	12.5	773.5	18.7
15.5	53.5	0	105.0	14.8	17.4	12.5	778.5	13.3
15.5	73.5	1	150.0	17.7	29.7	12.5	773.5	18.5

TABLE 2 Cont.

FLUME SLOPE DEGREES	NOMINAL DEPTH d MM	VALVE SETTING	WATER FLOW L/S	AIR DEMAND L/S	SUB-NAPPE PRESSURE MM WATER	AIR TEMP C	AIR PRESSURE MM Hg	WATER TEMP C
15.5	73.5	0	112.5	10.0	7.3	11.9	774.5	18.9
15.5	73.5	4	93.7	4.0	2.5	12.5	773.5	18.7
15.5	110.0	0	205.3	10.0	8.6	11.7	770.0	16.0
15.5	73.5	2	131.2	13.2	17.2	12.5	773.5	18.7
15.5	110.0	0	171.6	5.4	1.8	11.9	774.5	18.9
15.5	73.5	3	131.2	13.0	17.7	12.5	773.5	18.7
15.5	73.5	4	131.2	12.3	19.9	12.5	773.5	18.7
15.5	110.0	0	205.3	15.8	9.3	11.7	770.0	16.0
15.5	110.0	0	171.6	1.9	0.6	12.5	773.5	20.5
15.5	53.5	4	105.0	12.9	20.3	12.5	778.5	13.3
15.5	110.0	4	171.6	4.4	2.1	11.9	774.5	18.9
15.5	73.5	2	131.2	13.4	17.4	12.5	773.5	16.3
15.5	73.5	4	131.2	12.7	20.3	12.5	773.5	16.3
15.5	73.5	4	93.7	4.8	2.2	11.9	774.5	18.9
15.5	73.5	0	93.7	5.0	2.0	11.9	774.5	18.9
15.5	53.5	0	92.8	11.5	11.9	12.5	778.5	15.5
15.5	73.5	0	112.5	9.1	8.0	12.5	773.5	18.7
15.5	110.0	3	205.3	11.0	9.5	11.7	770.0	16.0
15.5	73.5	0	112.5	10.4	7.6	11.9	774.5	18.9
15.5	53.5	3	92.8	11.2	12.5	12.5	778.5	15.5
15.5	73.5	0	93.7	3.4	1.8	12.5	773.5	18.7
15.5	53.5	0	81.6	8.6	6.5	12.5	778.5	15.5
15.5	73.5	2	112.5	9.3	9.5	12.5	773.5	18.7
15.5	73.5	3	131.2	13.4	18.1	12.5	773.5	16.3
15.5	110.0	4	205.3	14.8	10.7	11.7	770.0	16.0
15.5	53.5	4	92.8	10.2	13.9	12.5	778.5	15.5
15.5	73.5	4	150.0	16.3	34.6	12.5	773.5	18.5

TABLE 3 TEST DATA FOR AERATOR NO. 7

FLUME SLOPE DEGREES	NOMINAL DEPTH d MM	VALVE SETTING	WATER FLOW L/S	AIR DEMAND L/S	SUB-NAPPE PRESSURE MM WATER	AIR TEMP C	AIR PRESSURE MM Hg	WATER TEMP C
45.3	110.0	4	205.3	27.4	54.8	13.9	754.3	17.3
45.3	110.0	4	171.6	18.9	5.0	13.9	754.3	17.3
45.3	110.0	4	171.6	20.1	28.1	13.9	754.3	17.3
45.3	110.0	4	171.6	19.6	29.6	13.9	754.3	17.3
45.3	110.0	4	136.9	12.4	8.9	13.9	754.3	17.3
45.3	110.0	3	171.6	23.4	25.2	13.9	754.3	17.3
45.3	110.0	3	171.6	27.9	22.7	13.9	754.3	17.3
45.3	110.0	2	171.6	26.2	23.9	13.9	754.3	17.3
45.3	110.0	2	171.6	24.5	18.7	13.9	754.3	17.3
45.3	110.0	2	171.6	27.0	23.1	13.9	754.3	17.3
45.3	110.0	0	171.6	23.9	23.7	13.9	754.3	17.3
45.3	110.0	0	171.6	28.1	24.0	13.9	754.3	17.3
45.3	110.0	0	136.9	16.7	5.8	13.9	754.3	17.3
45.3	110.0	0	205.3	39.8	46.2	13.9	754.3	17.3
45.3	110.0	0	103.1	5.5	1.2	13.9	754.3	17.3
45.3	110.0	0	171.6	22.9	4.3	13.9	754.3	17.3
45.3	80.0	4	127.5	20.8	27.1	13.9	767.5	14.9
45.3	80.0	4	63.7	6.8	3.3	13.1	732.4	18.5
45.3	80.0	4	105.9	15.7	19.7	13.9	767.5	14.9
45.3	80.0	4	127.5	22.9	30.9	13.1	732.4	18.5
45.3	80.0	3	127.5	26.1	28.2	13.9	767.5	14.9
45.3	80.0	3	127.5	30.5	28.4	13.1	732.4	18.5
45.3	80.0	2	127.5	28.2	19.0	13.9	767.5	14.9
45.3	80.0	0	105.9	19.9	16.8	13.9	767.5	14.9
45.3	80.0	0	127.5	35.8	27.8	13.1	732.4	18.5
45.3	80.0	0	127.5	28.6	29.0	13.9	767.5	14.9
45.3	80.0	0	127.5	28.7	19.4	13.9	767.5	14.9
45.3	80.0	0	149.1	45.6	44.4	13.1	732.4	18.5
45.3	80.0	0	85.3	16.5	8.2	13.9	767.5	14.9
45.3	80.0	0	63.7	9.5	2.5	13.1	732.4	18.5
45.3	80.0	0	127.5	36.1	28.5	13.1	732.4	18.5
45.3	53.5	4	81.6	13.8	15.1	13.9	767.5	14.9
45.3	53.5	4	69.4	11.5	9.2	13.9	767.5	14.9
45.3	53.5	4	92.8	15.2	17.8	13.9	767.5	14.9
45.3	53.5	4	58.1	9.0	6.2	13.9	767.5	14.9
45.3	53.5	4	46.9	8.1	4.3	13.1	732.4	19.4
45.3	53.5	3	69.4	15.6	8.8	13.9	767.5	14.9
45.3	53.5	3	92.8	21.5	16.7	13.9	767.5	14.9
45.3	53.5	3	81.6	19.0	14.2	13.9	767.5	14.9
45.3	53.5	2	92.8	23.8	16.9	13.9	767.5	14.9
45.3	53.5	0	92.8	24.5	17.1	13.9	767.5	14.9
45.3	53.5	0	81.6	22.2	13.8	13.9	767.5	14.9
45.3	53.5	0	58.1	14.1	5.4	13.9	767.5	14.9
45.3	53.5	0	69.4	15.0	9.0	13.9	767.5	14.9
45.3	53.5	0	69.4	18.9	8.7	13.9	767.5	14.9
45.3	53.5	0	46.9	11.5	3.3	13.1	732.4	19.4
45.3	53.5	0	69.4	17.3	8.9	13.9	767.5	14.9
45.3	53.5	0	92.8	24.4	16.3	13.9	767.5	14.9
45.3	53.5	0	81.6	22.6	13.9	13.9	767.5	14.9
15.5	110.0	4	171.6	13.0	10.8	12.8	769.0	22.9
15.5	110.0	3	171.6	14.9	8.1	12.8	769.0	22.9
15.5	110.0	2	171.6	15.2	7.4	12.8	769.0	22.9
15.5	110.0	2	136.9	4.6	1.1	12.8	769.0	22.9
15.5	110.0	0	103.1	9.1	0.8	12.8	769.0	22.9
15.5	110.0	0	171.6	15.2	6.6	12.8	769.0	22.9

TABLE 3 Cont.

FLUME SLOPE DEGREES	NOMINAL DEPTH d MM	VALVE SETTING	WATER FLOW L/S	AIR DEMAND L/S	SUB-NAPPE PRESSURE MM WATER	AIR TEMP C	AIR PRESSURE MM Hg	WATER TEMP C
15.5	110.0	0	136.9	5.0	0.9	11.9	774.5	18.9
15.5	110.0	0	136.9	3.1	0.9	12.8	769.0	22.9
15.5	80.0	4	149.1	22.0	56.3	12.8	769.0	20.5
15.5	80.0	4	105.9	13.6	10.8	13.3	770.0	24.4
15.5	80.0	4	85.3	4.2	2.2	13.3	770.0	24.4
15.5	80.0	4	127.5	21.8	25.2	13.3	770.0	24.4
15.5	80.0	3	149.1	25.2	51.5	12.8	769.0	20.5
15.5	80.0	3	105.9	16.1	8.8	13.3	770.0	24.4
15.5	80.0	3	127.5	25.5	21.7	13.3	770.0	24.4
15.5	80.0	2	127.5	28.2	19.9	13.3	770.0	24.4
15.5	80.0	2	149.1	28.8	46.0	12.8	769.0	20.5
15.5	80.0	1	149.1	25.6	52.2	12.8	769.0	22.9
15.5	80.0	1	149.1	29.2	47.0	12.8	769.0	22.9
15.5	80.0	0	149.1	26.2	52.3	12.8	769.0	22.9
15.5	80.0	0	149.1	31.3	44.9	12.8	769.0	22.9
15.5	80.0	0	127.5	28.2	18.3	13.3	770.0	24.4
15.5	80.0	0	64.0	0.0	0.0	13.3	770.0	24.4
15.5	80.0	0	85.3	6.0	1.2	13.3	770.0	24.4
15.5	80.0	0	105.9	17.5	7.4	13.3	770.0	24.4
15.5	80.0	0	149.1	35.3	36.5	12.8	769.0	20.5
15.5	80.0	0	127.5	29.0	19.1	13.3	770.0	24.4
15.5	53.5	4	81.6	14.7	14.1	11.9	774.5	21.5
15.5	53.5	4	105.0	20.8	26.4	11.9	774.5	21.5
15.5	53.5	4	69.4	11.4	9.0	11.9	774.5	21.5
15.5	53.5	4	92.8	17.8	20.1	11.9	774.5	21.5
15.5	53.5	4	58.1	7.7	4.4	11.9	774.5	21.5
15.5	53.5	4	105.0	21.0	28.2	11.9	774.5	21.5
15.5	53.5	3	92.8	23.6	18.6	11.9	774.5	21.5
15.5	53.5	3	69.4	14.8	7.9	11.9	774.5	21.5
15.5	53.5	3	105.0	27.5	24.9	11.9	774.5	21.5
15.5	53.5	3	81.6	19.2	12.8	11.9	774.5	21.5
15.5	53.5	2	92.8	26.2	18.2	11.9	774.5	21.5
15.5	53.5	2	105.0	30.3	24.6	11.9	774.5	21.5
15.5	53.5	0	81.6	23.3	11.8	11.9	774.5	21.5
15.5	53.5	0	58.1	10.9	3.0	11.9	774.5	21.5
15.5	53.5	0	92.8	27.6	18.0	11.9	774.5	21.5
15.5	53.5	0	81.6	22.7	12.0	11.9	774.5	21.5
15.5	53.5	0	92.8	27.4	18.2	11.9	774.5	21.5
15.5	53.5	0	69.4	17.3	7.2	11.9	774.5	21.5
15.5	53.5	0	105.0	32.1	24.2	11.9	774.5	21.5
15.5	53.5	0	69.4	17.1	7.2	11.9	774.5	21.5

TABLE 4 TEST DATA FOR AERATOR NO. 9

FLUME SLOPE DEGREES	NOMINAL DEPTH d MM	VALVE SETTING	WATER FLOW L/S	AIR DEMAND L/S	SUB-NAPPE PRESSURE MM WATER	AIR TEMP C	AIR PRESSURE MM Hg	WATER TEMP C
45.3	80.0	4	105.9	14.5	15.7	12.8	760.3	19.3
45.3	80.0	4	85.3	8.5	5.0	12.8	760.3	19.3
45.3	80.0	4	127.5	18.9	27.7	12.8	760.3	19.3
45.3	80.0	0	85.3	10.9	2.8	12.8	760.3	19.3
45.3	80.0	0	63.7	3.1	0.5	12.8	760.3	19.3
45.3	80.0	0	105.9	18.2	11.4	12.8	760.3	19.3
45.3	80.0	0	127.5	25.4	32.6	12.8	760.3	19.3
45.3	53.5	4	58.1	9.6	5.9	14.2	747.5	20.9
45.3	53.5	4	69.4	12.0	9.3	14.2	747.5	20.9
45.3	53.5	4	92.8	16.2	17.7	12.8	760.3	23.7
45.3	53.5	4	81.6	13.7	14.6	14.2	747.5	20.9
45.3	53.5	3	81.6	18.4	12.4	14.2	747.5	20.9
45.3	53.5	3	92.8	20.2	15.9	12.8	760.3	23.7
45.3	53.5	0	46.9	6.8	1.2	14.2	747.5	20.9
45.3	53.5	0	58.1	13.1	4.3	14.2	747.5	20.9
45.3	53.5	0	81.6	23.0	11.2	14.2	747.5	20.9
45.3	53.5	0	92.8	23.0	15.2	12.8	760.3	23.7
45.3	53.5	0	105.0	26.0	19.6	12.8	760.3	23.7
45.3	53.5	0	69.4	15.2	8.8	14.2	747.5	20.9
45.3	53.5	0	81.6	19.1	12.0	14.2	747.5	20.9
45.3	53.5	0	92.8	23.1	14.8	12.8	760.3	23.7
15.5	110.0	4	63.7	7.3	0.6	11.9	774.5	18.9
15.5	110.0	4	205.3	16.9	15.3	10.0	772.5	19.3
15.5	110.0	4	171.6	7.9	4.4	10.0	772.5	20.3
15.5	110.0	4	136.9	7.8	1.5	10.0	772.5	20.3
15.5	110.0	4	136.9	7.5	1.8	10.0	772.5	20.3
15.5	110.0	4	127.5	18.4	18.7	10.0	772.5	20.3
15.5	110.0	3	205.3	19.5	16.5	10.0	772.5	19.3
15.5	110.0	3	136.9	13.9	2.2	10.0	772.5	20.3
15.5	110.0	3	127.5	22.0	14.3	10.0	772.5	20.3
15.5	110.0	3	171.6	9.5	2.9	10.0	772.5	20.3
15.5	110.0	3	136.9	13.5	2.2	10.0	772.5	20.3
15.5	110.0	2	205.3	20.6	15.4	10.0	772.5	19.3
15.5	110.0	0	63.7	13.9	2.1	11.9	774.5	18.9
15.5	110.0	0	136.9	18.3	2.7	10.0	772.5	20.3
15.5	110.0	0	171.6	9.9	2.4	10.0	772.5	19.3
15.5	110.0	0	136.9	18.5	2.3	10.0	772.5	20.3
15.5	110.0	0	127.5	23.5	11.5	10.0	772.5	20.3
15.5	110.0	0	171.6	9.5	2.1	10.0	772.5	20.3
15.5	110.0	0	103.0	0.0	0.0	10.0	772.5	20.3
15.5	110.0	0	171.6	9.1	2.0	10.0	772.5	20.3
15.5	110.0	0	205.3	19.8	16.2	10.0	772.5	19.3
15.5	110.0	0	136.9	18.3	4.5	10.0	772.5	20.3
15.5	110.0	0	127.5	24.5	11.5	10.0	772.5	20.3
15.5	80.0	4	127.5	16.6	19.8	10.0	772.5	14.7
15.5	80.0	4	149.1	23.6	33.0	13.6	765.5	19.3
15.5	80.0	4	105.9	10.1	6.1	10.0	772.5	14.7
15.5	80.0	4	85.3	4.3	1.1	10.0	772.5	19.3
15.5	80.0	3	105.9	11.2	4.3	10.0	772.5	14.7
15.5	80.0	3	127.5	18.5	18.4	10.0	772.5	14.7
15.5	80.0	3	149.1	28.4	25.5	13.6	765.5	19.3
15.5	80.0	2	105.9	11.4	3.4	10.0	772.5	14.7
15.5	80.0	2	127.5	19.1	16.9	10.0	772.5	14.7
15.5	80.0	2	127.5	18.2	17.7	10.0	772.5	14.7
15.5	80.0	2	149.1	30.5	23.0	13.6	765.5	19.3

TABLE 4 Cont.

FLUME SLOPE DEGREES	NOMINAL DEPTH d MM	VALVE SETTING	WATER FLOW L/S	AIR DEMAND L/S	SUB-NAPPE PRESSURE MM WATER	AIR TEMP C	AIR PRESSURE MM Hg	WATER TEMP C
15.5	80.0	2	127.5	21.4	11.1	10.0	772.5	14.7
15.5	80.0	0	85.3	5.2	0.7	10.0	772.5	19.3
15.5	80.0	0	105.9	11.4	3.0	10.0	772.5	14.7
15.5	80.0	0	149.1	32.0	22.6	13.6	765.5	19.3
15.5	80.0	0	63.7	12.0	0.1	10.0	772.5	19.3
15.5	80.0	0	127.5	18.7	17.4	10.0	772.5	14.7
15.5	53.5	4	92.8	14.9	14.5	13.6	765.5	17.0
15.5	53.5	4	105.0	17.2	20.0	13.3	763.0	15.5
15.5	53.5	4	69.4	9.6	5.7	13.6	765.5	17.0
15.5	53.5	4	81.6	12.8	11.3	13.6	765.5	17.0
15.5	53.5	3	92.8	18.1	12.4	13.6	765.5	17.0
15.5	53.5	3	69.4	11.1	4.0	13.6	765.5	17.0
15.5	53.5	3	81.6	14.4	9.5	13.6	765.5	17.0
15.5	53.5	3	105.0	22.2	16.9	13.3	763.0	15.5
15.5	53.5	2	81.6	15.6	8.7	13.6	765.5	17.0
15.5	53.5	2	105.0	25.5	15.8	13.3	763.0	15.5
15.5	53.5	2	69.4	11.8	3.5	13.6	765.5	17.0
15.5	53.5	2	92.8	19.4	11.8	13.6	765.5	17.0
15.5	53.5	0	105.0	26.6	15.1	13.3	763.0	15.5
15.5	53.5	0	69.4	11.5	3.0	13.6	765.5	19.3
15.5	53.5	0	81.6	16.5	8.1	13.6	765.5	17.0
15.5	53.5	0	92.8	20.2	11.3	13.6	765.5	17.0
15.5	53.5	0	92.8	22.4	10.8	13.6	765.5	17.0
15.5	53.5	0	105.0	25.5	16.7	13.3	763.0	15.5
15.5	53.5	0	69.4	10.8	4.6	13.6	765.5	17.0

TABLE 5 DATA ANALYSIS FOR AERATOR NO. 1

FLUME SLOPE DEGREES	NOMINAL DEPTH d MM	VEL V M/S	BETA qa/qw	FROUDE NUMBER F	d/h1	EULER NUMBER E*1000
45.3	110.0	4.148	0.067	3.994	13.75	5.130
45.3	110.0	6.221	0.129	5.989	13.75	10.544
45.3	110.0	6.221	0.103	5.989	13.75	13.763
45.3	110.0	3.124	0.038	3.008	13.75	1.307
45.3	110.0	3.124	0.038	3.008	13.75	1.307
45.3	110.0	5.200	0.098	5.006	13.75	11.102
45.3	110.0	4.148	0.064	3.994	13.75	2.793
45.3	110.0	5.200	0.098	5.006	13.75	6.784
45.3	110.0	5.200	0.116	5.006	13.75	5.805
45.3	110.0	5.200	0.110	5.006	13.75	10.412
45.3	110.0	6.221	0.122	5.989	13.75	12.623
45.3	110.0	6.221	0.158	5.989	13.75	8.162
45.3	110.0	6.221	0.179	5.989	13.75	7.300
45.3	110.0	3.124	0.056	3.008	13.75	1.005
45.3	110.0	6.221	0.121	5.989	13.75	12.394
45.3	110.0	2.091	0.000	2.013	13.75	0.000
45.3	110.0	5.200	0.112	5.006	13.75	9.941
45.3	110.0	6.221	0.133	5.989	13.75	12.851
45.3	110.0	5.200	0.104	5.006	13.75	10.158
45.3	110.0	5.200	0.124	5.006	13.75	4.680
45.3	110.0	4.148	0.075	3.994	13.75	4.275
45.3	110.0	3.124	0.043	3.008	13.75	1.407
45.3	110.0	5.200	0.127	5.006	13.75	4.716
45.3	110.0	4.148	0.088	3.994	13.75	1.653
45.3	110.0	3.124	0.035	3.008	13.75	1.407
45.3	110.0	6.221	0.164	5.989	13.75	7.198
45.3	110.0	2.073	0.025	1.995	13.75	0.457
45.3	80.0	6.213	0.161	7.013	10.00	10.548
45.3	80.0	6.213	0.221	7.013	10.00	8.718
45.3	80.0	6.213	0.223	7.013	10.00	8.286
45.3	80.0	6.213	0.254	7.013	10.00	7.879
45.3	73.5	5.950	0.162	7.007	9.19	13.854
45.3	73.5	4.249	0.142	5.004	9.19	10.865
45.3	73.5	3.401	0.112	4.006	9.19	6.868
45.3	73.5	5.102	0.163	6.008	9.19	13.680
45.3	73.5	5.950	0.190	7.007	9.19	13.688
45.3	73.5	5.102	0.188	6.008	9.19	13.416
45.3	73.5	5.102	0.196	6.008	9.19	12.587
45.3	73.5	5.950	0.204	7.007	9.19	14.048
45.3	73.5	5.950	0.200	7.007	9.19	13.744
45.3	73.5	5.102	0.198	6.008	9.19	12.926
45.3	73.5	4.249	0.170	5.004	9.19	9.887
45.3	73.5	3.401	0.132	4.006	9.19	5.681
45.3	73.5	5.950	0.208	7.007	9.19	14.519
45.3	73.5	2.549	0.116	3.002	9.19	4.077
45.3	53.5	5.084	0.192	7.018	6.69	10.665
45.3	53.5	5.782	0.169	7.981	6.69	8.246
45.3	53.5	5.084	0.184	7.018	6.69	8.198
45.3	53.5	5.782	0.189	7.981	6.69	7.894
45.3	53.5	5.084	0.214	7.018	6.69	8.387
45.3	53.5	2.922	0.162	4.034	6.69	5.285
45.3	53.5	3.620	0.177	4.997	6.69	7.037
45.3	53.5	5.782	0.206	7.981	6.69	7.952
45.3	53.5	5.084	0.199	7.018	6.69	8.084
45.3	53.5	6.542	0.198	9.030	6.69	7.633
45.3	53.5	4.324	0.187	5.969	6.69	7.608
45.3	53.5	5.782	0.208	7.981	6.69	8.275

TABLE 5 Cont.

FLUME SLOPE DEGREES	NOMINAL DEPTH d MM	VEL V M/S	BETA qa/qw	FROUDE NUMBER F	d/h1	EULER NUMBER E*1000
15.5	110.0	4.148	0.049	3.994	13.75	1.482
15.5	110.0	6.221	0.077	5.989	13.75	6.945
15.5	110.0	5.200	0.045	5.006	13.75	2.286
15.5	110.0	5.200	0.048	5.006	13.75	1.959
15.5	110.0	6.221	0.080	5.989	13.75	6.109
15.5	110.0	4.148	0.069	3.994	13.75	1.482
15.5	110.0	5.200	0.051	5.006	13.75	1.959
15.5	110.0	6.221	0.080	5.989	13.75	5.982
15.5	110.0	6.221	0.089	5.989	13.75	6.210
15.5	110.0	3.121	0.000	3.005	13.75	0.000
15.5	110.0	4.148	0.082	3.994	13.75	1.824
15.5	110.0	5.200	0.050	5.006	13.75	1.850
15.5	73.5	3.401	0.053	4.006	9.19	1.526
15.5	73.5	5.102	0.133	6.008	9.19	9.685
15.5	73.5	5.950	0.144	7.007	9.19	13.411
15.5	73.5	6.803	0.162	8.011	9.19	11.320
15.5	73.5	5.950	0.147	7.007	9.19	13.522
15.5	73.5	4.249	0.094	5.004	9.19	4.726
15.5	73.5	5.102	0.124	6.008	9.19	8.969
15.5	73.5	5.102	0.135	6.008	9.19	8.065
15.5	73.5	5.950	0.155	7.007	9.19	12.912
15.5	73.5	6.803	0.180	8.011	9.19	9.518
15.5	73.5	6.803	0.186	8.011	9.19	9.497
15.5	73.5	5.950	0.154	7.007	9.19	12.940
15.5	73.5	4.249	0.100	5.004	9.19	3.748
15.5	73.5	5.102	0.140	6.008	9.19	7.876
15.5	73.5	3.401	0.080	4.006	9.19	1.865
15.5	73.5	6.803	0.189	8.011	9.19	9.327
15.5	73.5	5.950	0.178	7.007	9.19	11.222
15.5	73.5	5.102	0.148	6.008	9.19	8.969
15.5	73.5	5.102	0.140	6.008	9.19	7.989
15.5	73.5	6.803	0.189	8.011	9.19	8.458
15.5	73.5	4.249	0.118	5.004	9.19	3.857
15.5	73.5	5.950	0.157	7.007	9.19	13.106
15.5	73.5	5.950	0.149	7.007	9.19	13.356
15.5	53.5	5.782	0.154	7.981	6.69	7.248
15.5	53.5	6.542	0.167	9.030	6.69	7.725
15.5	53.5	5.084	0.152	7.018	6.69	6.793
15.5	53.5	4.324	0.125	5.969	6.69	4.985
15.5	53.5	6.542	0.192	9.030	6.69	7.472
15.5	53.5	5.782	0.178	7.981	6.69	6.896
15.5	53.5	4.324	0.141	5.969	6.69	4.670
15.5	53.5	5.084	0.167	7.018	6.69	6.490
15.5	53.5	5.084	0.173	7.018	6.69	6.338
15.5	53.5	5.782	0.185	7.981	6.69	6.749
15.5	53.5	6.542	0.205	9.030	6.69	7.587
15.5	53.5	5.084	0.178	7.018	6.69	6.262
15.5	53.5	5.782	0.189	7.981	6.69	6.720
15.5	53.5	4.324	0.144	5.969	6.69	4.355
15.5	53.5	6.542	0.206	9.030	6.69	7.449

TABLE 6 DATA ANALYSIS FOR AERATOR NO. 3

FLUME SLOPE DEGREES	NOMINAL DEPTH d MM	VEL V M/S	BETA qa/qw	FROUDE NUMBER F	d/h1	EULER NUMBER E*1000
45.3	110.0	4.148	0.035	3.994	13.75	1.881
45.3	110.0	3.124	0.064	3.008	13.75	2.915
45.3	110.0	5.200	0.068	5.006	13.75	5.514
45.3	110.0	5.200	0.075	5.006	13.75	4.680
45.3	110.0	5.200	0.080	5.006	13.75	4.499
45.3	110.0	4.148	0.048	3.994	13.75	1.368
45.3	110.0	2.073	0.111	1.995	13.75	3.653
45.3	110.0	6.221	0.101	5.989	13.75	7.857
45.3	110.0	4.148	0.036	3.994	13.75	1.311
45.3	110.0	6.221	0.105	5.989	13.75	8.440
45.3	110.0	6.221	0.104	5.989	13.75	7.908
45.3	110.0	5.200	0.082	5.006	13.75	4.426
45.3	110.0	3.124	0.106	3.008	13.75	4.422
45.3	73.5	4.249	0.111	5.004	9.19	6.302
45.3	73.5	5.950	0.135	7.007	9.19	9.310
45.3	73.5	5.102	0.132	6.008	9.19	4.070
45.3	73.5	5.102	0.156	6.008	9.19	4.070
45.3	73.5	5.950	0.151	7.007	9.19	9.643
45.3	73.5	5.950	0.160	7.007	9.19	9.172
45.3	73.5	5.102	0.156	6.008	9.19	4.221
45.3	73.5	4.249	0.129	5.004	9.19	5.215
45.3	73.5	5.102	0.156	6.008	9.19	7.876
45.3	73.5	5.950	0.164	7.007	9.19	9.837
45.3	73.5	3.401	0.085	4.006	9.19	2.289
45.3	73.5	2.540	0.000	2.991	9.19	0.000
45.3	53.5	4.324	0.151	5.969	6.69	6.139
45.3	53.5	5.782	0.154	7.981	6.69	6.426
45.3	53.5	5.084	0.147	7.018	6.69	6.110
45.3	53.5	5.782	0.195	7.981	6.69	6.485
45.3	53.5	4.324	0.182	5.969	6.69	5.352
45.3	53.5	5.084	0.189	7.018	6.69	5.996
45.3	53.5	3.620	0.165	4.997	6.69	4.267
45.3	53.5	2.922	0.115	4.034	6.69	2.528
15.5	53.5	4.324	0.062	5.969	6.69	1.312
15.5	110.0	5.200	0.029	5.006	13.75	0.653
15.5	73.5	5.950	0.104	7.007	9.19	4.766
15.5	110.0	5.200	0.013	5.006	13.75	0.290
15.5	73.5	5.950	0.103	7.007	9.19	4.683
15.5	53.5	6.542	0.135	9.030	6.69	4.057
15.5	73.5	5.102	0.087	6.008	9.19	3.015
15.5	73.5	5.102	0.073	6.008	9.19	4.070
15.5	73.5	6.803	0.115	8.011	9.19	6.572
15.5	53.5	5.084	0.102	7.018	6.69	2.884
15.5	53.5	6.542	0.132	9.030	6.69	4.172
15.5	53.5	5.084	0.097	7.018	6.69	3.226
15.5	73.5	6.803	0.118	8.011	9.19	6.338
15.5	110.0	5.200	0.028	5.006	13.75	0.580
15.5	53.5	5.782	0.123	7.981	6.69	3.609
15.5	73.5	5.102	0.084	6.008	9.19	3.693
15.5	53.5	4.324	0.069	5.969	6.69	1.154
15.5	110.0	6.221	0.051	5.989	13.75	2.256
15.5	73.5	6.803	0.121	8.011	9.19	6.360
15.5	73.5	5.102	0.077	6.008	9.19	3.580
15.5	53.5	6.542	0.141	9.030	6.69	3.988

TABLE 6 Cont.

FLUME SLOPE DEGREES	NOMINAL DEPTH d MM	VEL V M/S	BETA qa/qw	FROUDE NUMBER F	d/h1	EULER NUMBER E*1000
15.5	73.5	6.803	0.118	8.011	9.19	6.296
15.5	73.5	5.102	0.089	6.008	9.19	2.751
15.5	73.5	4.249	0.043	5.004	9.19	1.358
15.5	110.0	6.221	0.049	5.989	13.75	2.180
15.5	73.5	5.950	0.101	7.007	9.19	4.766
15.5	110.0	5.200	0.031	5.006	13.75	0.653
15.5	73.5	5.950	0.099	7.007	9.19	4.904
15.5	73.5	5.950	0.094	7.007	9.19	5.514
15.5	110.0	6.221	0.077	5.989	13.75	2.357
15.5	110.0	5.200	0.011	5.006	13.75	0.218
15.5	53.5	6.542	0.123	9.030	6.69	4.653
15.5	110.0	5.200	0.026	5.006	13.75	0.762
15.5	73.5	5.950	0.102	7.007	9.19	4.821
15.5	73.5	5.950	0.097	7.007	9.19	5.625
15.5	73.5	4.249	0.051	5.004	9.19	1.195
15.5	73.5	4.249	0.053	5.004	9.19	1.087
15.5	53.5	5.782	0.124	7.981	6.69	3.492
15.5	73.5	5.102	0.081	6.008	9.19	3.015
15.5	110.0	6.221	0.054	5.989	13.75	2.408
15.5	73.5	5.102	0.092	6.008	9.19	2.864
15.5	53.5	5.782	0.121	7.981	6.69	3.668
15.5	73.5	4.249	0.036	5.004	9.19	0.978
15.5	53.5	5.084	0.105	7.018	6.69	2.467
15.5	73.5	5.102	0.083	6.008	9.19	3.580
15.5	73.5	5.950	0.102	7.007	9.19	5.015
15.5	110.0	6.221	0.072	5.989	13.75	2.712
15.5	53.5	5.782	0.110	7.981	6.69	4.079
15.5	73.5	6.803	0.109	8.011	9.19	7.335

TABLE 7 DATA ANALYSIS FOR AERATOR NO. 7

FLUME SLOPE DEGREES	NOMINAL DEPTH d MM	VEL V M/S	BETA qa/qw	FROUDE NUMBER F	d/h1	EULER NUMBER E*1000
45.3	110.0	6.221	0.133	5.989	6.88	13.890
45.3	110.0	5.200	0.110	5.006	6.88	1.814
45.3	110.0	5.200	0.117	5.006	6.88	10.195
45.3	110.0	5.200	0.114	5.006	6.88	10.739
45.3	110.0	4.148	0.091	3.994	6.88	5.073
45.3	110.0	5.200	0.136	5.006	6.88	9.142
45.3	110.0	5.200	0.163	5.006	6.88	8.235
45.3	110.0	5.200	0.153	5.006	6.88	8.671
45.3	110.0	5.200	0.143	5.006	6.88	6.784
45.3	110.0	5.200	0.157	5.006	6.88	8.381
45.3	110.0	5.200	0.139	5.006	6.88	8.598
45.3	110.0	5.200	0.164	5.006	6.88	8.707
45.3	110.0	4.148	0.122	3.994	6.88	3.306
45.3	110.0	6.221	0.194	5.989	6.88	11.710
45.3	110.0	3.124	0.053	3.008	6.88	1.206
45.3	110.0	5.200	0.133	5.006	6.88	1.560
45.3	80.0	5.313	0.163	5.997	5.00	9.420
45.3	80.0	2.654	0.107	2.996	5.00	4.595
45.3	80.0	4.413	0.148	4.981	5.00	9.926
45.3	80.0	5.313	0.180	5.997	5.00	10.741
45.3	80.0	5.313	0.205	5.997	5.00	9.802
45.3	80.0	5.313	0.239	5.997	5.00	9.872
45.3	80.0	5.313	0.221	5.997	5.00	6.604
45.3	80.0	4.413	0.188	4.981	5.00	8.465
45.3	80.0	5.313	0.281	5.997	5.00	9.663
45.3	80.0	5.313	0.224	5.997	5.00	10.080
45.3	80.0	5.313	0.225	5.997	5.00	6.743
45.3	80.0	6.213	0.306	7.013	5.00	11.285
45.3	80.0	3.554	0.193	4.012	5.00	6.368
45.3	80.0	2.654	0.149	2.996	5.00	3.481
45.3	80.0	5.313	0.283	5.997	5.00	9.906
45.3	53.5	5.084	0.169	7.018	3.34	5.731
45.3	53.5	4.324	0.166	5.969	3.34	4.827
45.3	53.5	5.782	0.164	7.981	3.34	5.223
45.3	53.5	3.620	0.155	4.997	3.34	4.642
45.3	53.5	2.922	0.173	4.034	3.34	4.940
45.3	53.5	4.324	0.225	5.969	3.34	4.617
45.3	53.5	5.782	0.232	7.981	3.34	4.900
45.3	53.5	5.084	0.233	7.018	3.34	5.389
45.3	53.5	5.782	0.256	7.981	3.34	4.959
45.3	53.5	5.782	0.264	7.981	3.34	5.018
45.3	53.5	5.084	0.272	7.018	3.34	5.237
45.3	53.5	3.620	0.243	4.997	3.34	4.043
45.3	53.5	4.324	0.216	5.969	3.34	4.722
45.3	53.5	4.324	0.272	5.969	3.34	4.565
45.3	53.5	2.922	0.245	4.034	3.34	3.791
45.3	53.5	4.324	0.249	5.969	3.34	4.670
45.3	53.5	5.782	0.263	7.981	3.34	4.783
45.3	53.5	5.084	0.277	7.018	3.34	5.275
15.5	110.0	5.200	0.076	5.006	6.88	3.918
15.5	110.0	5.200	0.087	5.006	6.88	2.939
15.5	110.0	5.200	0.089	5.006	6.88	2.685
15.5	110.0	4.148	0.034	3.994	6.88	0.627
15.5	110.0	3.124	0.088	3.008	6.88	0.804

TABLE 7 Cont.

FLUME SLOPE DEGREES	NOMINAL DEPTH d MM	VEL V M/S	BETA q <sub>a</sub> /q <sub>w</sub>	FROUDE NUMBER F	d/h <sub>1</sub>	EULER NUMBER E*1000
15.5	110.0	5.200	0.089	5.006	6.88	2.394
15.5	110.0	4.148	0.037	3.994	6.88	0.513
15.5	110.0	4.148	0.023	3.994	6.88	0.513
15.5	80.0	6.213	0.148	7.013	5.00	14.310
15.5	80.0	4.413	0.128	4.981	5.00	5.442
15.5	80.0	3.554	0.049	4.012	5.00	1.709
15.5	80.0	5.313	0.171	5.997	5.00	8.759
15.5	80.0	6.213	0.169	7.013	5.00	13.090
15.5	80.0	4.413	0.152	4.981	5.00	4.434
15.5	80.0	5.313	0.200	5.997	5.00	7.543
15.5	80.0	5.313	0.221	5.997	5.00	6.917
15.5	80.0	6.213	0.193	7.013	5.00	11.692
15.5	80.0	6.213	0.172	7.013	5.00	13.268
15.5	80.0	6.213	0.196	7.013	5.00	11.946
15.5	80.0	6.213	0.176	7.013	5.00	13.293
15.5	80.0	6.213	0.210	7.013	5.00	11.413
15.5	80.0	5.313	0.221	5.997	5.00	6.361
15.5	80.0	2.667	0.000	3.010	5.00	0.000
15.5	80.0	3.554	0.070	4.012	5.00	0.932
15.5	80.0	4.413	0.165	4.981	5.00	3.728
15.5	80.0	6.213	0.237	7.013	5.00	9.277
15.5	80.0	5.313	0.227	5.997	5.00	6.646
15.5	53.5	5.084	0.180	7.018	3.34	5.351
15.5	53.5	6.542	0.198	9.030	3.34	6.051
15.5	53.5	4.324	0.164	5.969	3.34	4.722
15.5	53.5	5.782	0.192	7.981	3.34	5.898
15.5	53.5	3.620	0.133	4.997	3.34	3.294
15.5	53.5	6.542	0.200	9.030	3.34	6.464
15.5	53.5	5.782	0.254	7.981	3.34	5.458
15.5	53.5	4.324	0.213	5.969	3.34	4.145
15.5	53.5	6.542	0.262	9.030	3.34	5.707
15.5	53.5	5.084	0.235	7.018	3.34	4.858
15.5	53.5	5.782	0.282	7.981	3.34	5.341
15.5	53.5	6.542	0.289	9.030	3.34	5.639
15.5	53.5	5.084	0.286	7.018	3.34	4.478
15.5	53.5	3.620	0.188	4.997	3.34	2.246
15.5	53.5	5.782	0.297	7.981	3.34	5.282
15.5	53.5	5.084	0.278	7.018	3.34	4.554
15.5	53.5	5.782	0.295	7.981	3.34	5.341
15.5	53.5	4.324	0.249	5.969	3.34	3.778
15.5	53.5	6.542	0.306	9.030	3.34	5.547
15.5	53.5	4.324	0.246	5.969	3.34	3.778

TABLE 8 DATA ANALYSIS FOR AERATOR NO. 9

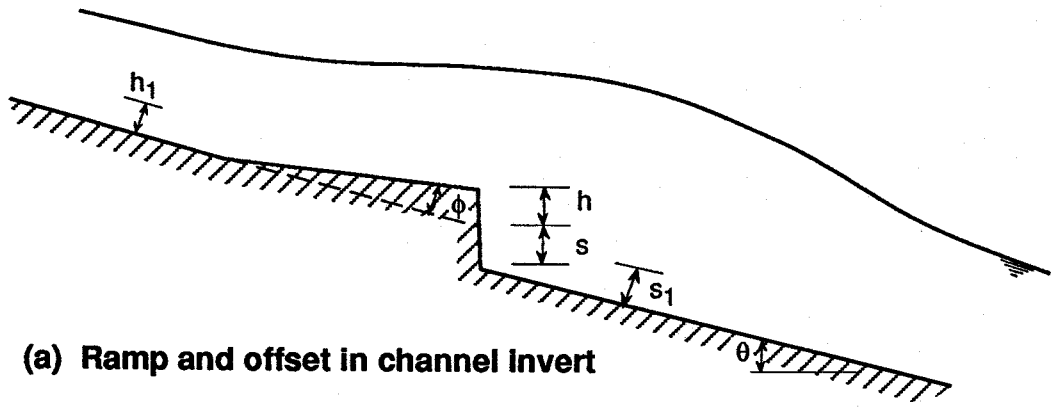
FLUME SLOPE DEGREES	NOMINAL DEPTH d MM	VEL V M/S	BETA $q_a/q_w$	FROUDE NUMBER F	d/h1	EULER NUMBER E*1000
45.3	80.0	4.413	0.137	4.981	5.00	7.910
45.3	80.0	3.554	0.100	4.012	5.00	3.883
45.3	80.0	5.313	0.148	5.997	5.00	9.628
45.3	80.0	3.554	0.128	4.012	5.00	2.174
45.3	80.0	2.654	0.049	2.996	5.00	0.696
45.3	80.0	4.413	0.172	4.981	5.00	5.744
45.3	80.0	5.313	0.199	5.997	5.00	11.332
45.3	53.5	3.620	0.165	4.997	3.34	4.417
45.3	53.5	4.324	0.173	5.969	3.34	4.880
45.3	53.5	5.782	0.175	7.981	3.34	5.194
45.3	53.5	5.084	0.168	7.018	3.34	5.541
45.3	53.5	5.084	0.225	7.018	3.34	4.706
45.3	53.5	5.782	0.218	7.981	3.34	4.666
45.3	53.5	2.922	0.145	4.034	3.34	1.379
45.3	53.5	3.620	0.225	4.997	3.34	3.219
45.3	53.5	5.084	0.282	7.018	3.34	4.251
45.3	53.5	5.782	0.248	7.981	3.34	4.460
45.3	53.5	6.542	0.248	9.030	3.34	4.493
45.3	53.5	4.324	0.219	5.969	3.34	4.617
45.3	53.5	5.084	0.234	7.018	3.34	4.554
45.3	53.5	5.782	0.249	7.981	3.34	4.343
15.5	110.0	1.930	0.115	1.858	6.88	1.448
15.5	110.0	6.221	0.082	5.989	6.88	3.878
15.5	110.0	5.200	0.046	5.006	6.88	1.596
15.5	110.0	4.148	0.057	3.994	6.88	0.855
15.5	110.0	4.148	0.055	3.994	6.88	1.026
15.5	110.0	3.864	0.144	3.719	6.88	12.289
15.5	110.0	6.221	0.095	5.989	6.88	4.182
15.5	110.0	4.148	0.102	3.994	6.88	1.254
15.5	110.0	3.864	0.173	3.719	6.88	9.398
15.5	110.0	5.200	0.055	5.006	6.88	1.052
15.5	110.0	4.148	0.099	3.994	6.88	1.254
15.5	110.0	6.221	0.100	5.989	6.88	3.903
15.5	110.0	1.930	0.218	1.858	6.88	5.529
15.5	110.0	4.148	0.134	3.994	6.88	1.539
15.5	110.0	5.200	0.058	5.006	6.88	0.871
15.5	110.0	4.148	0.135	3.994	6.88	1.311
15.5	110.0	3.864	0.184	3.719	6.88	7.557
15.5	110.0	5.200	0.055	5.006	6.88	0.762
15.5	110.0	3.121	0.000	3.005	6.88	0.000
15.5	110.0	5.200	0.053	5.006	6.88	0.726
15.5	110.0	6.221	0.096	5.989	6.88	4.106
15.5	110.0	4.148	0.134	3.994	6.88	2.565
15.5	110.0	3.864	0.192	3.719	6.88	7.557
15.5	80.0	5.313	0.130	5.997	5.00	6.882
15.5	80.0	6.213	0.158	7.013	5.00	8.388
15.5	80.0	4.413	0.095	4.981	5.00	3.073
15.5	80.0	3.554	0.050	4.012	5.00	0.854
15.5	80.0	4.413	0.106	4.981	5.00	2.167
15.5	80.0	5.313	0.145	5.997	5.00	6.396
15.5	80.0	6.213	0.190	7.013	5.00	6.482
15.5	80.0	4.413	0.108	4.981	5.00	1.713
15.5	80.0	5.313	0.150	5.997	5.00	5.874
15.5	80.0	5.313	0.143	5.997	5.00	6.152
15.5	80.0	6.213	0.205	7.013	5.00	5.846

TABLE 8 Cont.

FLUME SLOPE DEGREES	NOMINAL DEPTH d MM	VEL V M/S	BETA qa/qw	FROUDE NUMBER F	d/h1	EULER NUMBER E*1000
15.5	80.0	5.313	0.168	5.997	5.00	3.858
15.5	80.0	3.554	0.061	4.012	5.00	0.544
15.5	80.0	4.413	0.108	4.981	5.00	1.512
15.5	80.0	6.213	0.215	7.013	5.00	5.744
15.5	80.0	2.654	0.188	2.996	5.00	0.139
15.5	80.0	5.313	0.147	5.997	5.00	6.048
15.5	53.5	5.782	0.161	7.981	3.34	4.255
15.5	53.5	6.542	0.164	9.030	3.34	4.584
15.5	53.5	4.324	0.138	5.969	3.34	2.991
15.5	53.5	5.084	0.157	7.018	3.34	4.289
15.5	53.5	5.782	0.195	7.981	3.34	3.639
15.5	53.5	4.324	0.160	5.969	3.34	2.099
15.5	53.5	5.084	0.176	7.018	3.34	3.605
15.5	53.5	6.542	0.211	9.030	3.34	3.874
15.5	53.5	5.084	0.191	7.018	3.34	3.302
15.5	53.5	6.542	0.243	9.030	3.34	3.622
15.5	53.5	4.324	0.170	5.969	3.34	1.836
15.5	53.5	5.782	0.209	7.981	3.34	3.463
15.5	53.5	6.542	0.253	9.030	3.34	3.461
15.5	53.5	4.324	0.166	5.969	3.34	1.574
15.5	53.5	5.084	0.202	7.018	3.34	3.074
15.5	53.5	5.782	0.218	7.981	3.34	3.316
15.5	53.5	5.782	0.241	7.981	3.34	3.169
15.5	53.5	6.542	0.243	9.030	3.34	3.828
15.5	53.5	4.324	0.156	5.969	3.34	2.414

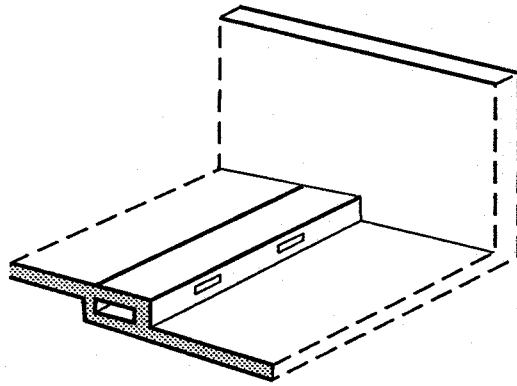
**FIGURES.**



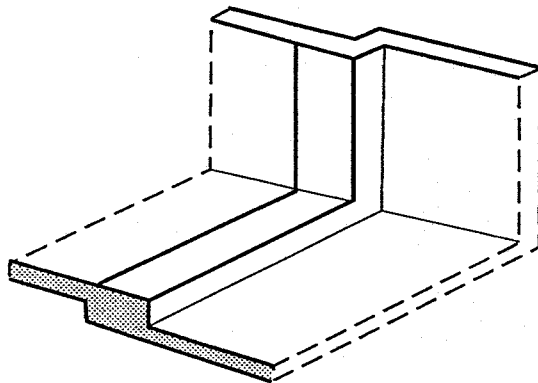


**(a) Ramp and offset in channel invert**

Ramp only  $s_1 = 0$   
 Offset only  $h_1 = 0$



**(b) Air supply via transverse duct and slots**



**(c) Air supply via offset in side wall**

**Fig 1 Geometry of aeration system**

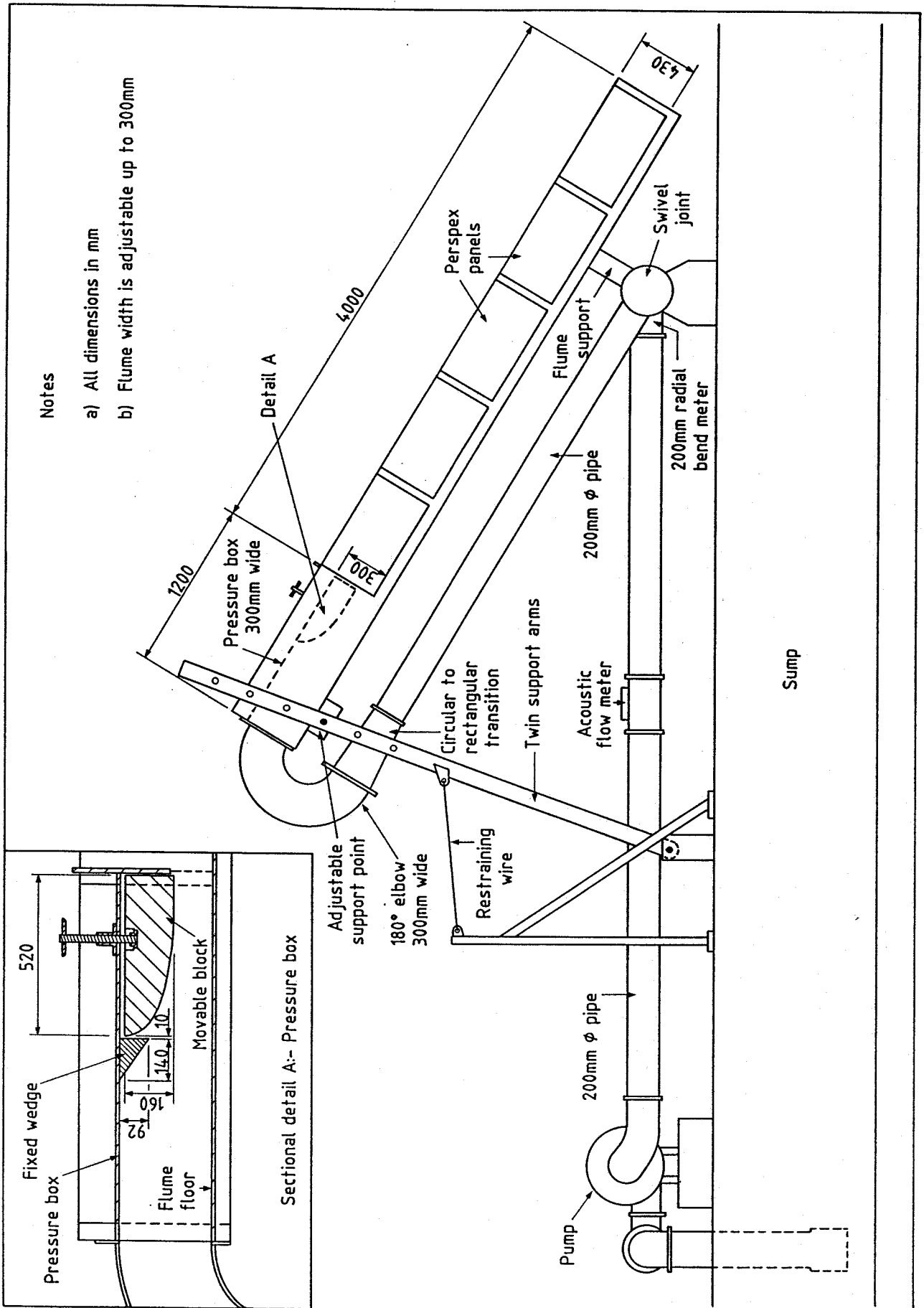
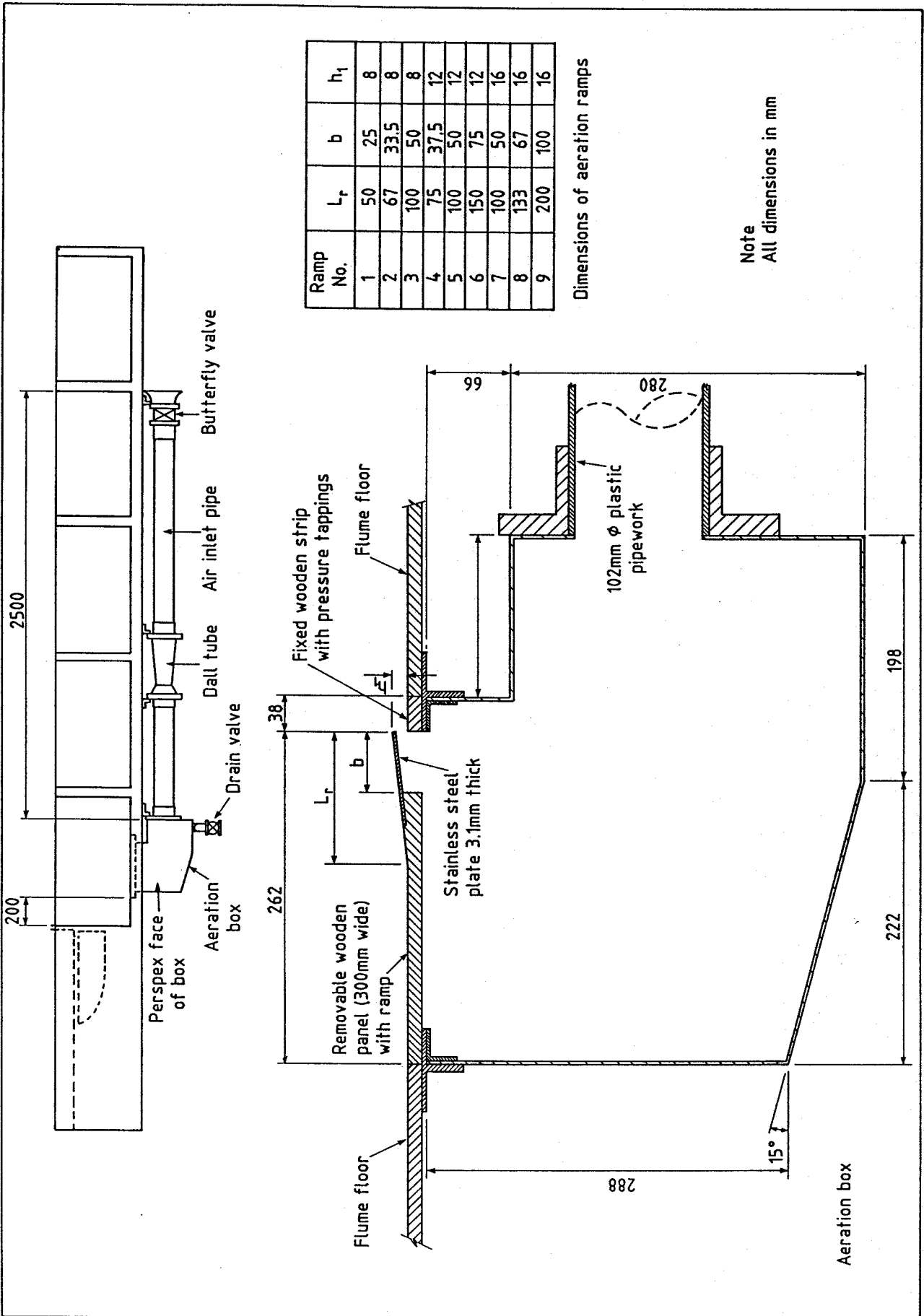


Fig 2 Layout of high velocity flume



Ramp No.	$L_r$	$b$	$h_1$
1	50	25	8
2	67	33.5	8
3	100	50	8
4	75	37.5	12
5	100	50	12
6	150	75	12
7	100	50	16
8	133	67	16
9	200	100	16

Dimensions of aeration ramps

Note  
All dimensions in mm

Fig 3 Air supply system and aeration ramps

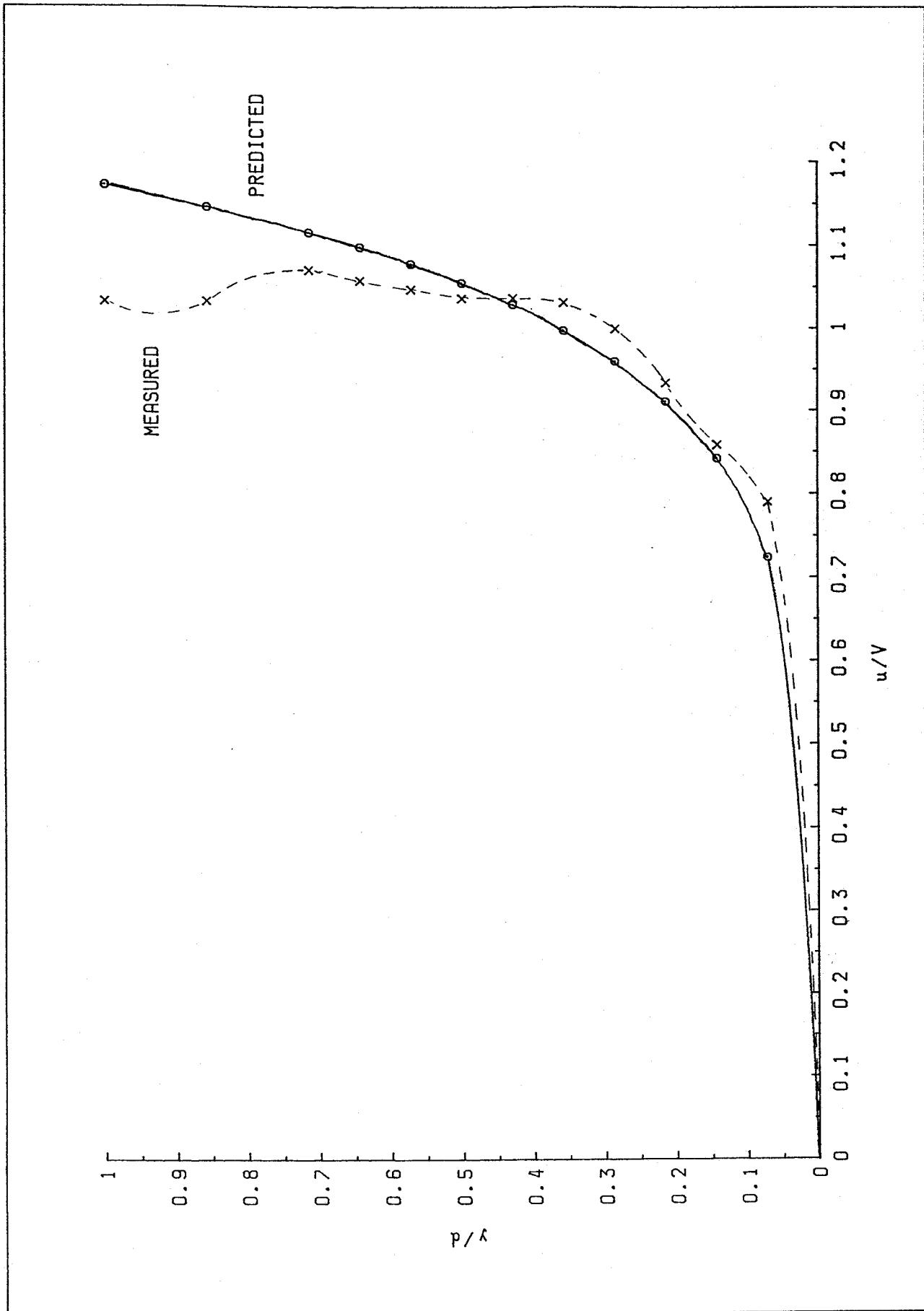


FIG 4 MEASURED AND PREDICTED VELOCITY PROFILES AT  $x=0.195m$

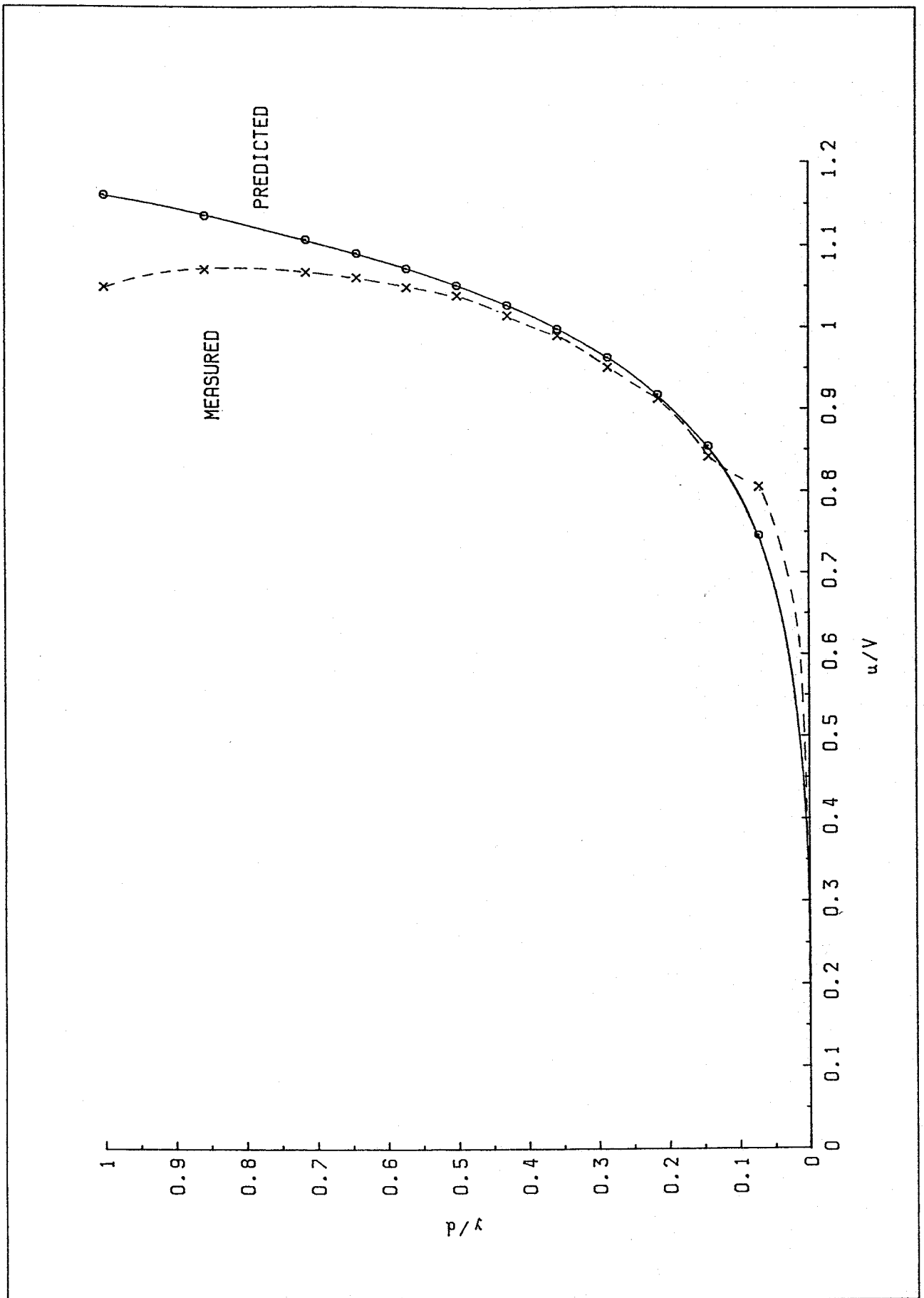


FIG 5. MEASURED AND PREDICTED VELOCITY PROFILES AT  $x=0.5m$

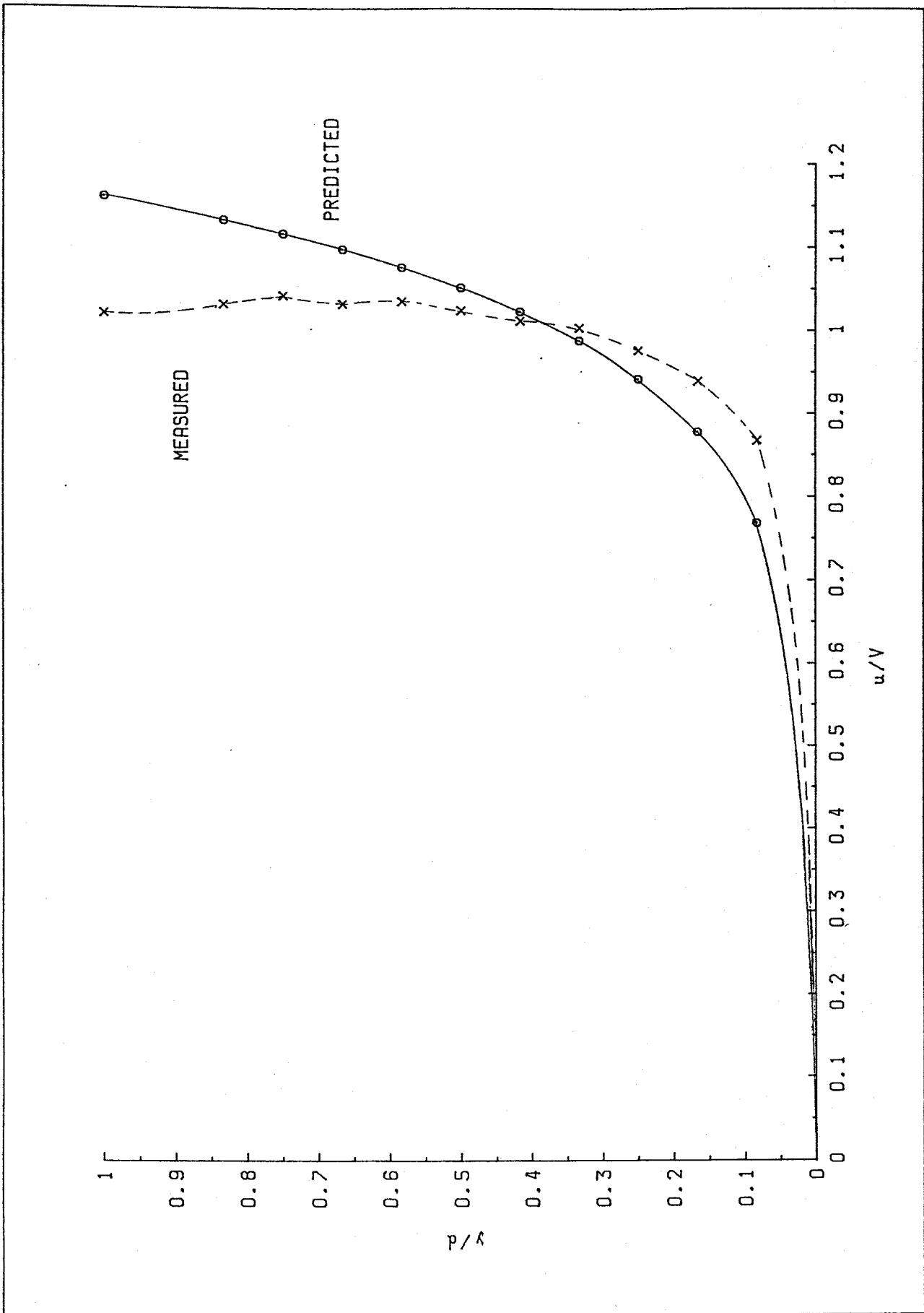


FIG 6 MEASURED AND PREDICTED VELOCITY PROFILES AT  $x=1.0m$

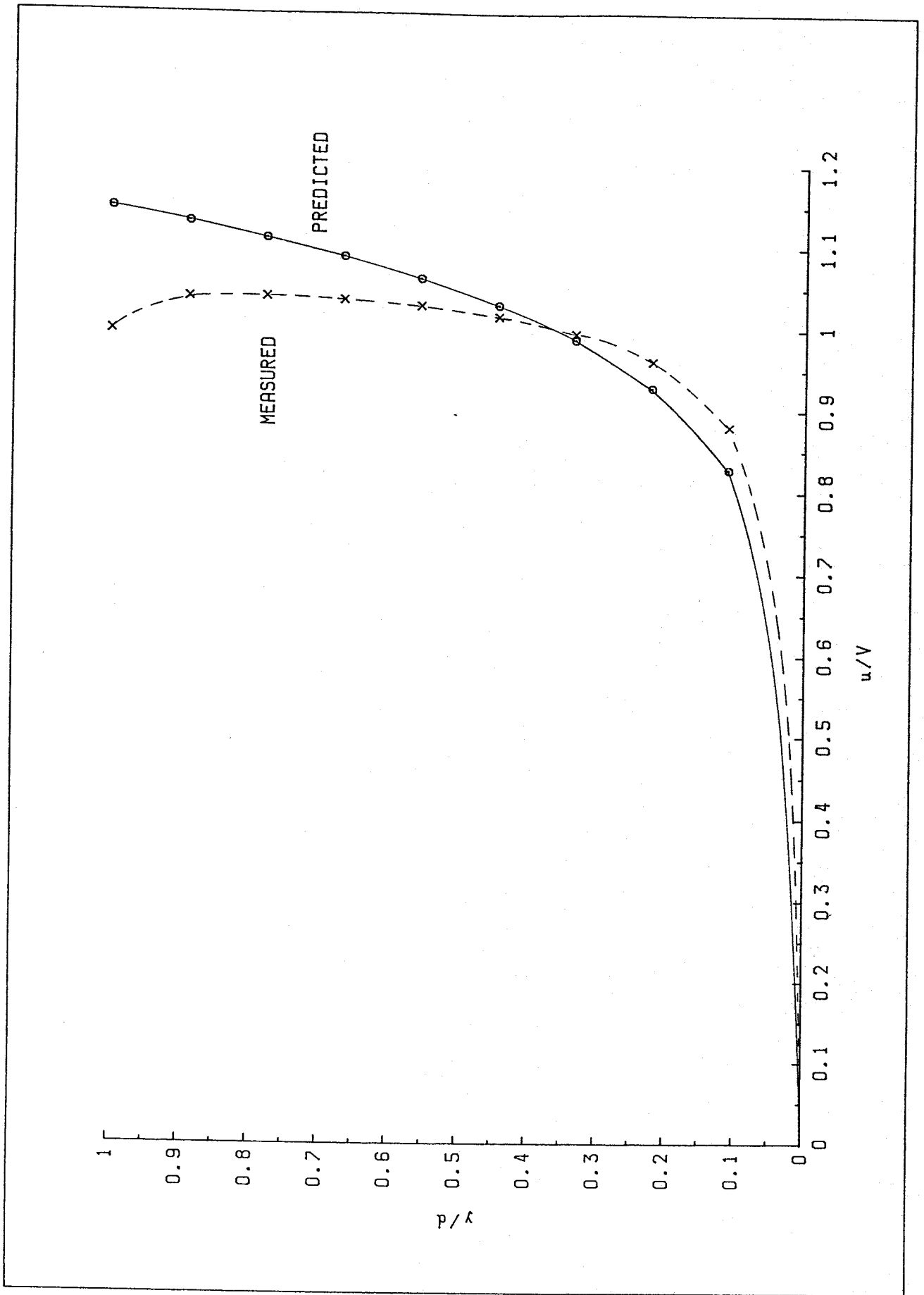


FIG 7 MEASURED AND PREDICTED VELOCITY PROFILES AT  $x=1.5\text{m}$

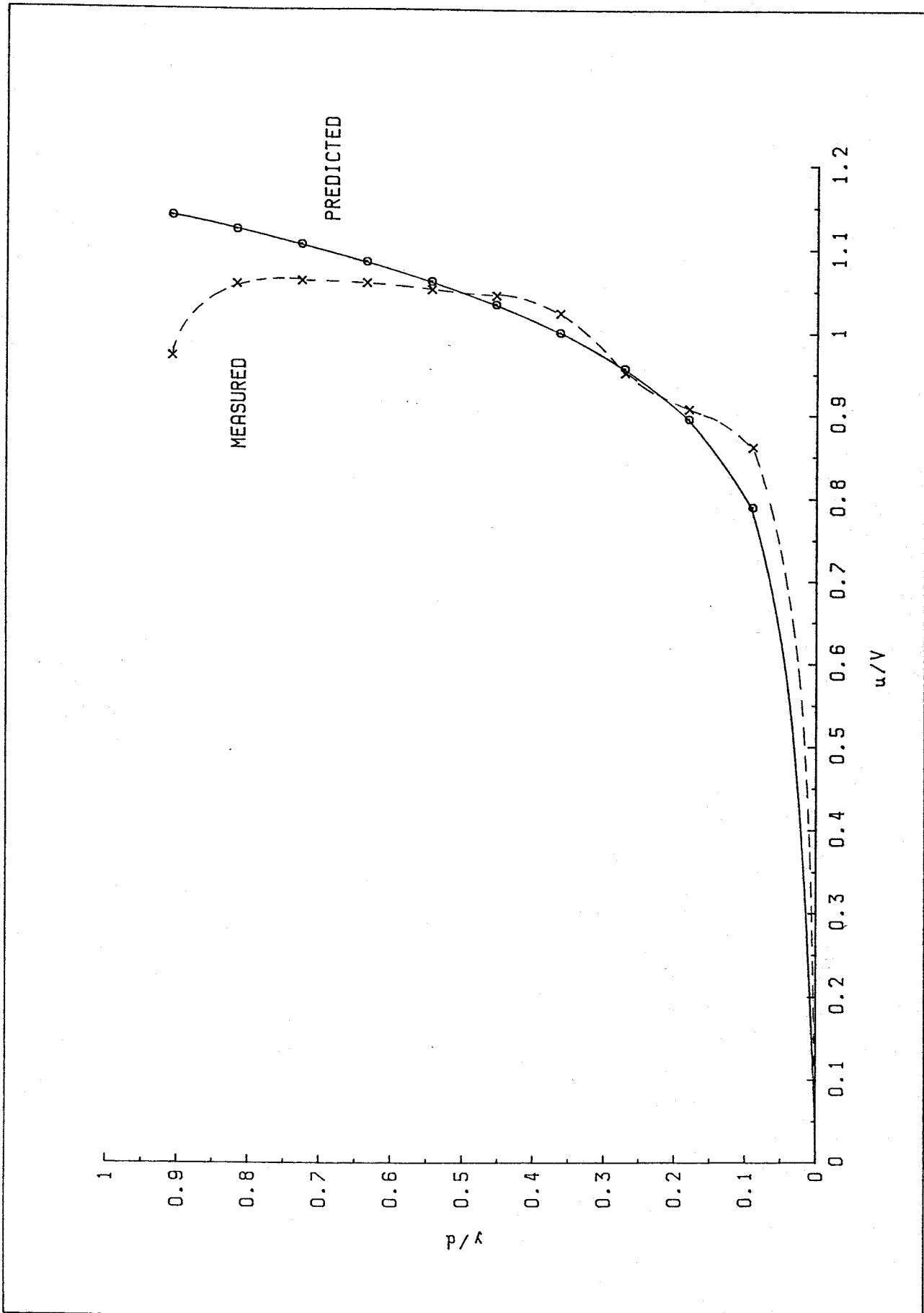
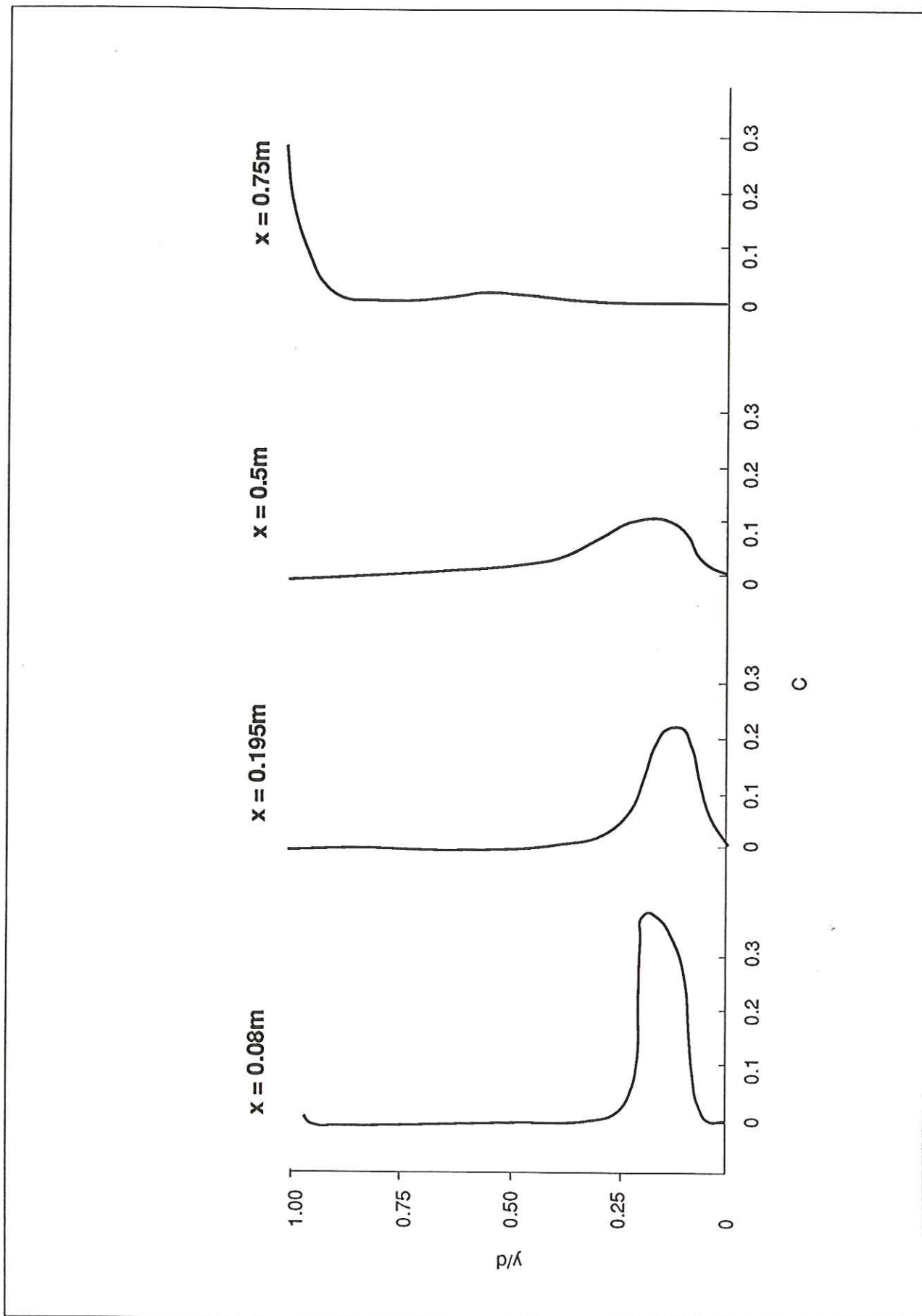


FIG 8 MEASURED AND PREDICTED VELOCITY PROFILES AT  $x=2.0m$



**Fig 9 Gas concentration profiles at  $x = 0.08\text{m}$ ,  $0.195\text{m}$ ,  $0.5\text{m}$  and  $0.75\text{m}$**

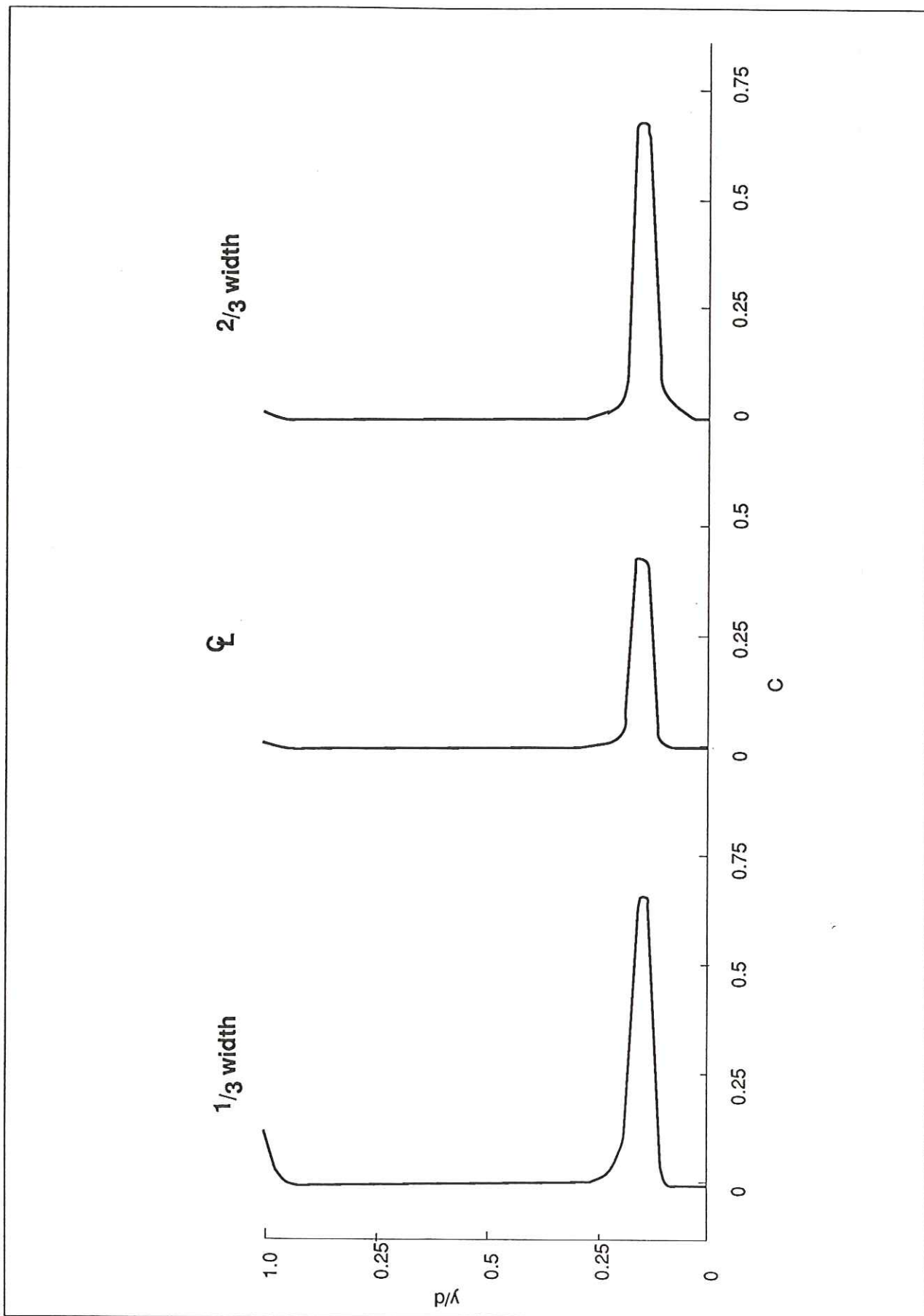


Fig 10 Transverse variation in gas concentration profiles at  $x = 0.08\text{m}$

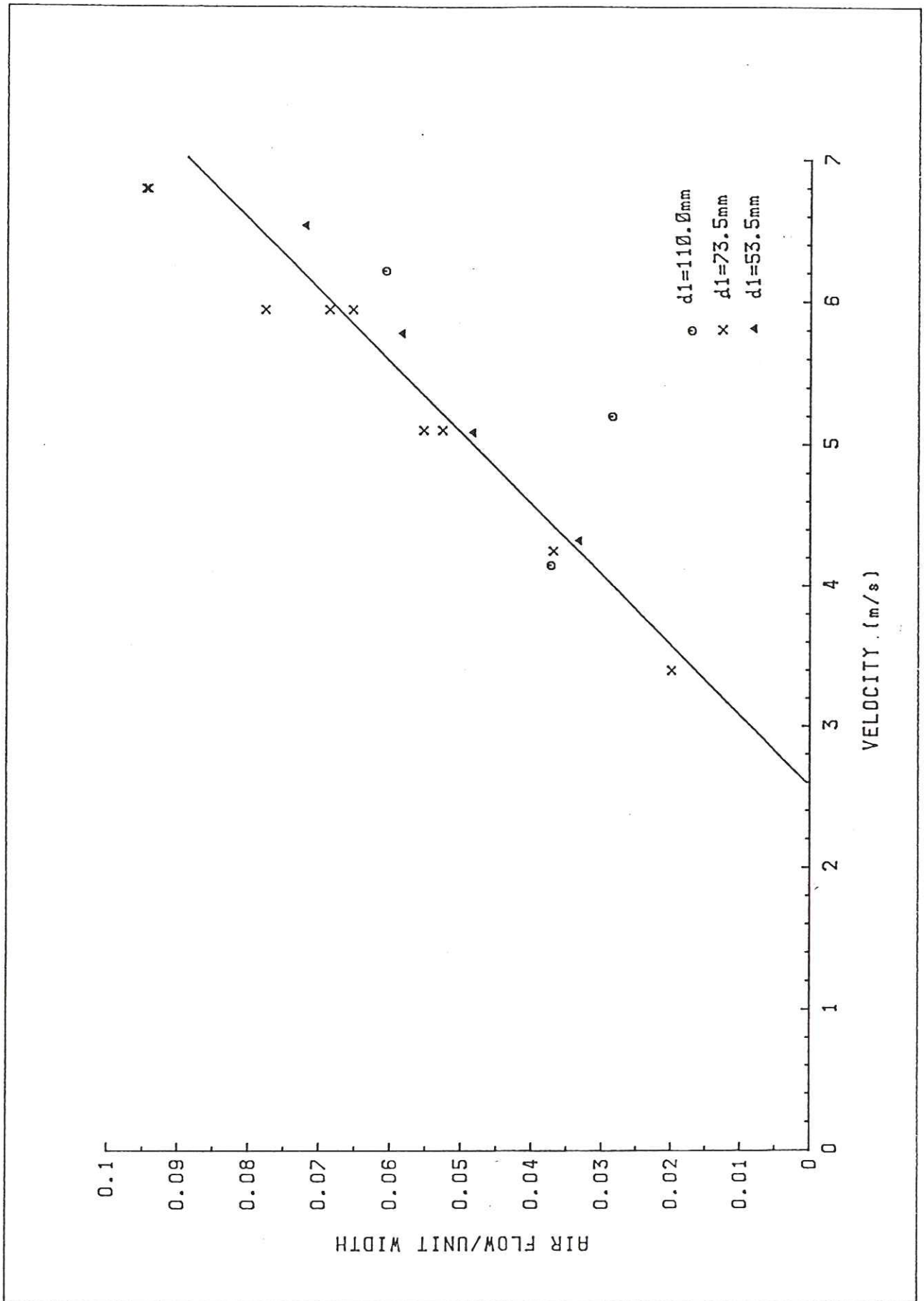


FIG 11 AIR DEMAND V's VELOCITY FOR AERATOR 1  
 VALVE SETTING 0 ; FLUME SLOPE 15.5 DEGREES

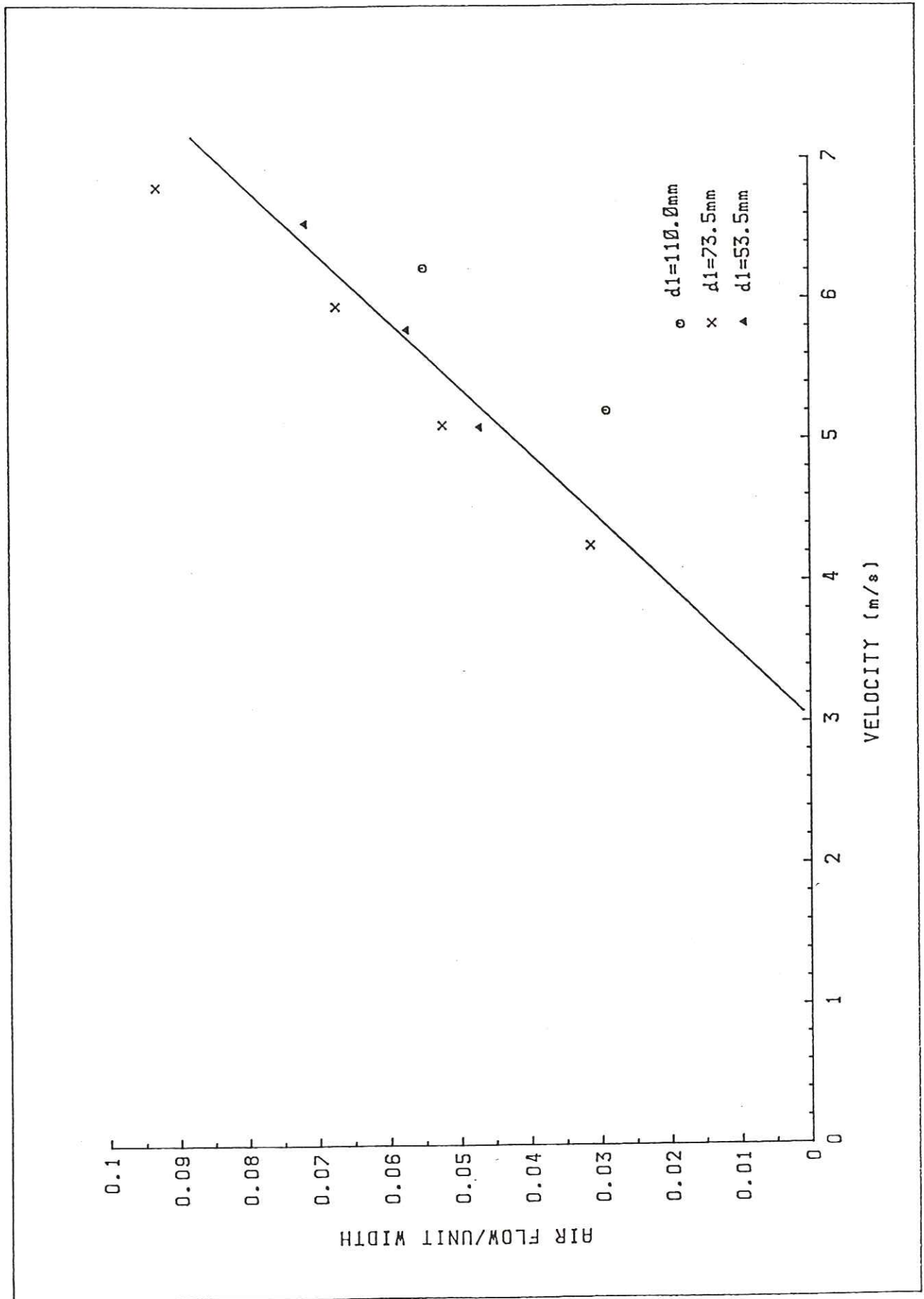


FIG 12 AIR DEMAND V'S VELOCITY FOR AERATOR 1  
VALVE SETTING 2 ; FLUME SLOPE 15.5 DEGREES

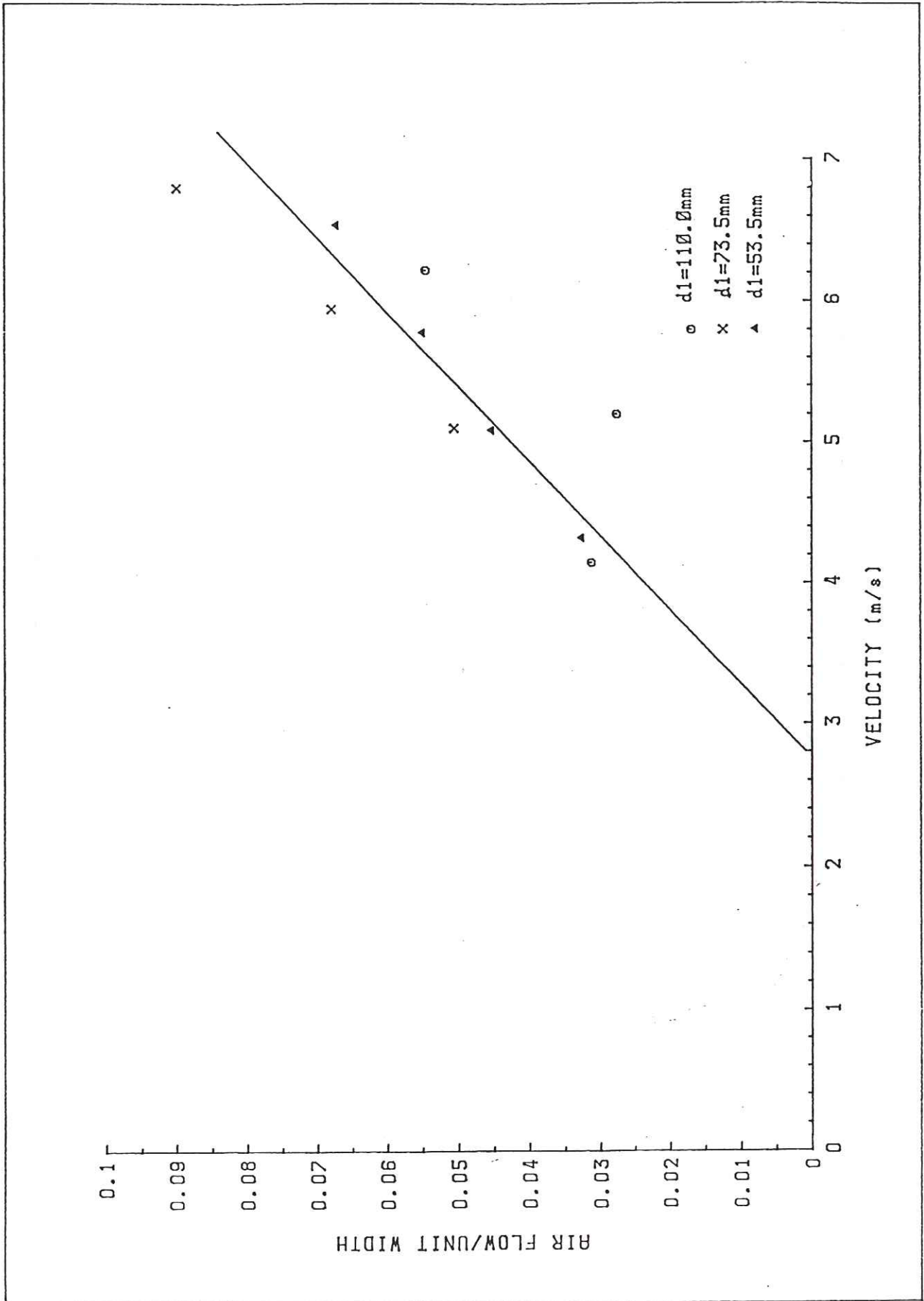


FIG 13 AIR DEMAND V's VELOCITY FOR AERATOR 1  
 VALVE SETTING 3 ; FLUME SLOPE 15.5 DEGREES

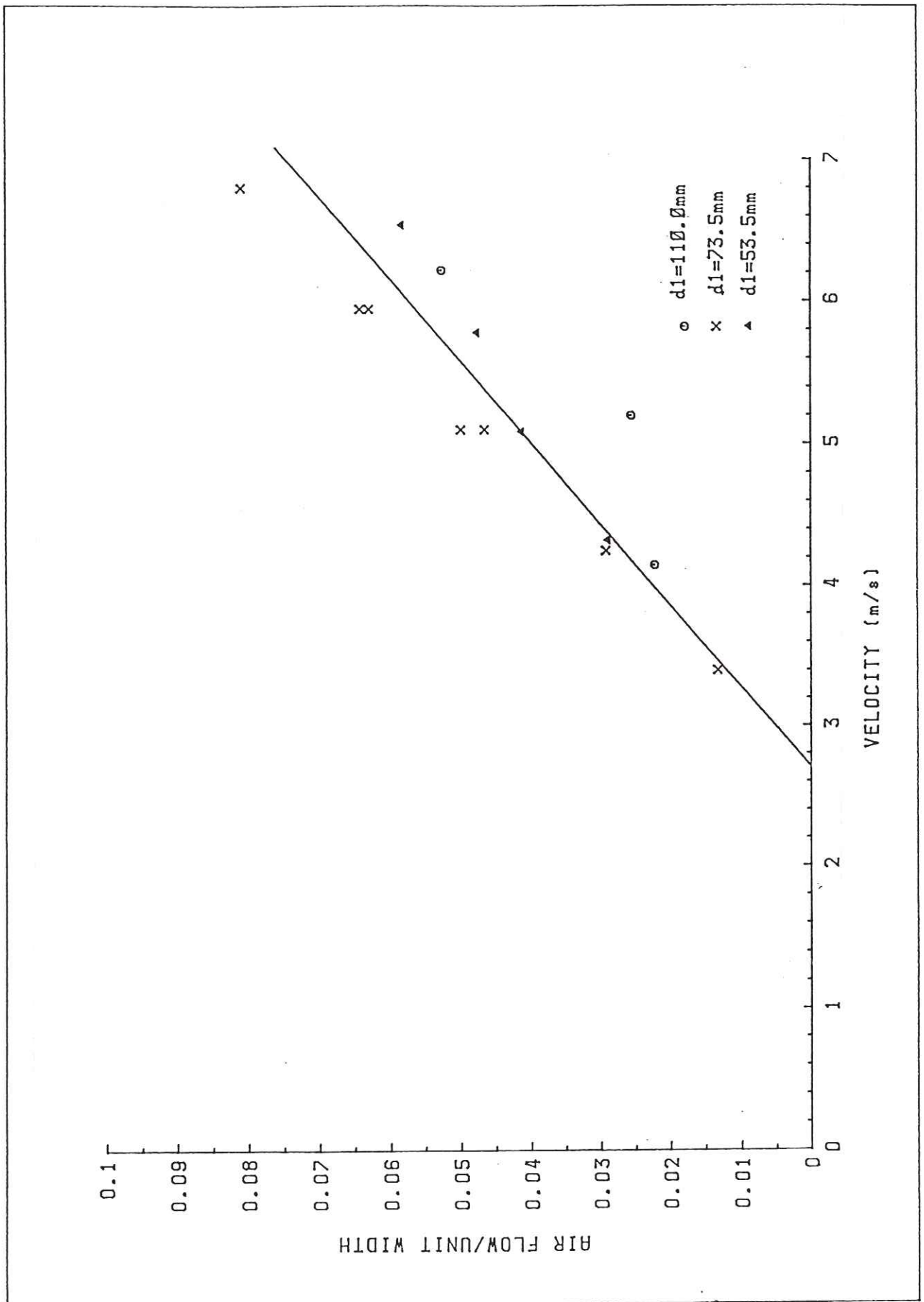


FIG 14 AIR DEMAND V'S VELOCITY FOR AERATOR 1  
VALVE SETTING 4 ; FLUME SLOPE 15.5 DEGREES

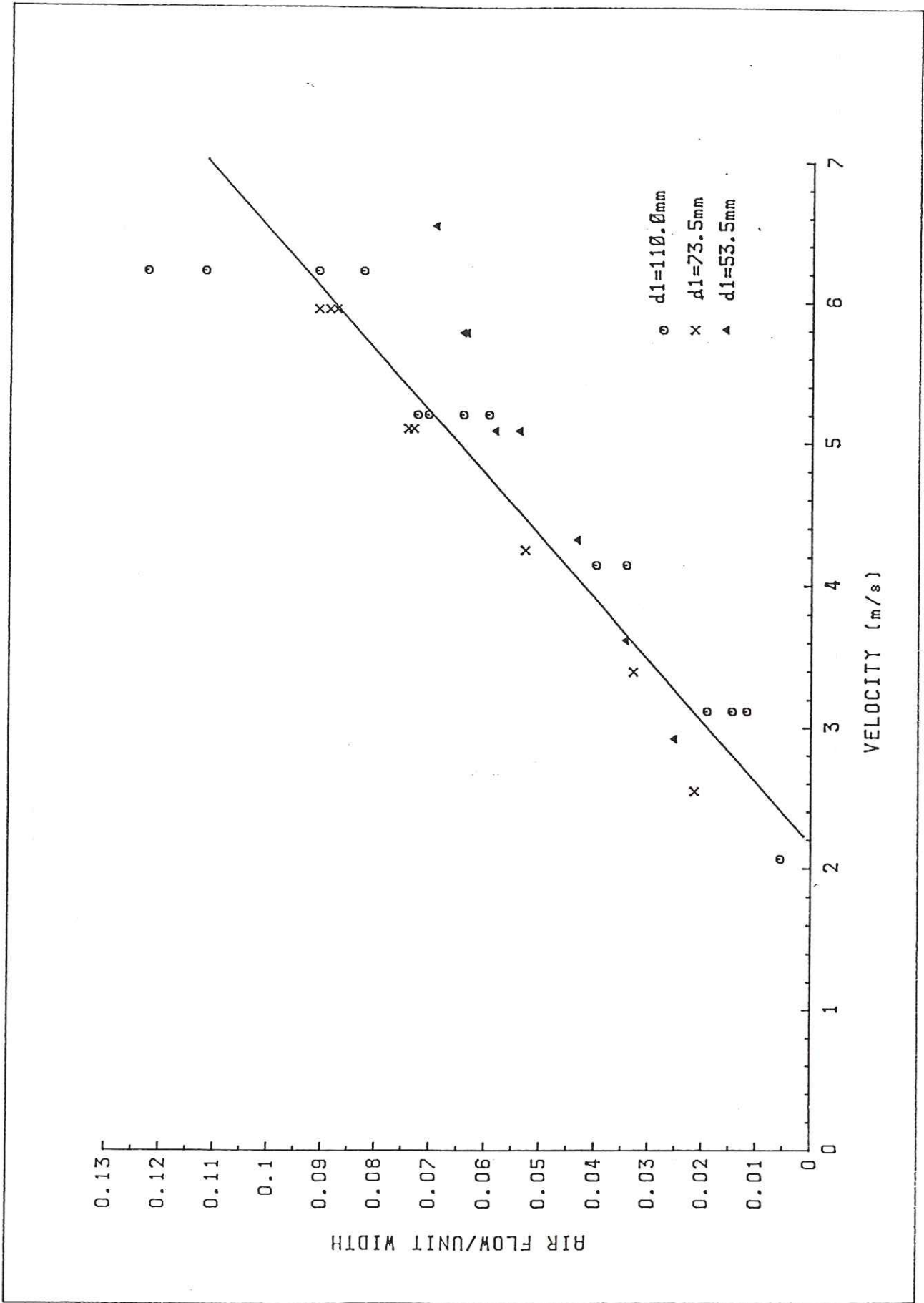


FIG 15 AIR DEMAND  $V$ 's VELOCITY FOR AERATOR 1  
 VALVE SETTING  $\emptyset$  ; FLUME SLOPE 45.3 DEGREES

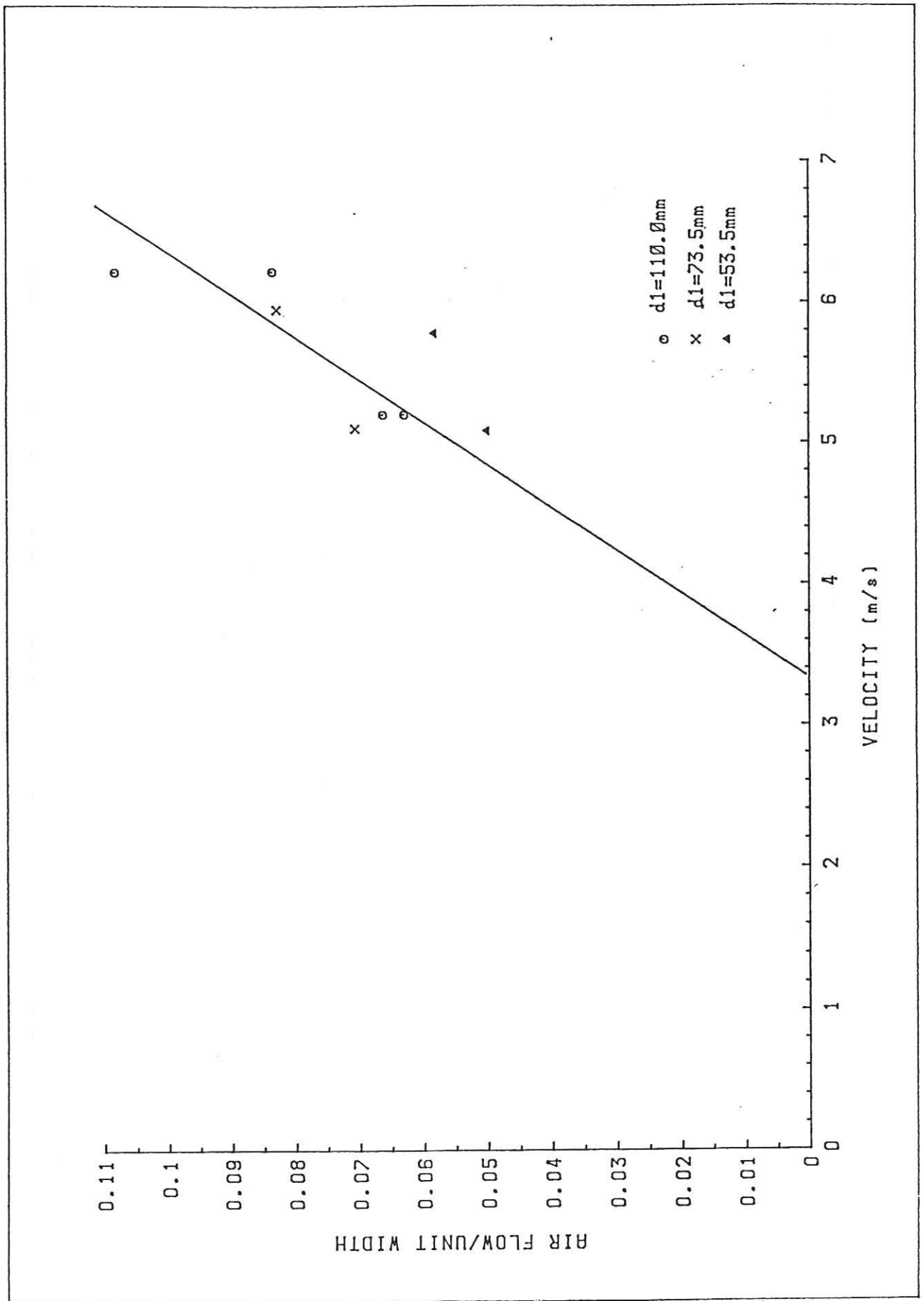


FIG 16 AIR DEMAND V's VELOCITY FOR AERATOR 1  
 VALVE SETTING 3 ; FLUME SLOPE 45.3 DEGREES

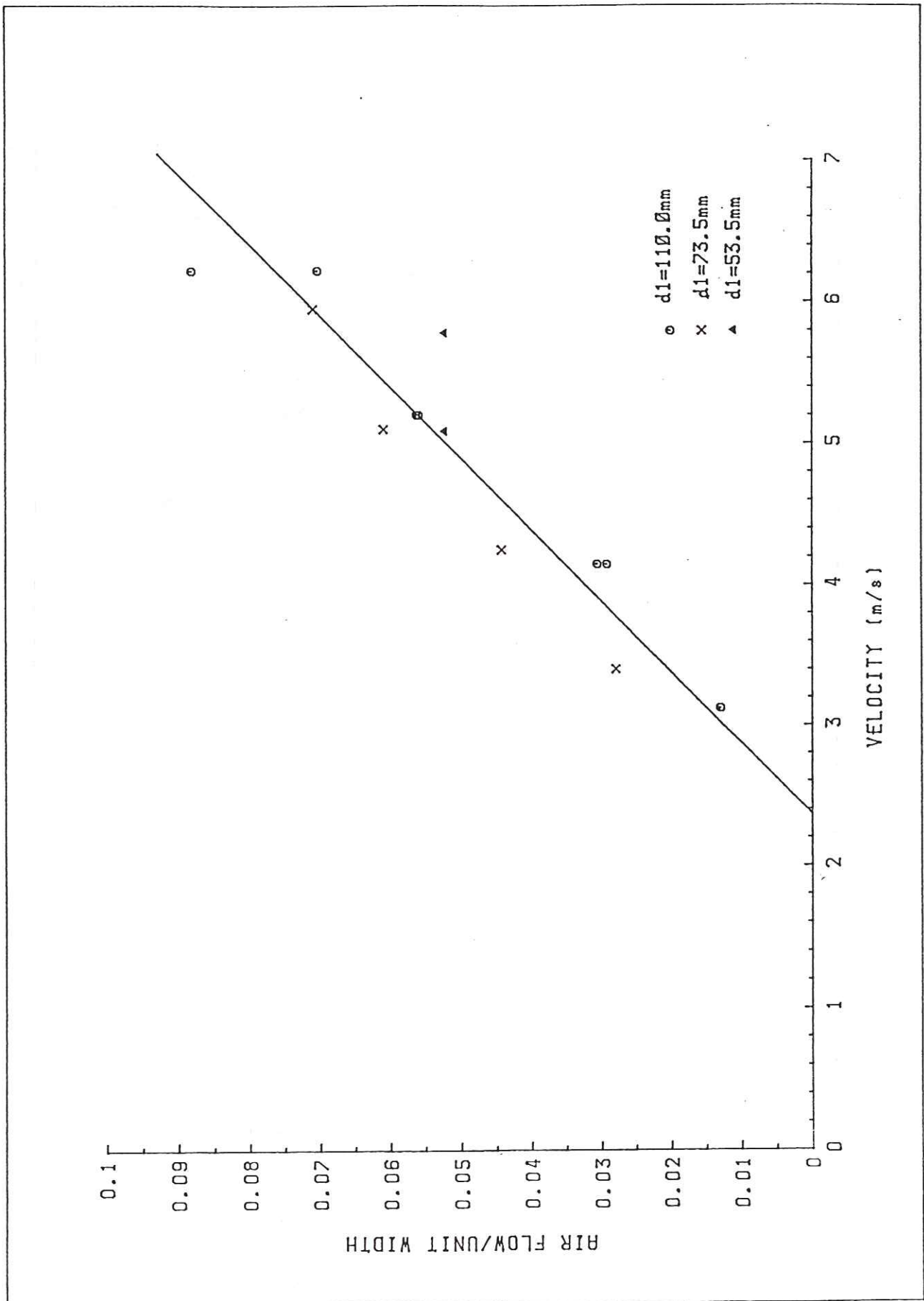


FIG 17 AIR DEMAND V'S VELOCITY FOR AERATOR 1  
 VALVE SETTING 4; FLUME SLOPE 45.3 DEGREES

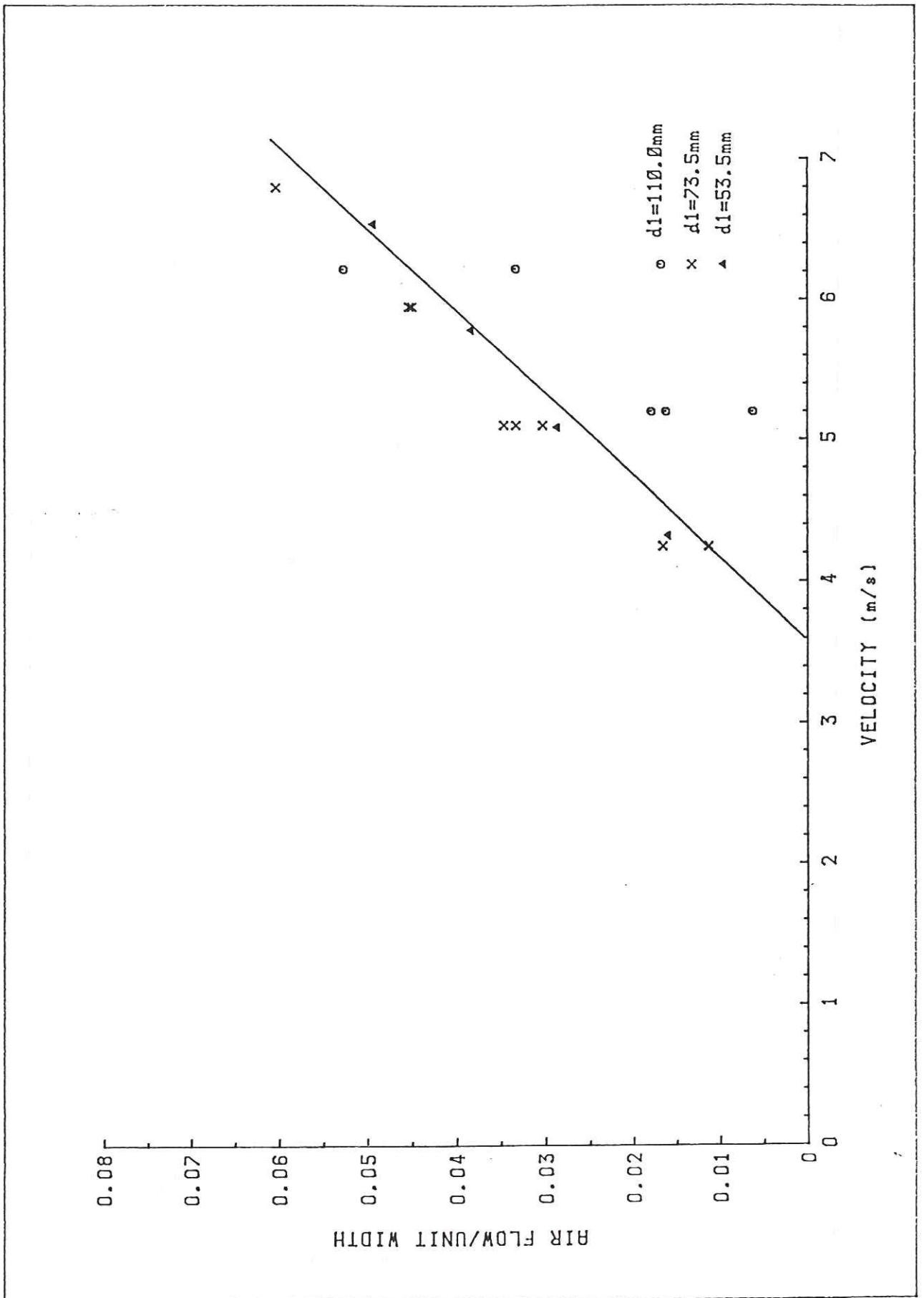


FIG 18 AIR DEMAND V'S VELOCITY FOR AERATOR 3  
 VALVE SETTING 0 ; FLUME SLOPE 15.5 DEGREES

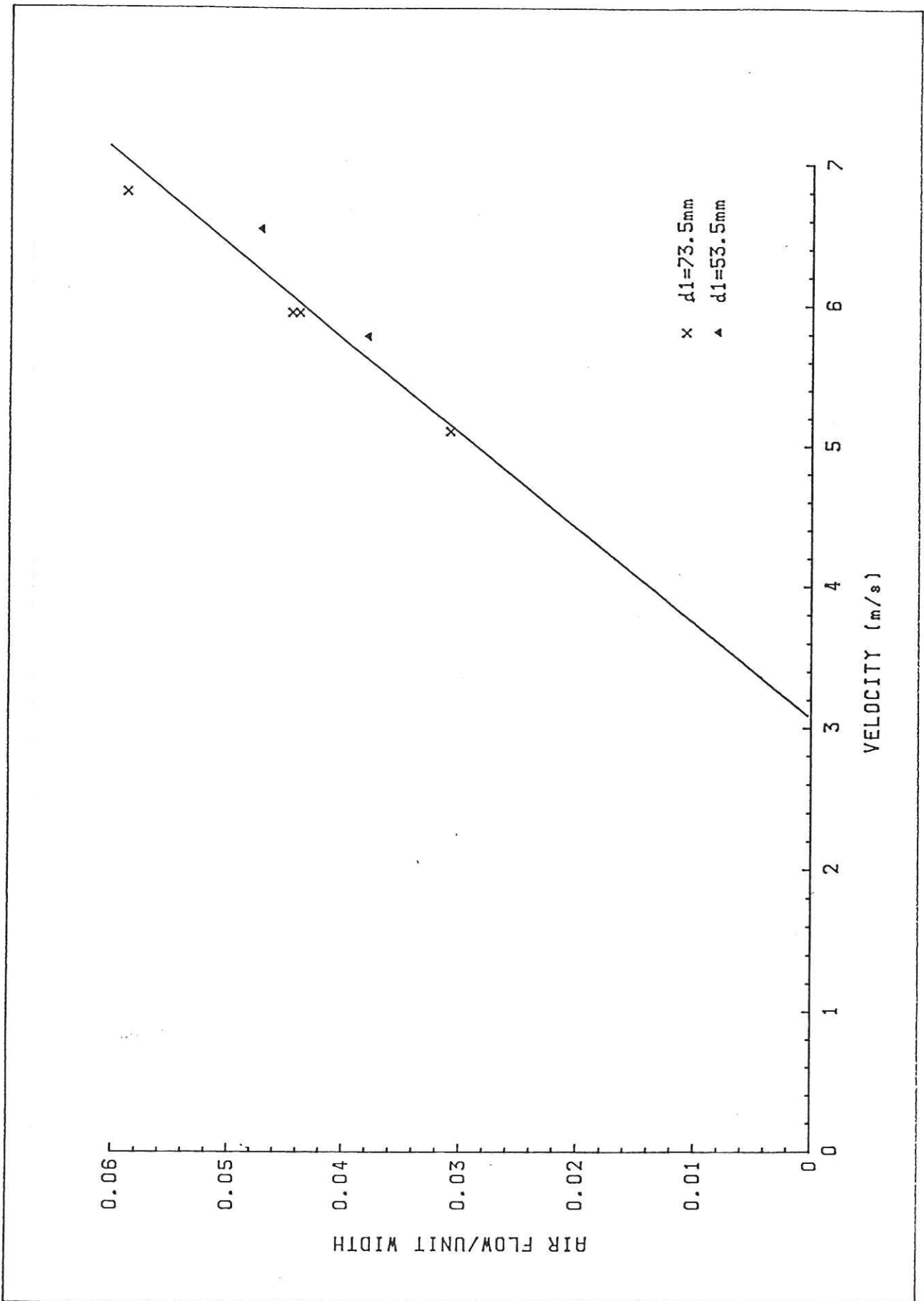
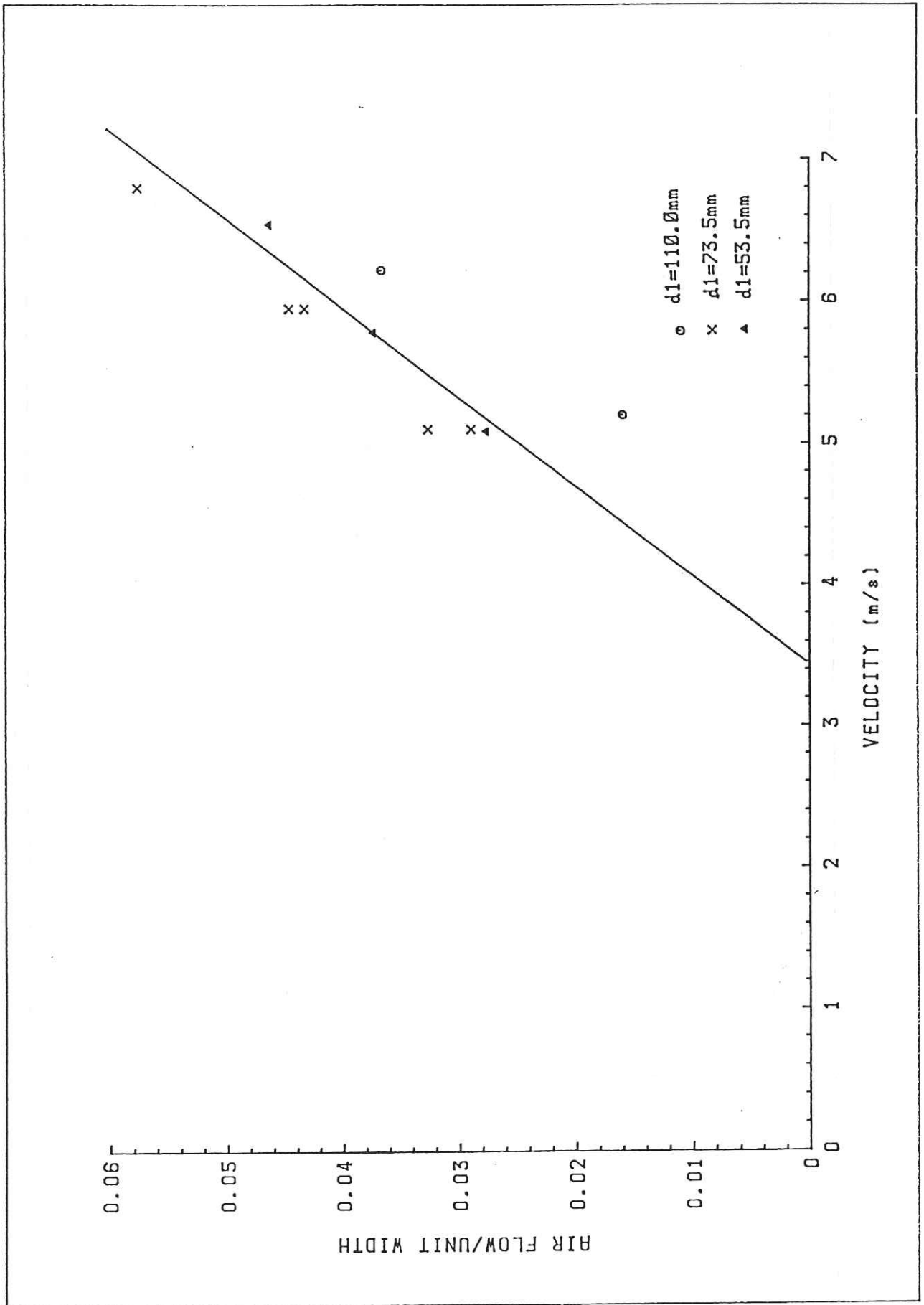


FIG 19 AIR DEMAND V's VELOCITY FOR AERATOR 3  
 VALVE SETTING 2 ; FLUME SLOPE 15.5 DEGREES



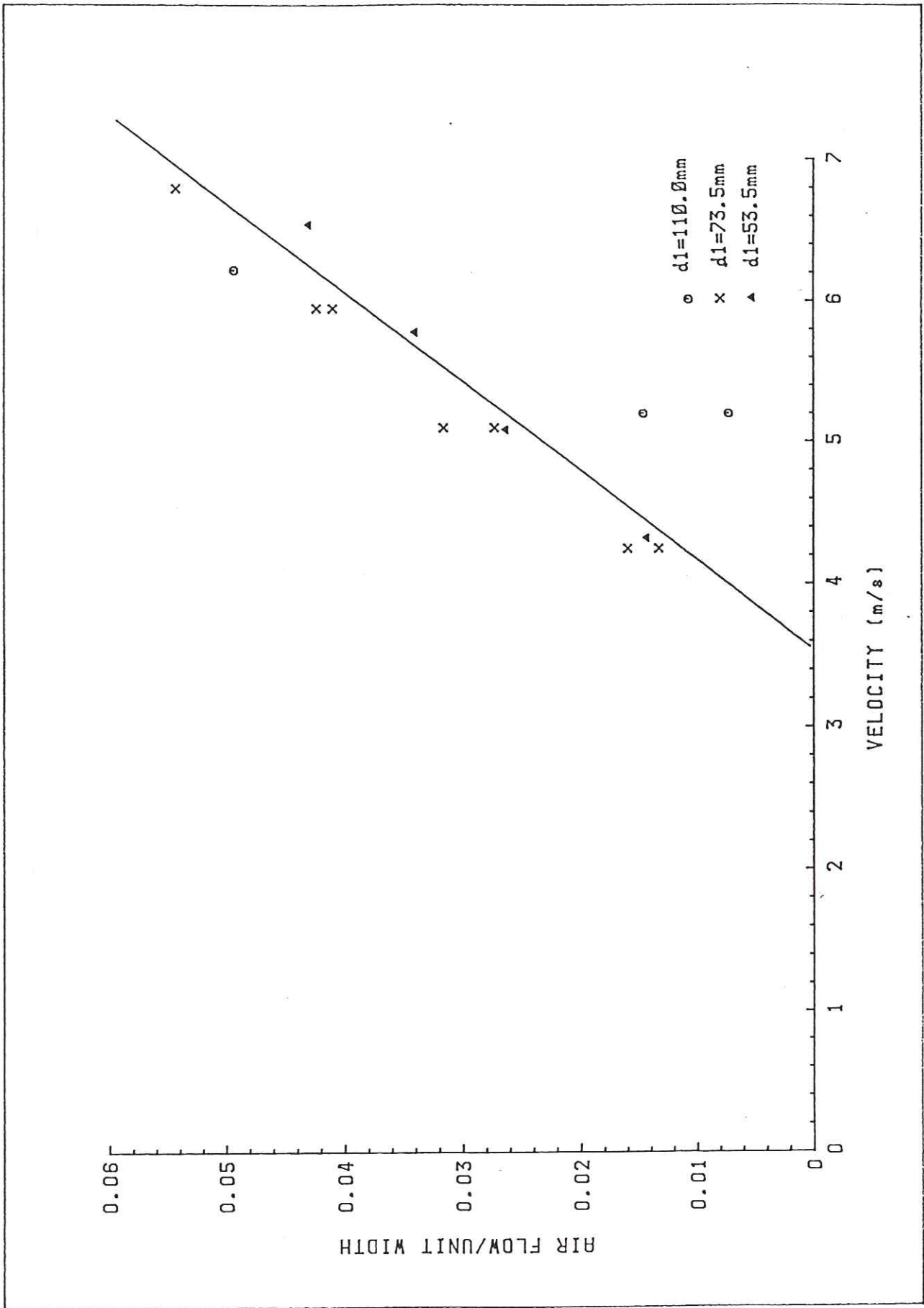


FIG 21 AIR DEMAND V's VELOCITY FOR AERATOR 3  
 VALVE SETTING 4 ; FLUME SLOPE 15.5 DEGREES

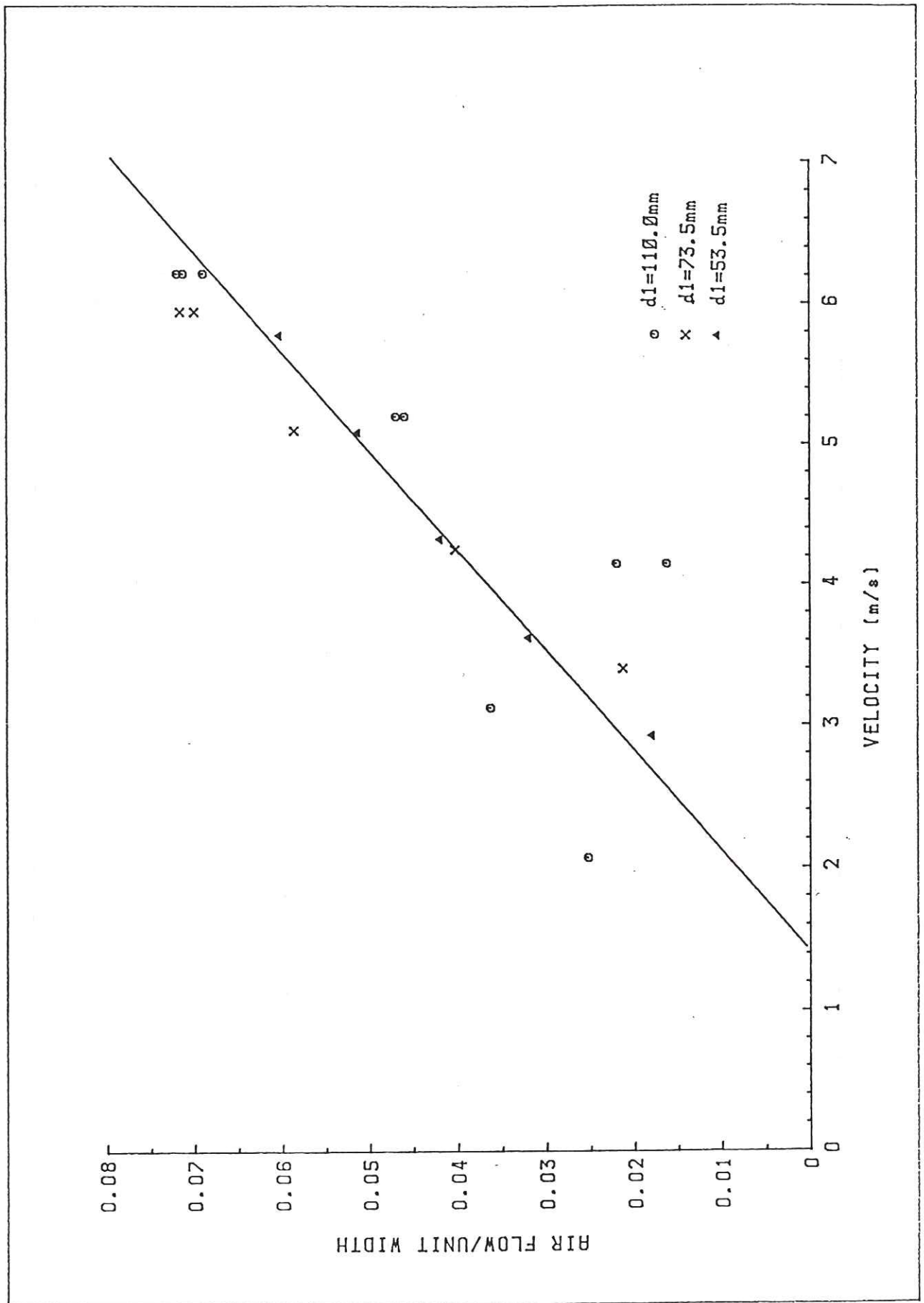


FIG 22 AIR DEMAND V'S VELOCITY FOR AERATOR 3  
 VALVE SETTING Ø ; FLUME SLOPE 45.3 DEGREES

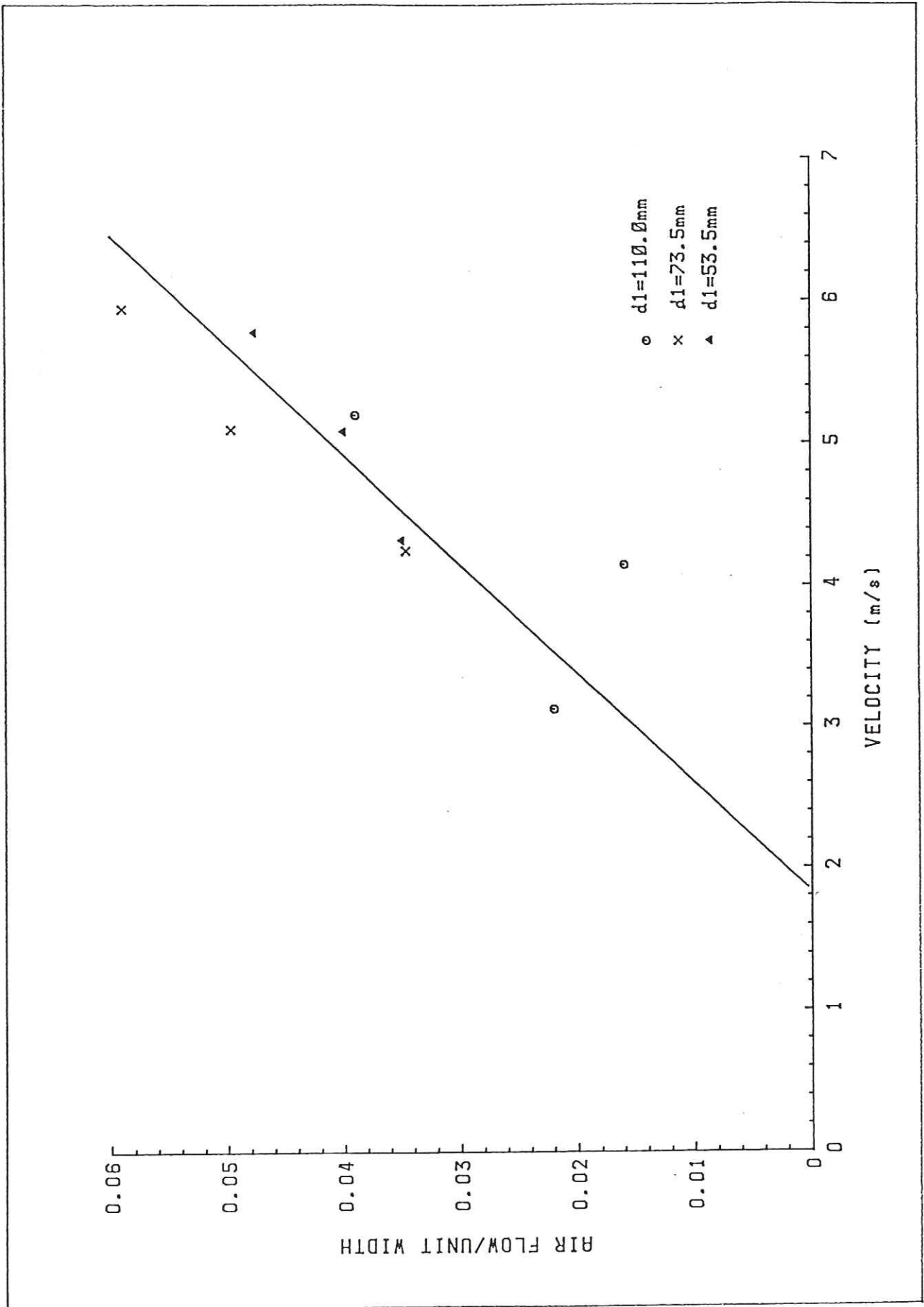


FIG 23 AIR DEMAND  $V$ 's VELOCITY FOR AERATOR 3  
VALVE SETTING 4 ; FLUME SLOPE 45.3 DEGREES

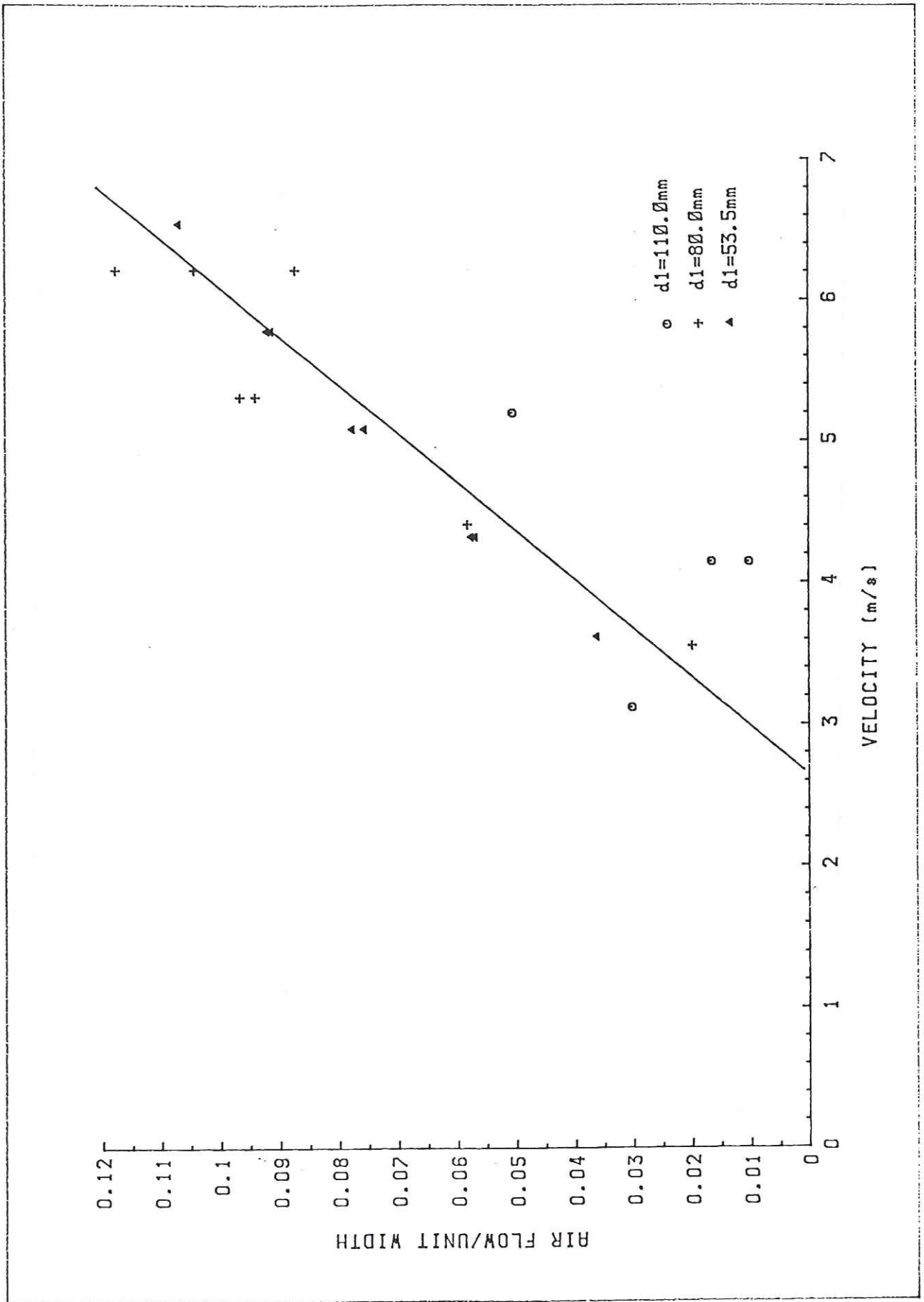


FIG 24 AIR DEMAND V'S VELOCITY FOR AERATOR 7  
 VALVE SETTING 0 ; FLUME SLOPE 15.5 DEGREES

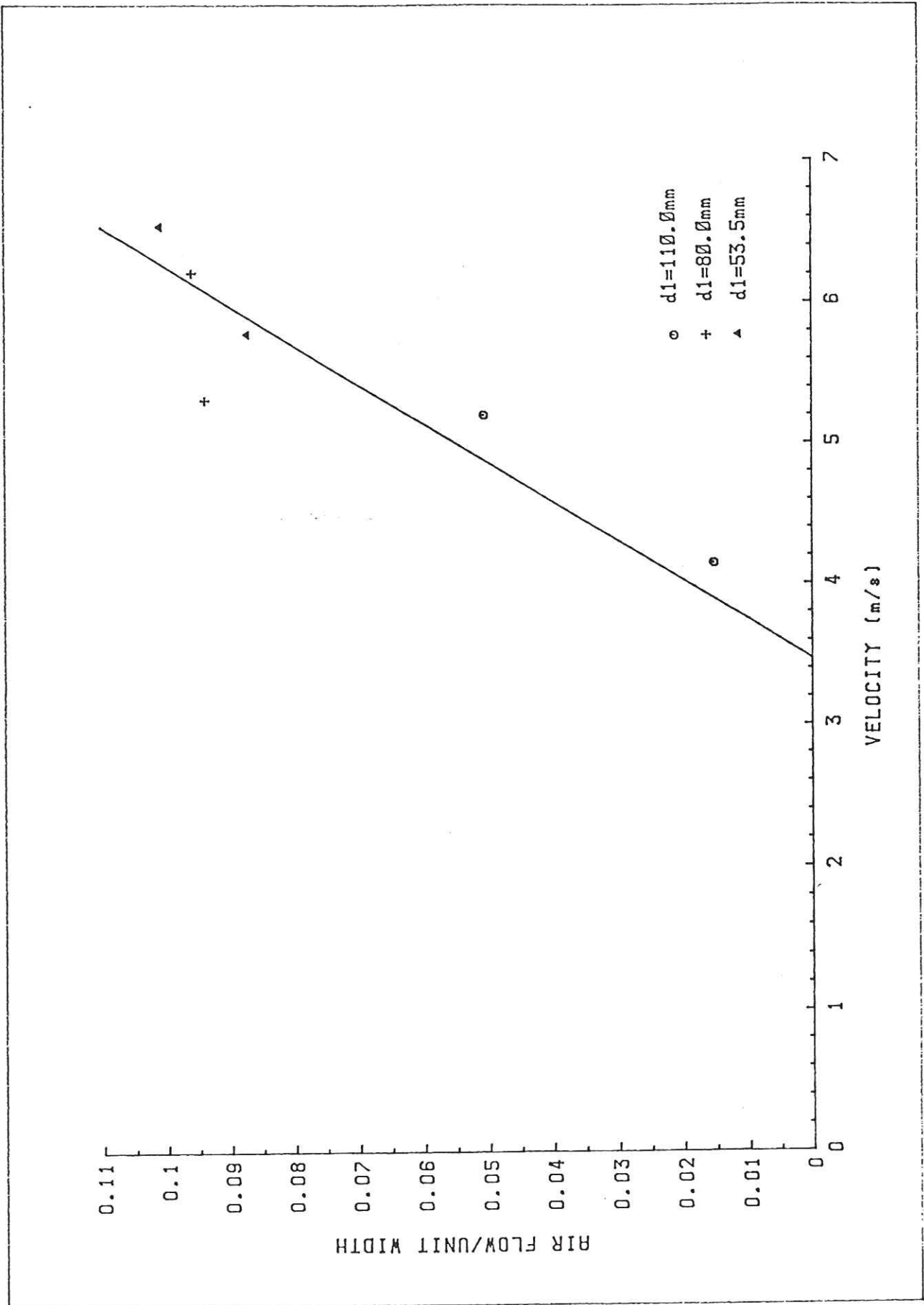


FIG 25 AIR DEMAND V's VELOCITY FOR AERATOR 7  
 VALVE SETTING 2 ; FLUME SLOPE 15.5 DEGREES

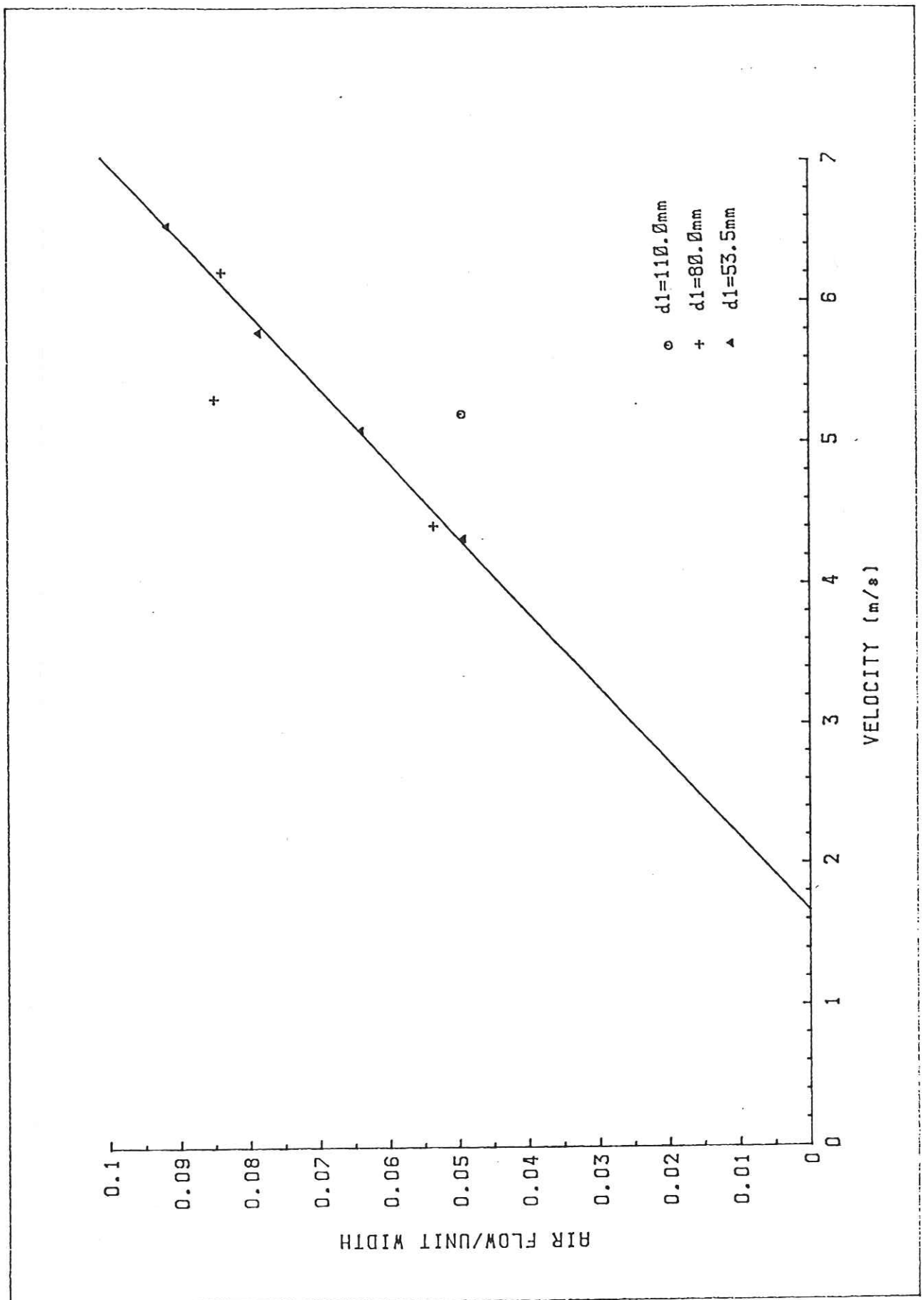


FIG 26 AIR DEMAND V's VELOCITY FOR AERATOR 7  
 VALVE SETTING 3 ; FLUME SLOPE 15.5 DEGREES

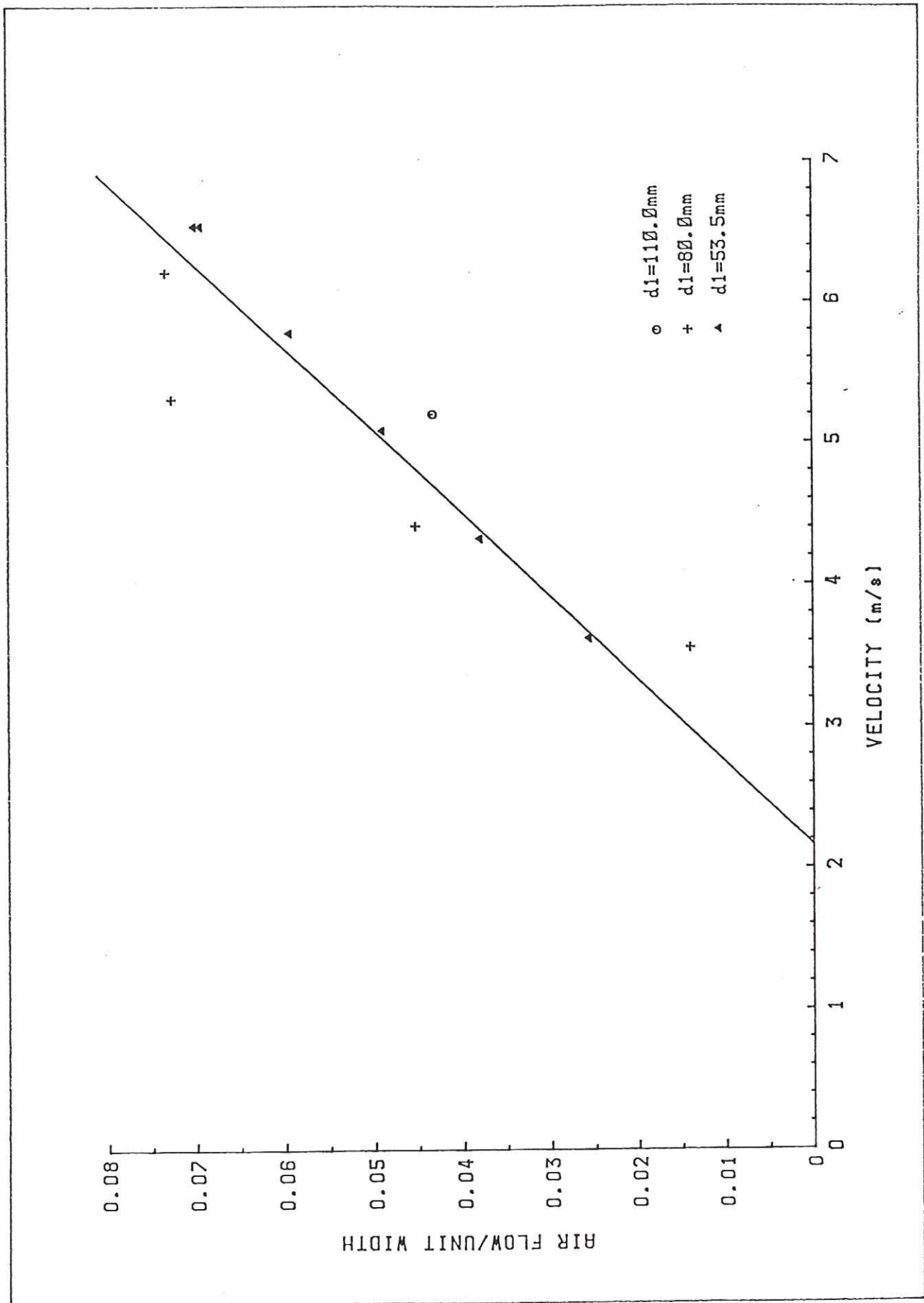


FIG 27 AIR DEMAND V' s VELOCITY FOR AERATOR 7.  
 VALVE SETTING 4 ; FLUME SLOPE 15.5 DEGREES

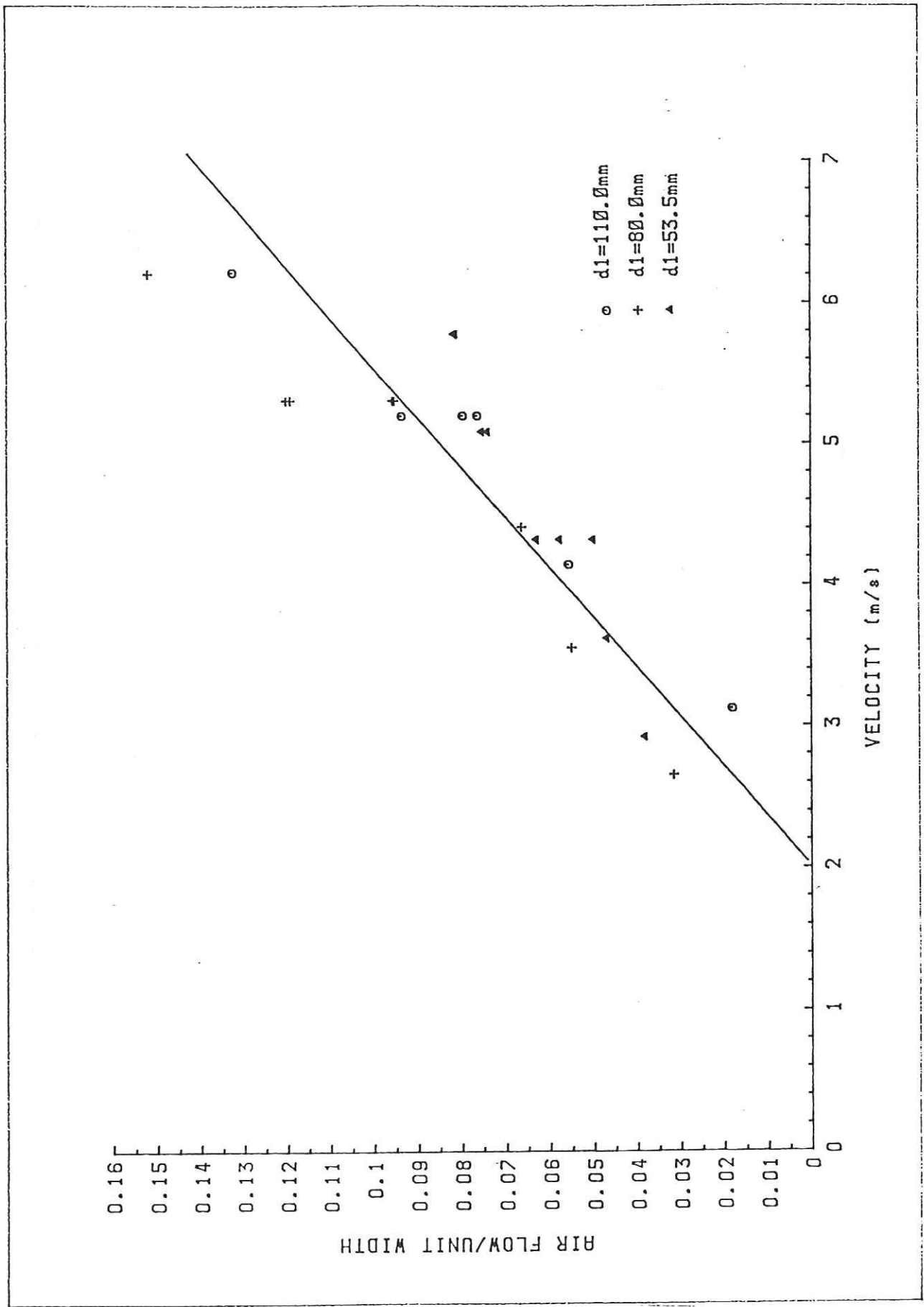


FIG 28 AIR DEMAND V' s VELOCITY FOR AERATOR 7  
 VALVE SETTING 0 ; FLUME SLOPE 45.3 DEGREES

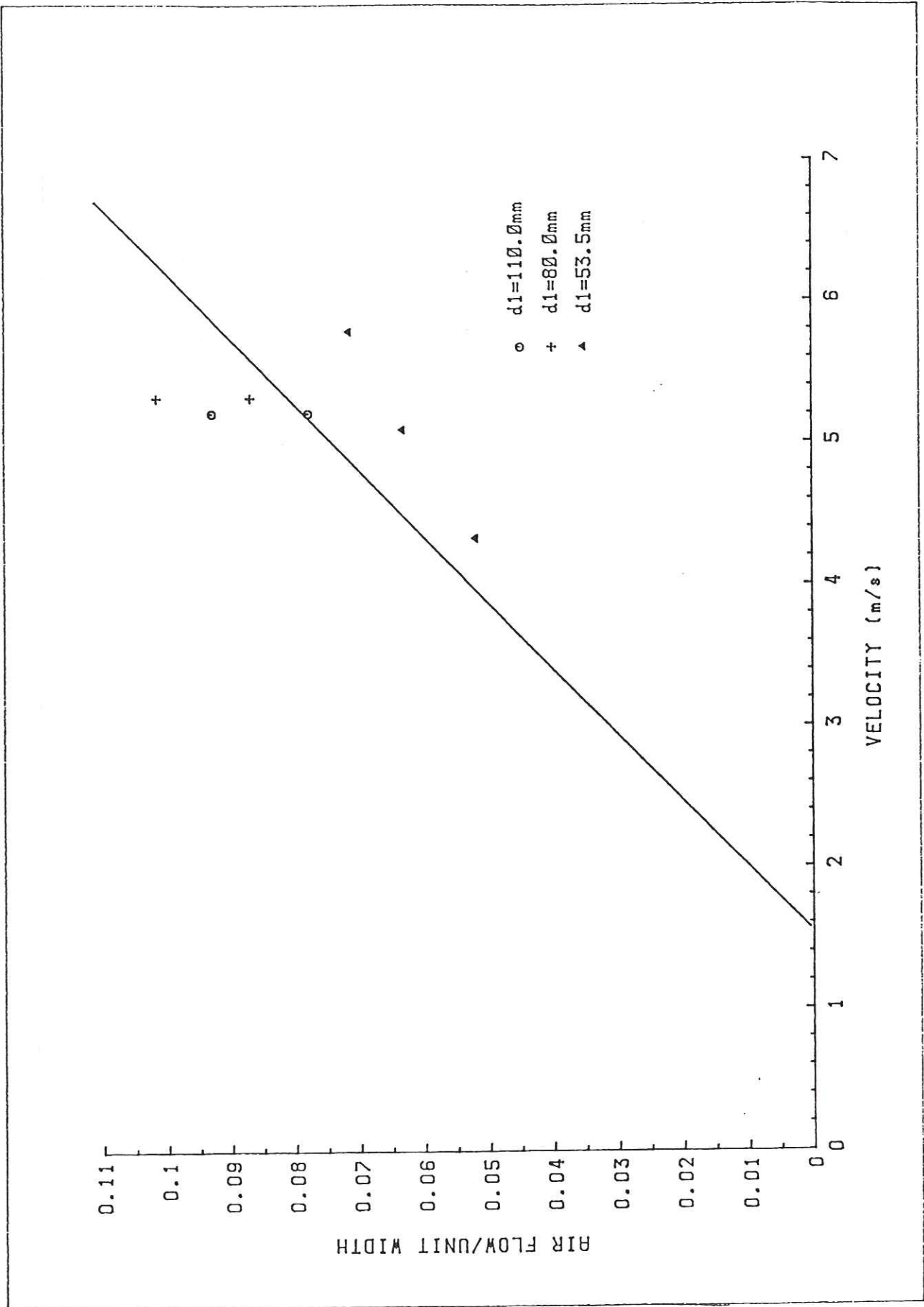


FIG 29 AIR DEMAND  $V$ 's VELOCITY FOR AERATOR 7  
 VALVE SETTING 3 ; FLUME SLOPE 45.3 DEGREES

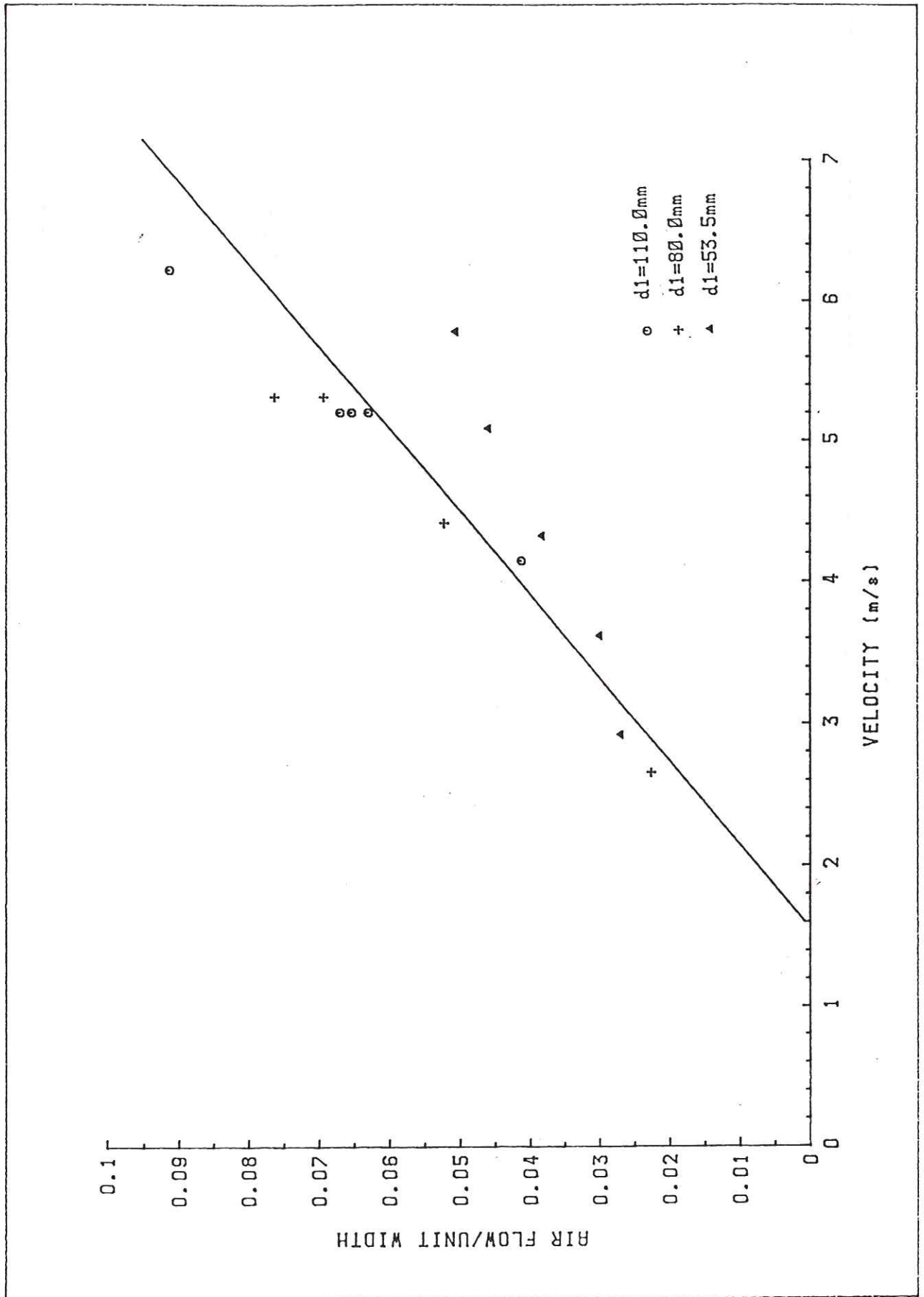


FIG 30 AIR DEMAND  $V$ 's VELOCITY FOR AERATOR 7  
 VALVE SETTING 4 ; FLUME SLOPE 45.3 DEGREES

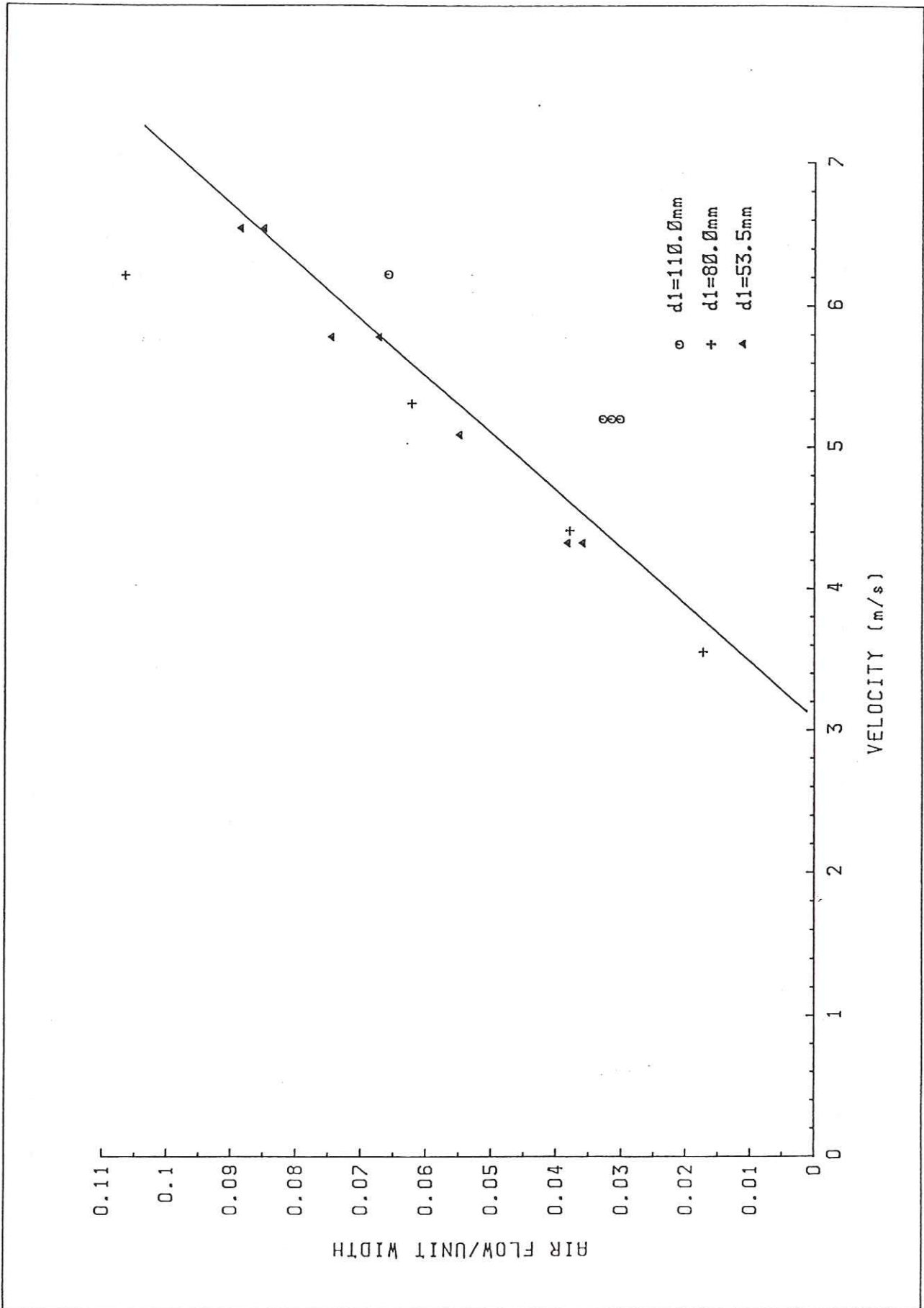


FIG 31 AIR DEMAND V's VELOCITY FOR AERATOR 9  
 VALVE SETTING Ø ; FLUME SLOPE 15.5 DEGREES

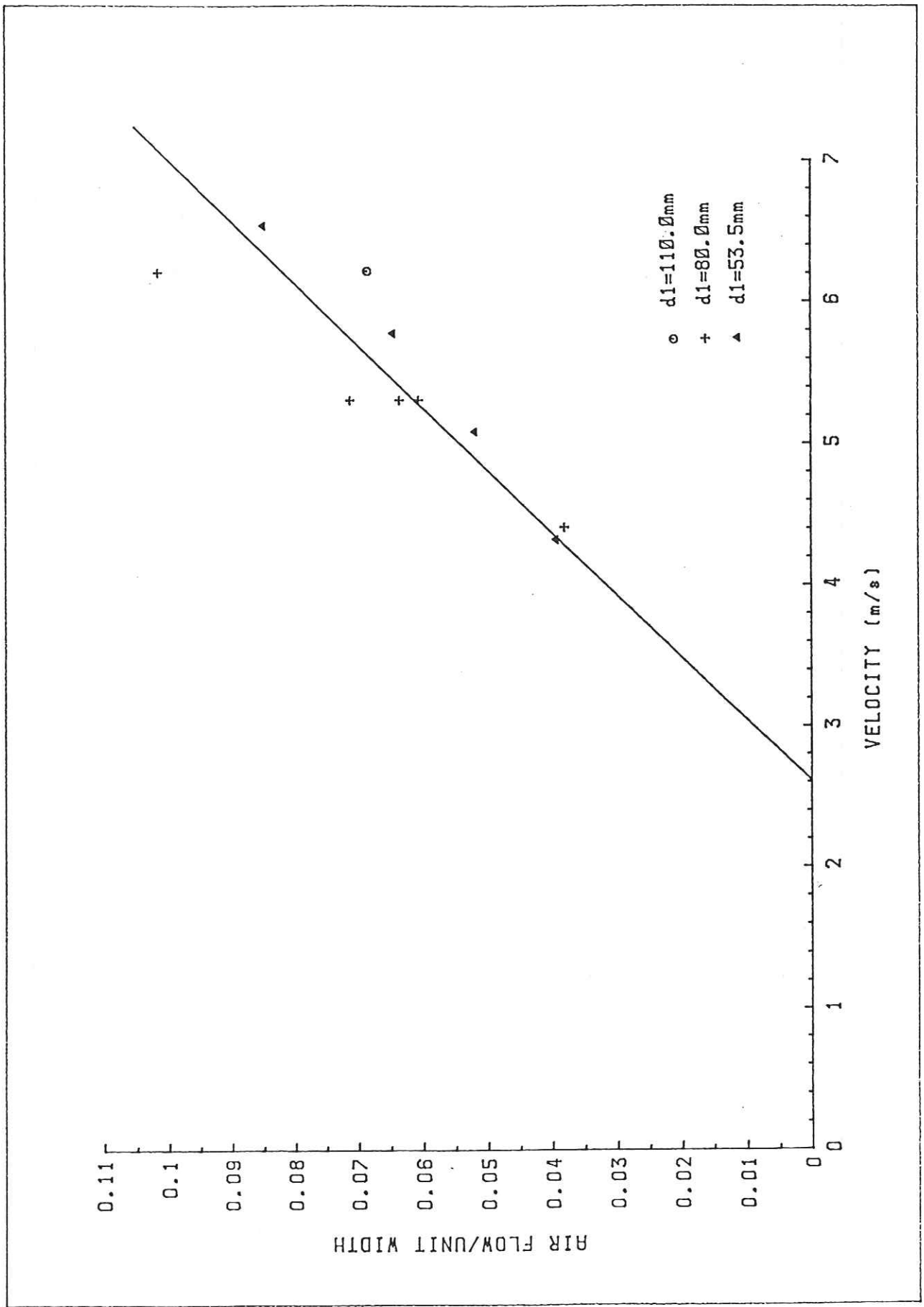


FIG 32 AIR DEMAND V's VELOCITY FOR AERATOR 9  
 VALVE SETTING 2 ; FLUME SLOPE 15.5 DEGREES

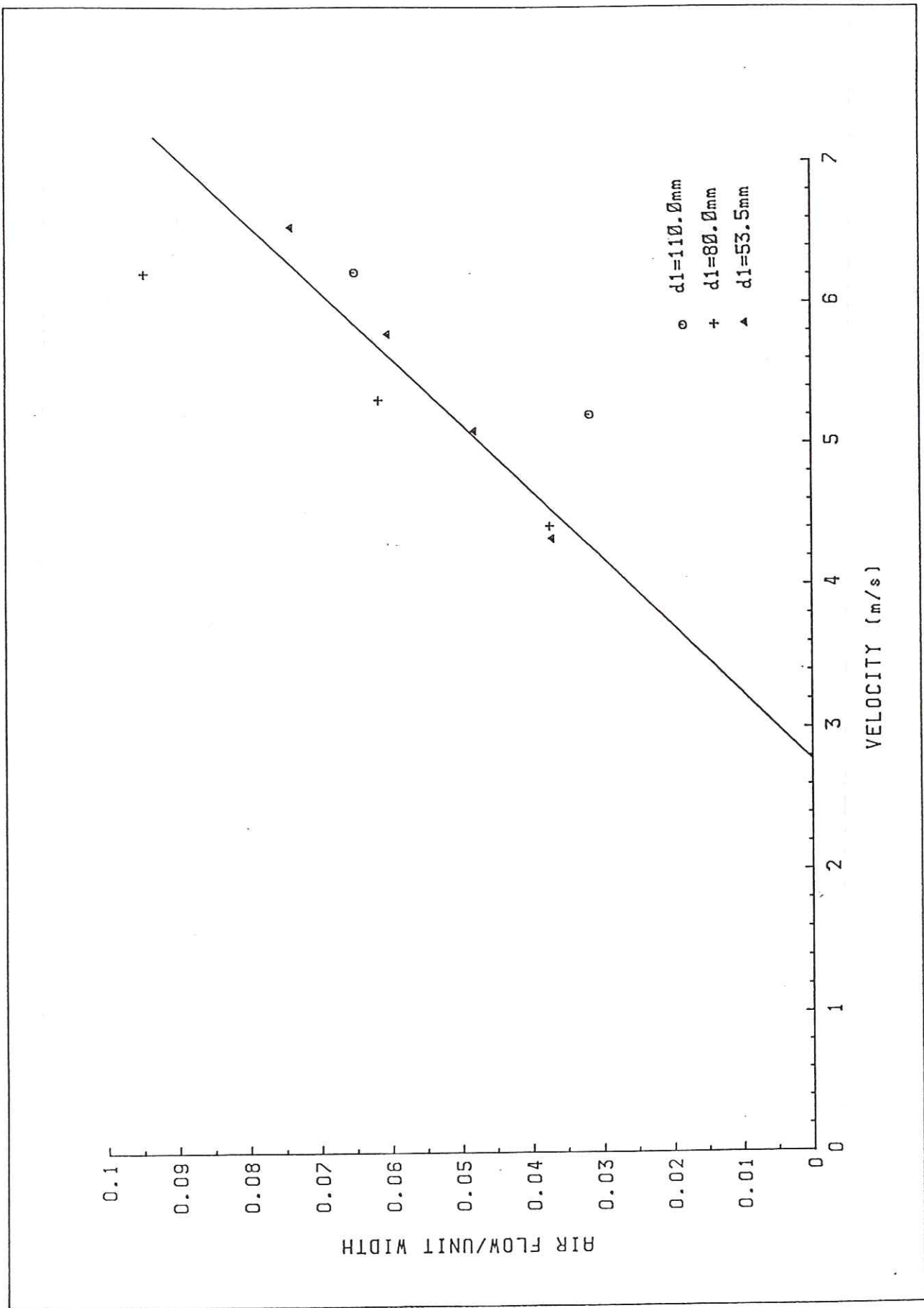


FIG 33 AIR DEMAND V's VELOCITY FOR AERATOR 9  
 VALVE SETTING 3 ; FLUME SLOPE 15.5 DEGREES

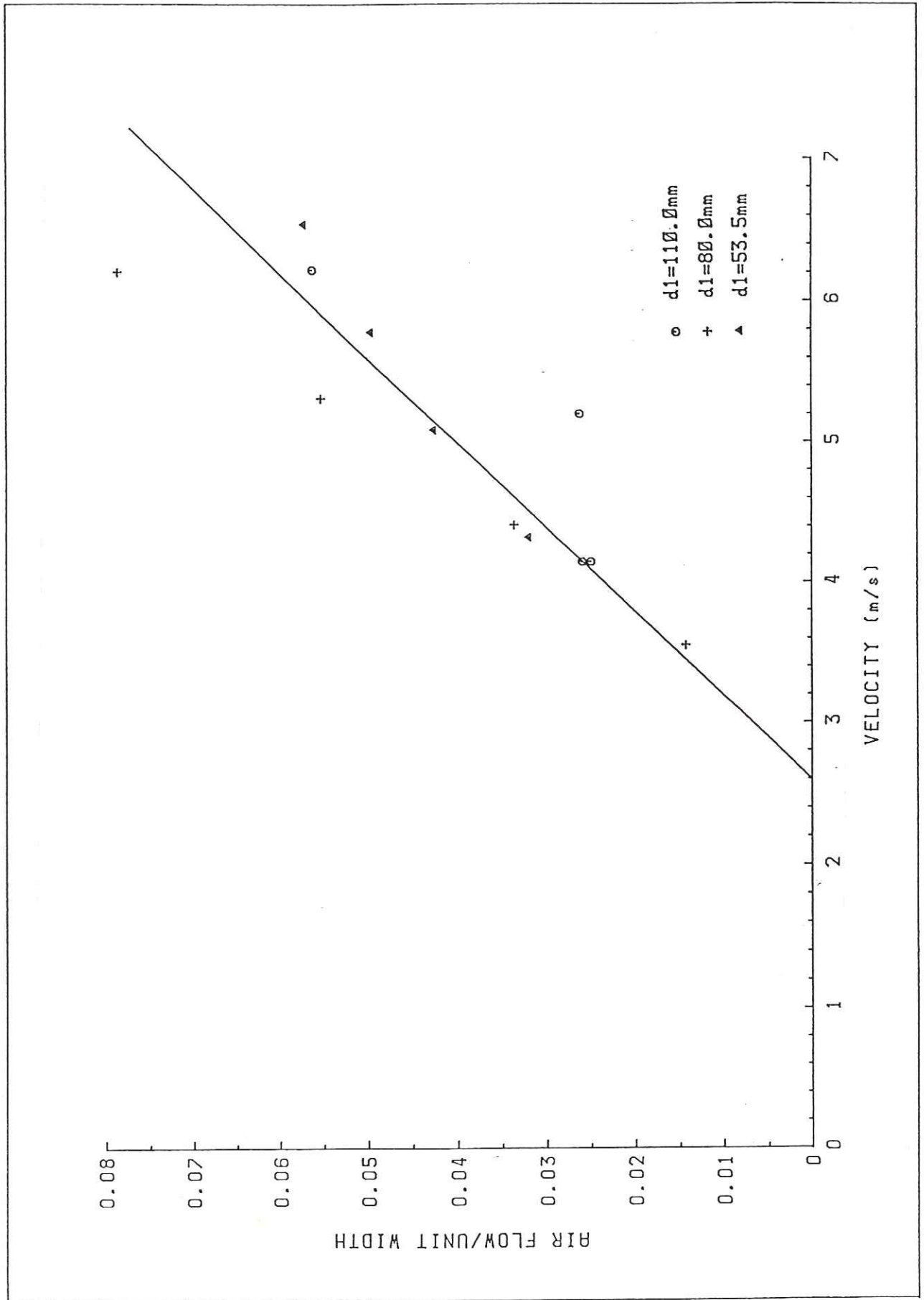


FIG 34 AIR DEMAND V's VELOCITY FOR AERATOR 9  
 VALVE SETTING 4 ; FLUME SLOPE 15.5 DEGREES

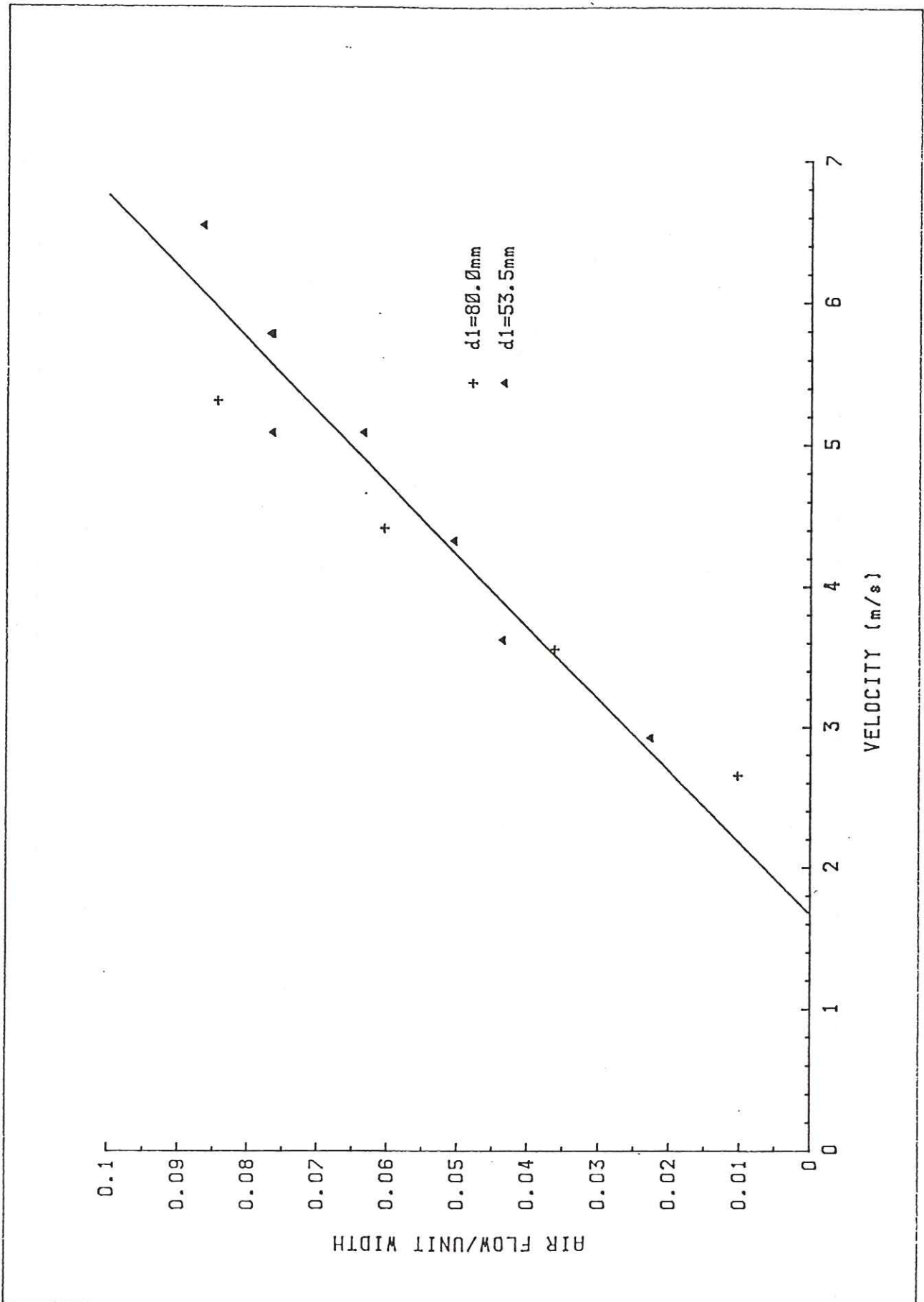


FIG 35 AIR DEMAND V'S VELOCITY FOR AERATOR 9  
 VALVE SETTING 0 ; FLUME SLOPE 45.3 DEGREES

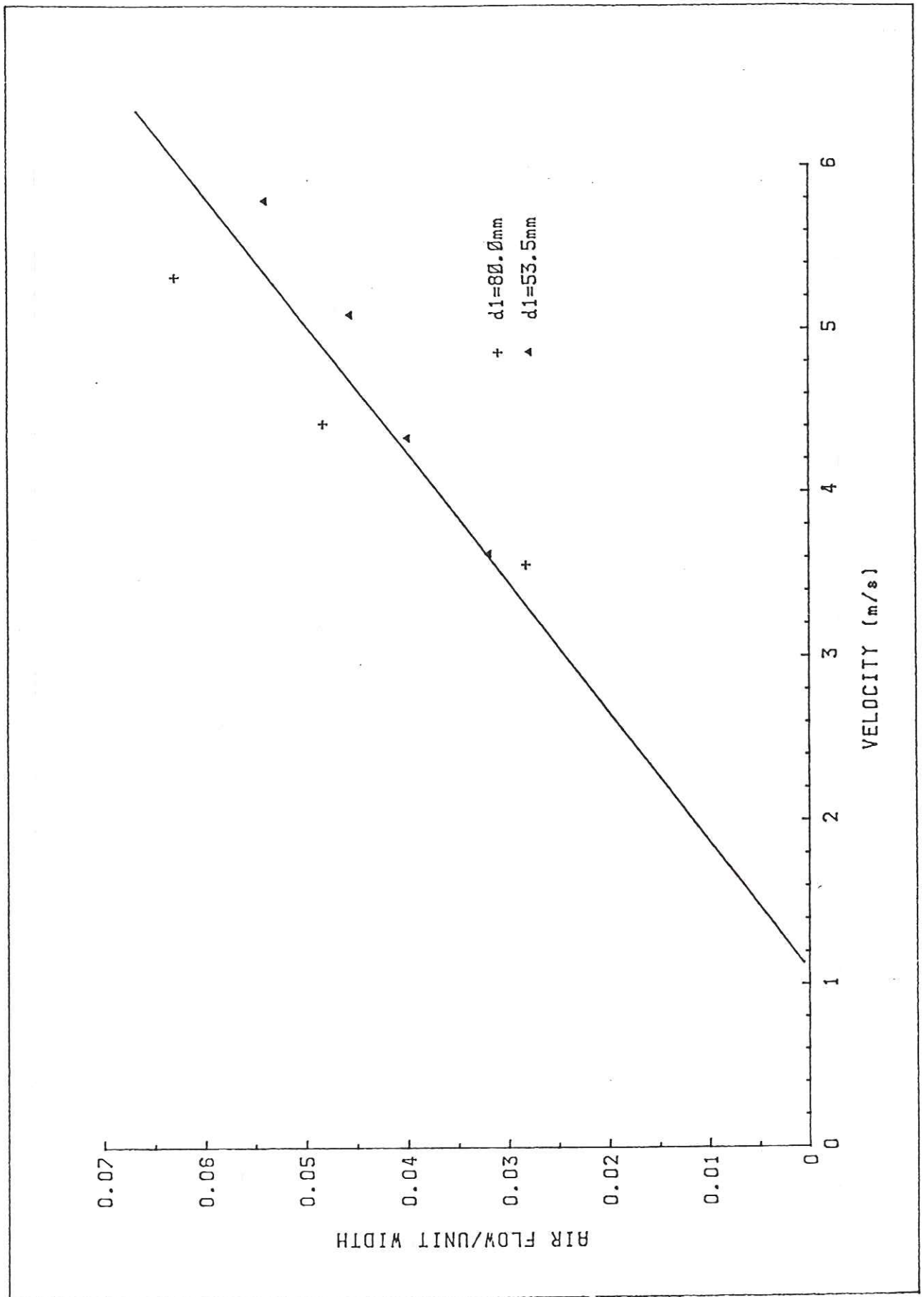


FIG 36 AIR DEMAND V'S VELOCITY FOR AERATOR 9  
 VALVE SETTING 4 ; FLUME SLOPE 45.3 DEGREES

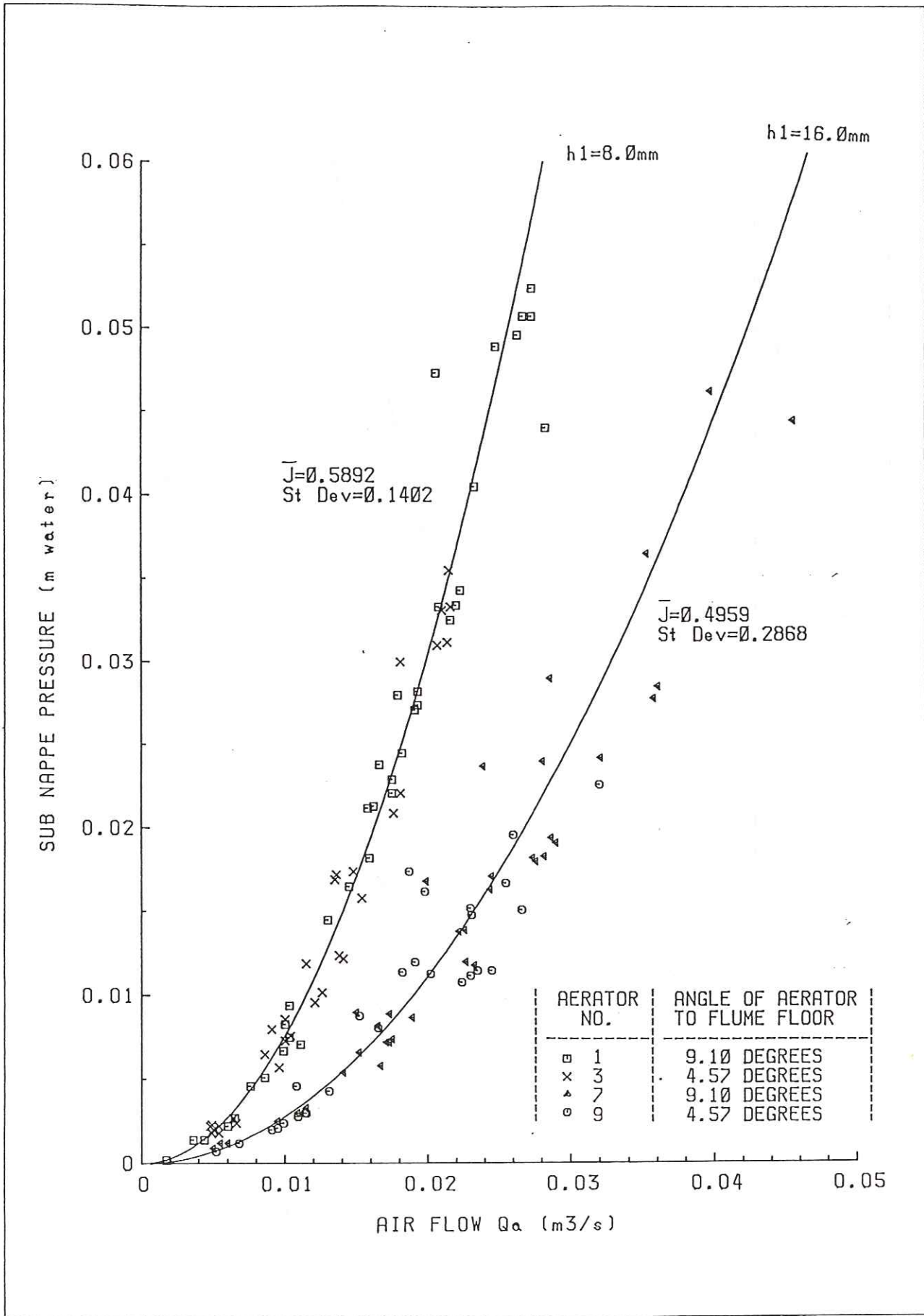


FIG 37 HEAD LOSS CHARACTERISTICS OF AIR SUPPLY SYSTEM FOR VALVE SETTING 0

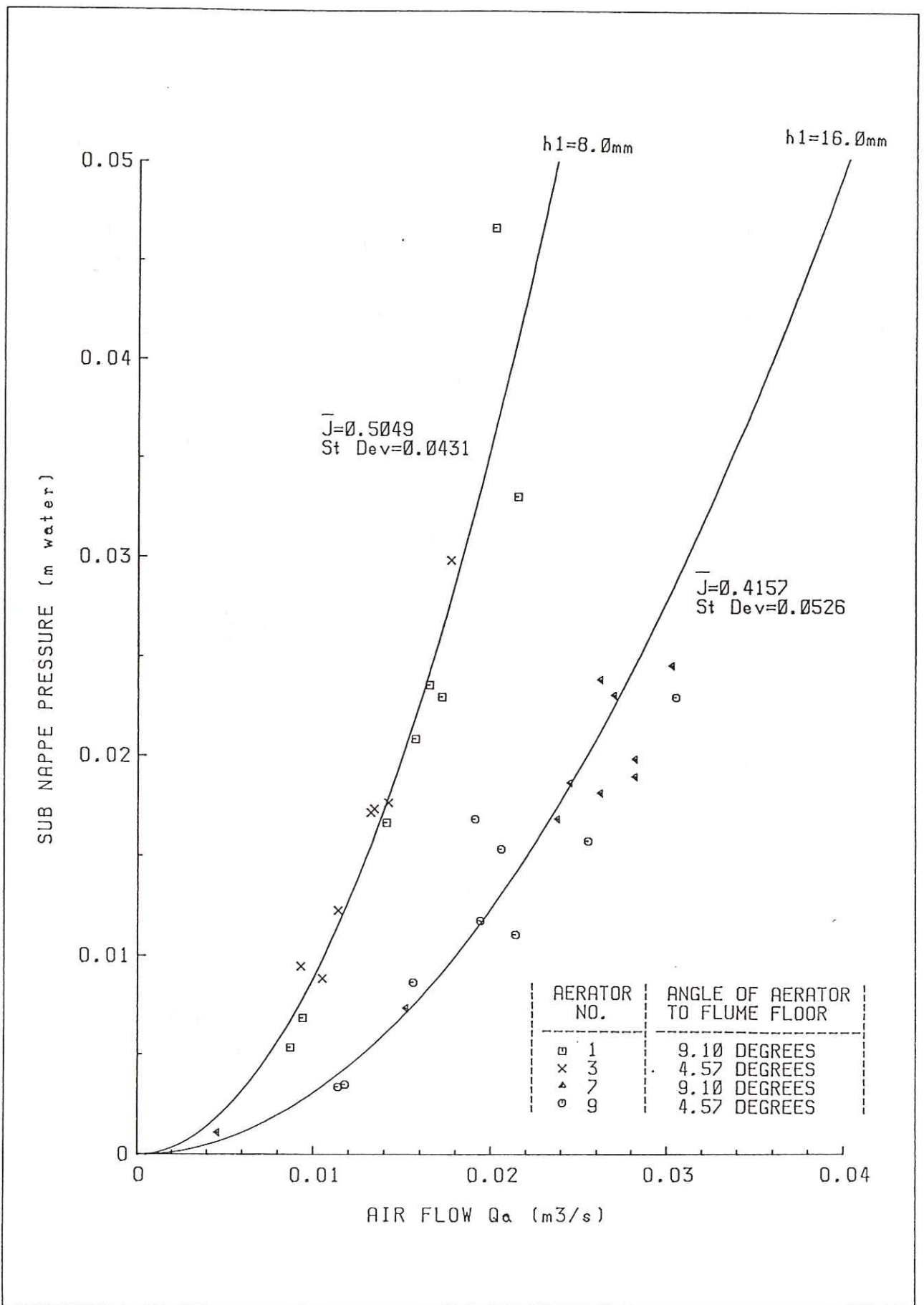


FIG 38 HEAD LOSS CHARACTERISTICS OF AIR SUPPLY SYSTEM FOR VALVE SETTING 2

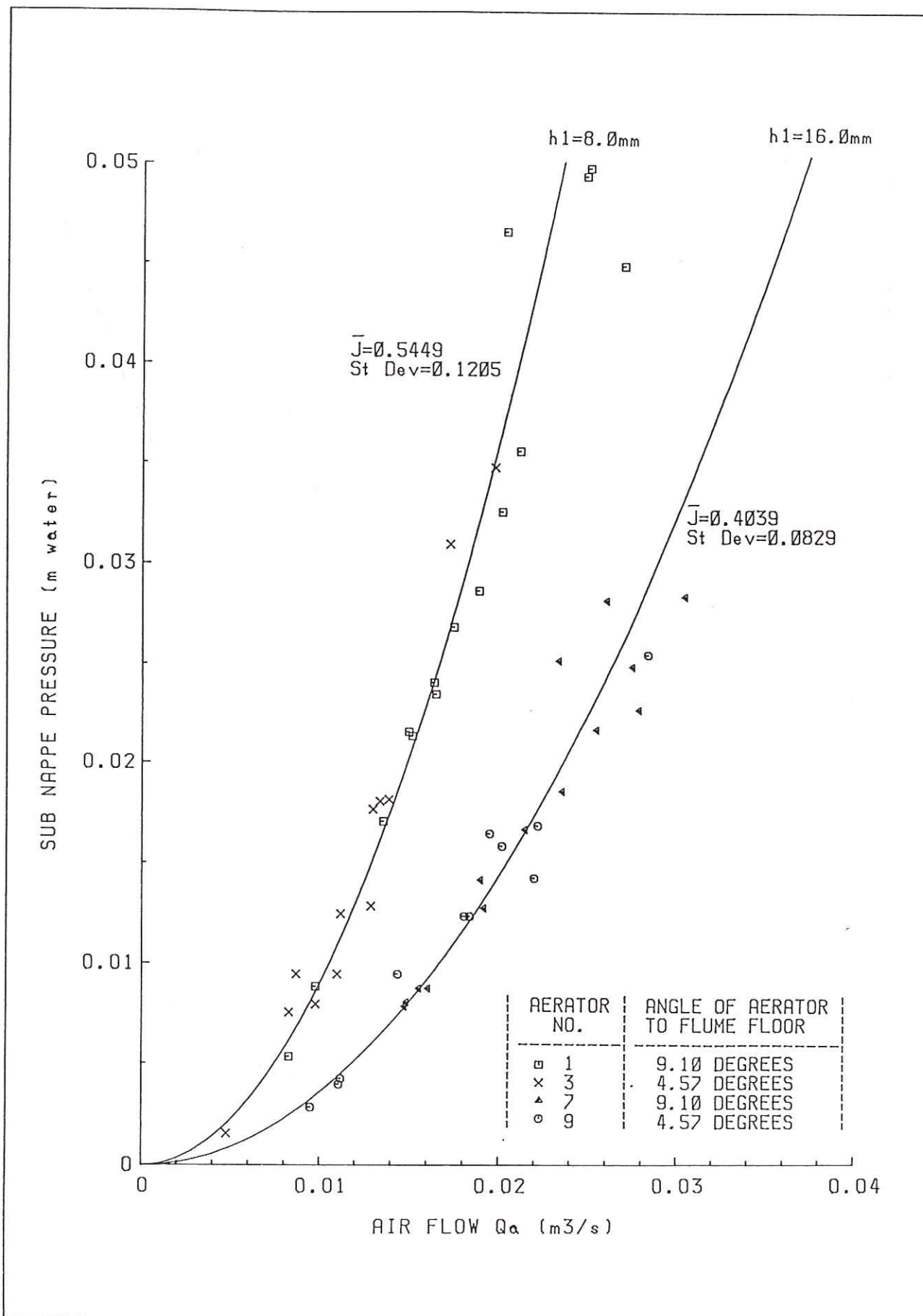


FIG 39 HEAD LOSS CHARACTERISTICS OF AIR SUPPLY SYSTEM FOR VALVE SETTING 3

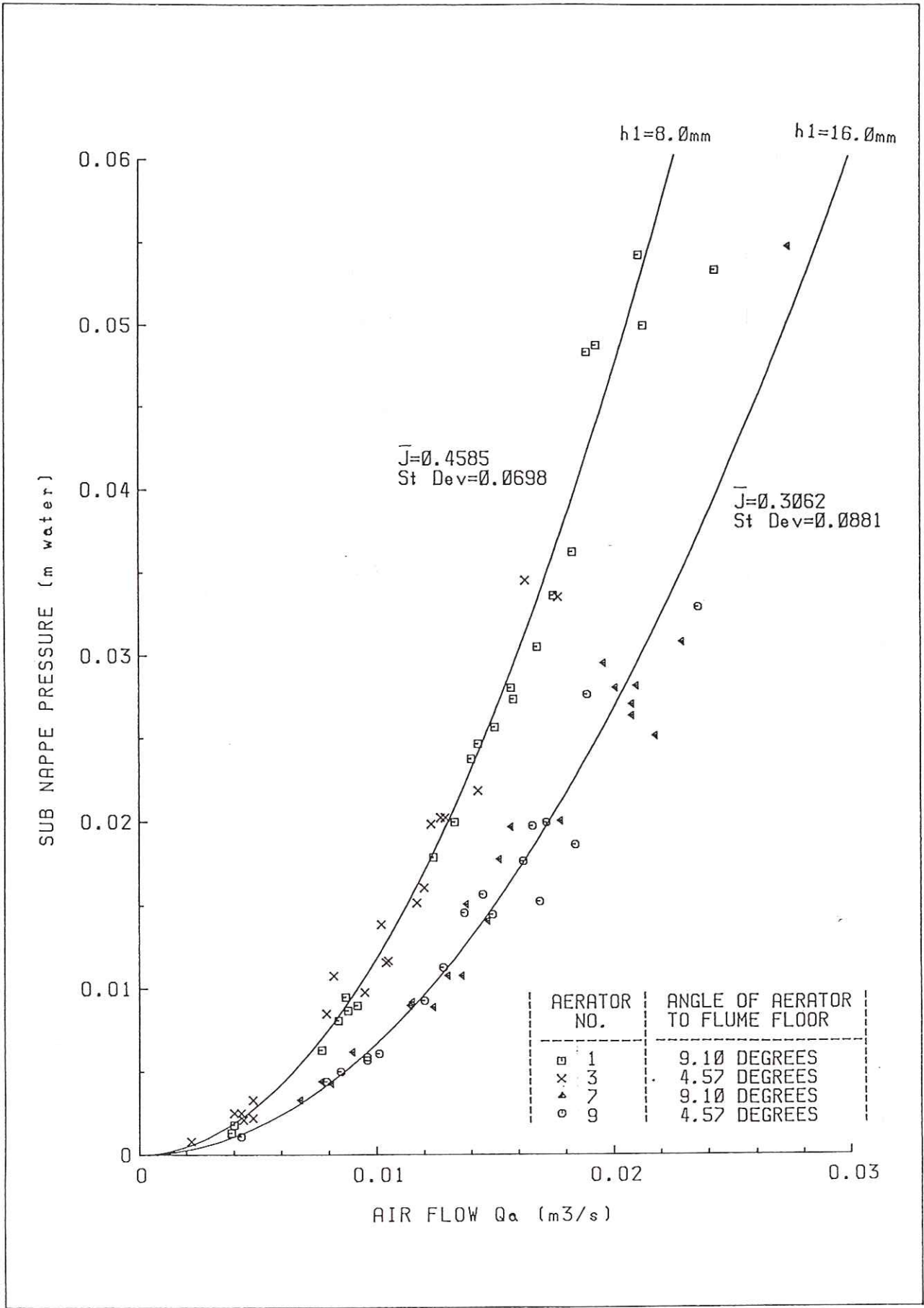


FIG 40 HEAD LOSS CHARACTERISTICS OF AIR SUPPLY SYSTEM FOR VALVE SETTING 4

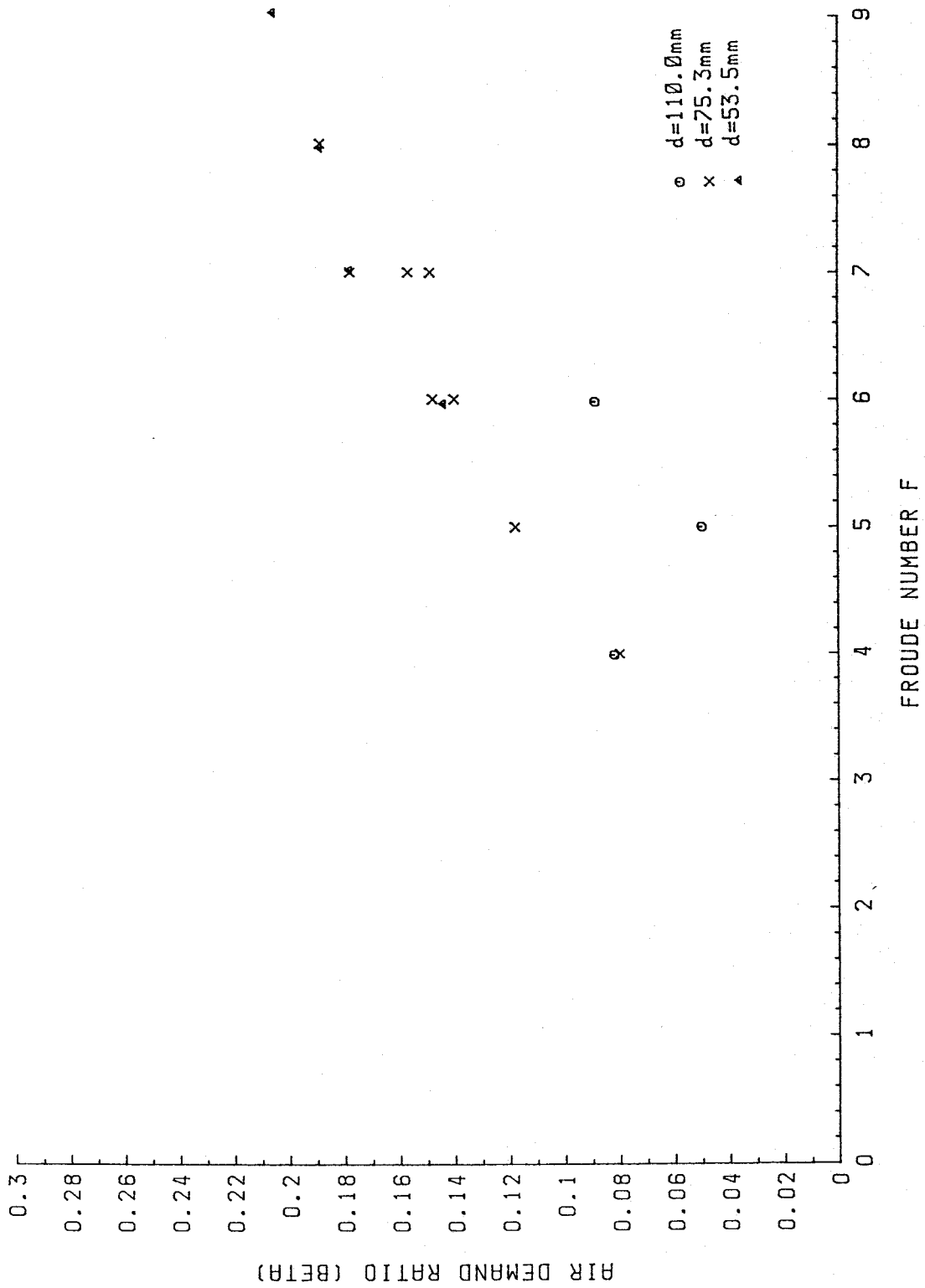


FIG 41 AIR DEMAND RATIO  $V$ 's FROUDE NUMBER  
 AERATOR 1; VALVE SETTING  $\emptyset$ ; FLUME SLOPE 15.5 DEGREES

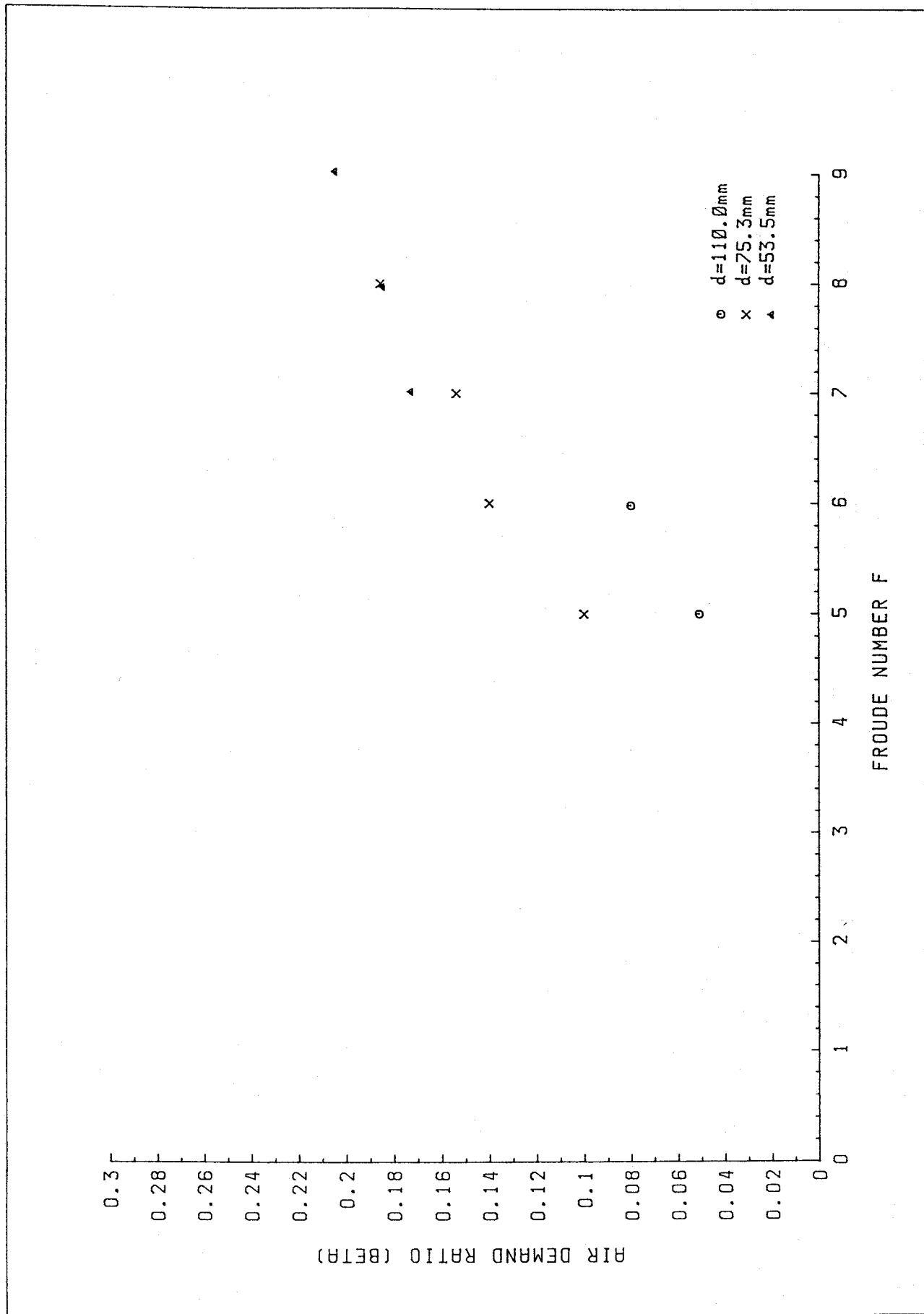


FIG 42 AIR DEMAND RATIO V's FROUDE NUMBER  
 AERATOR 1; VALVE SETTING 2; FLUME SLOPE 15.5 DEGREES

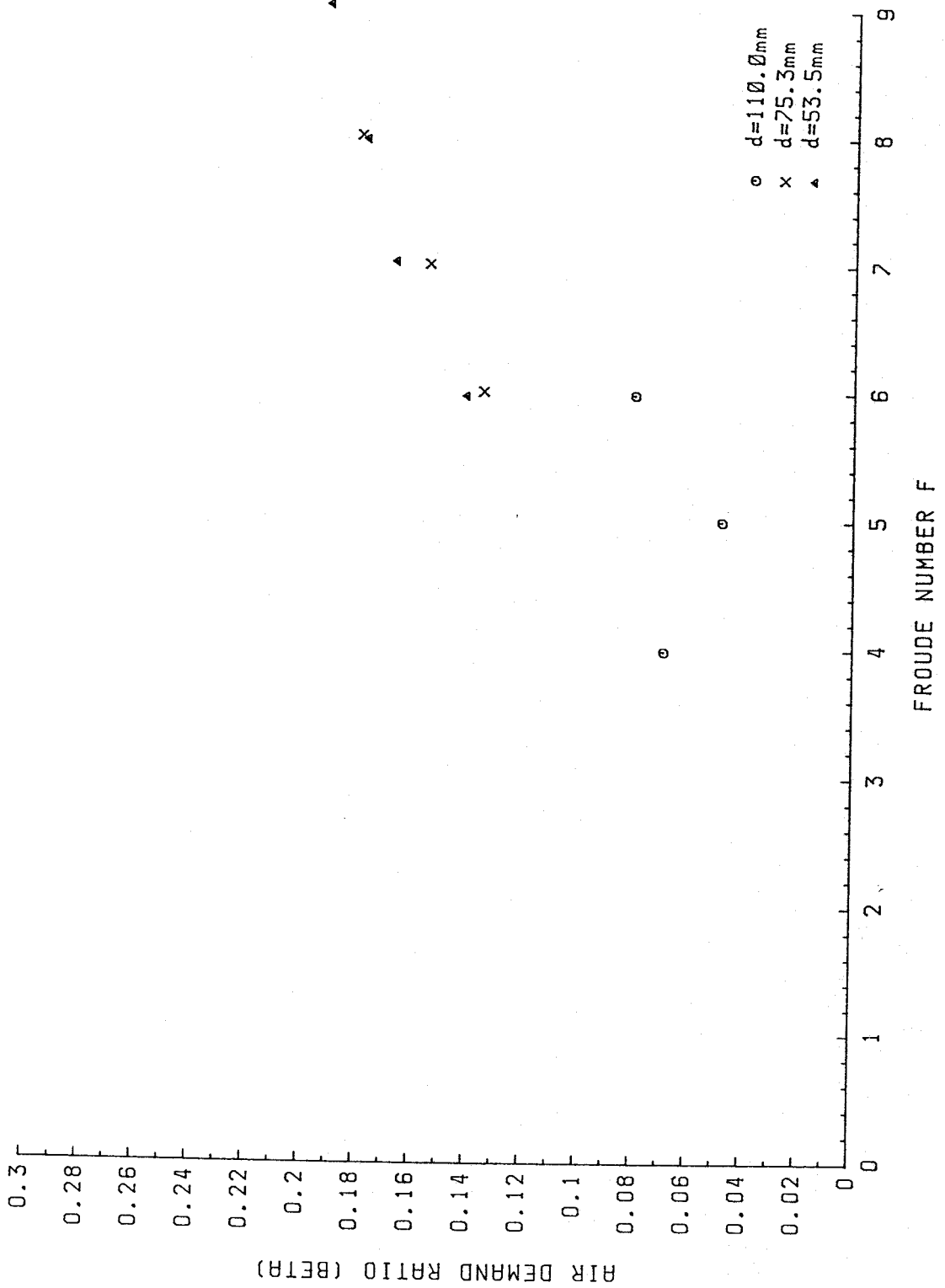


FIG 43 AIR DEMAND RATIO  $V$ 's FROUDE NUMBER  
 AERATOR 1; VALVE SETTING 3; FLUME SLOPE 15.5 DEGREES

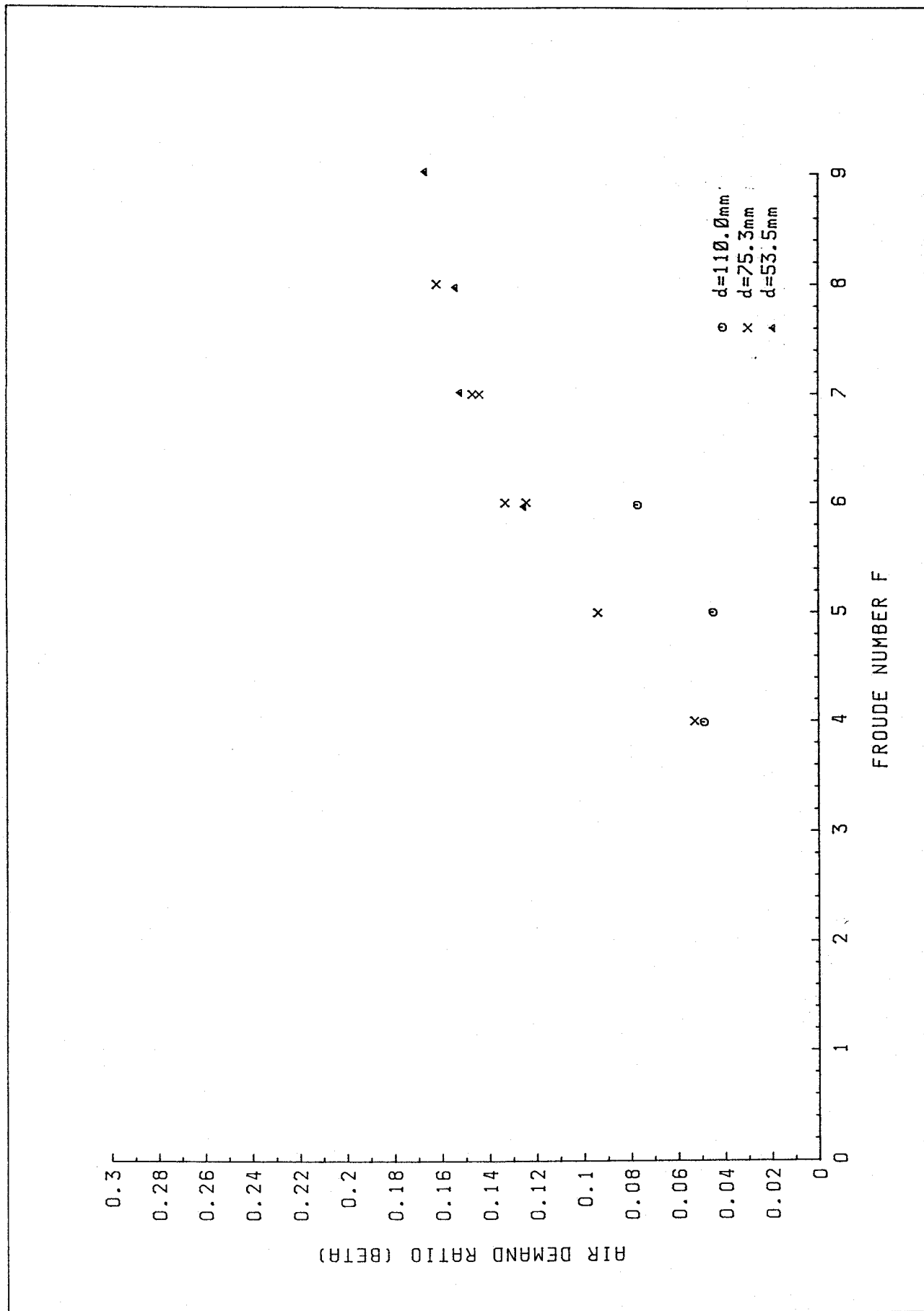


FIG 44 AIR DEMAND RATIO V's FROUDE NUMBER  
 AERATOR 1; VALVE SETTING 4; FLUME SLOPE 15.5 DEGREES

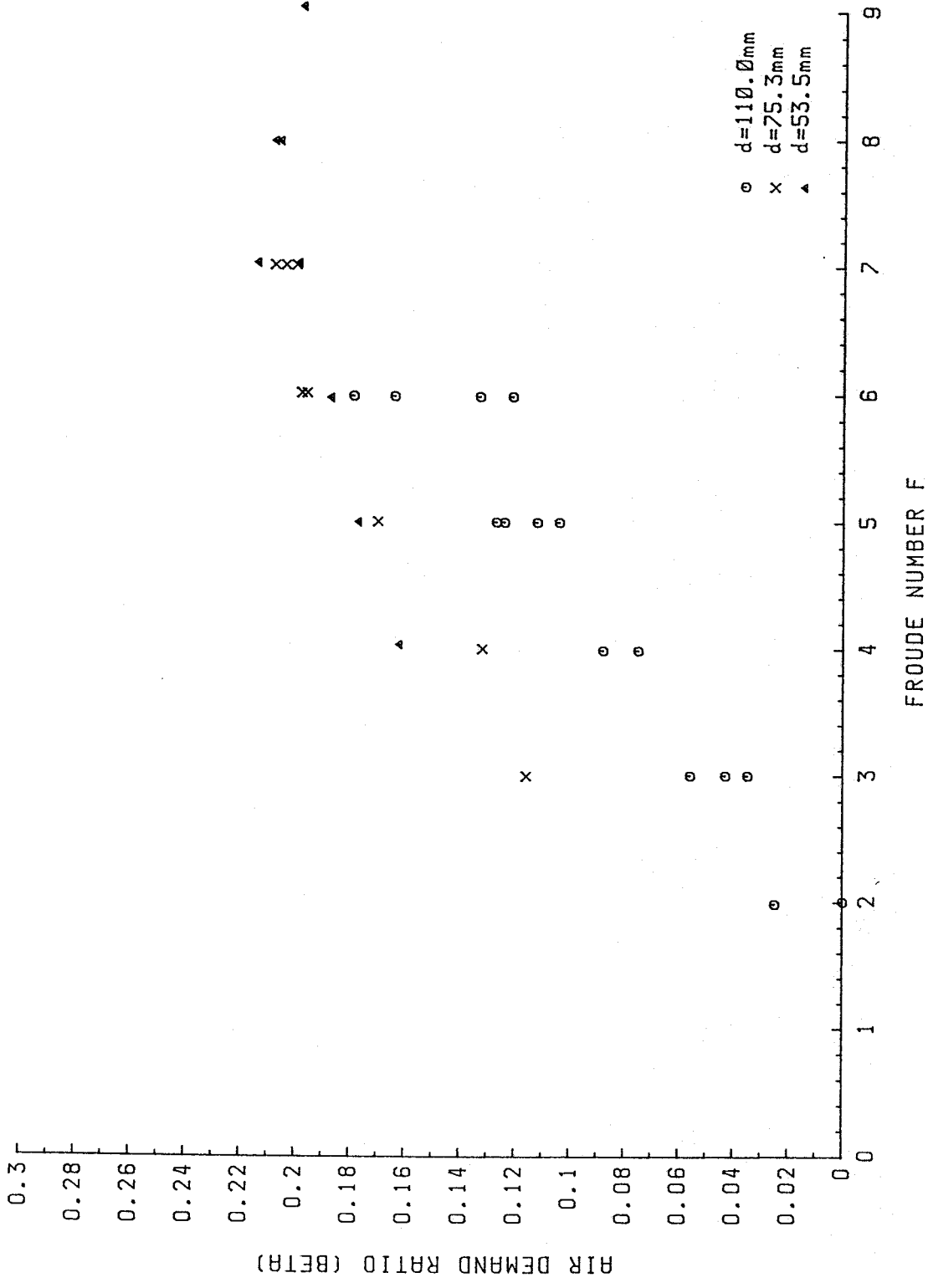


FIG 45 AIR DEMAND RATIO V's FROUDE NUMBER  
 AERATOR 1; VALVE SETTING 0; FLUME SLOPE 45.3 DEGREES

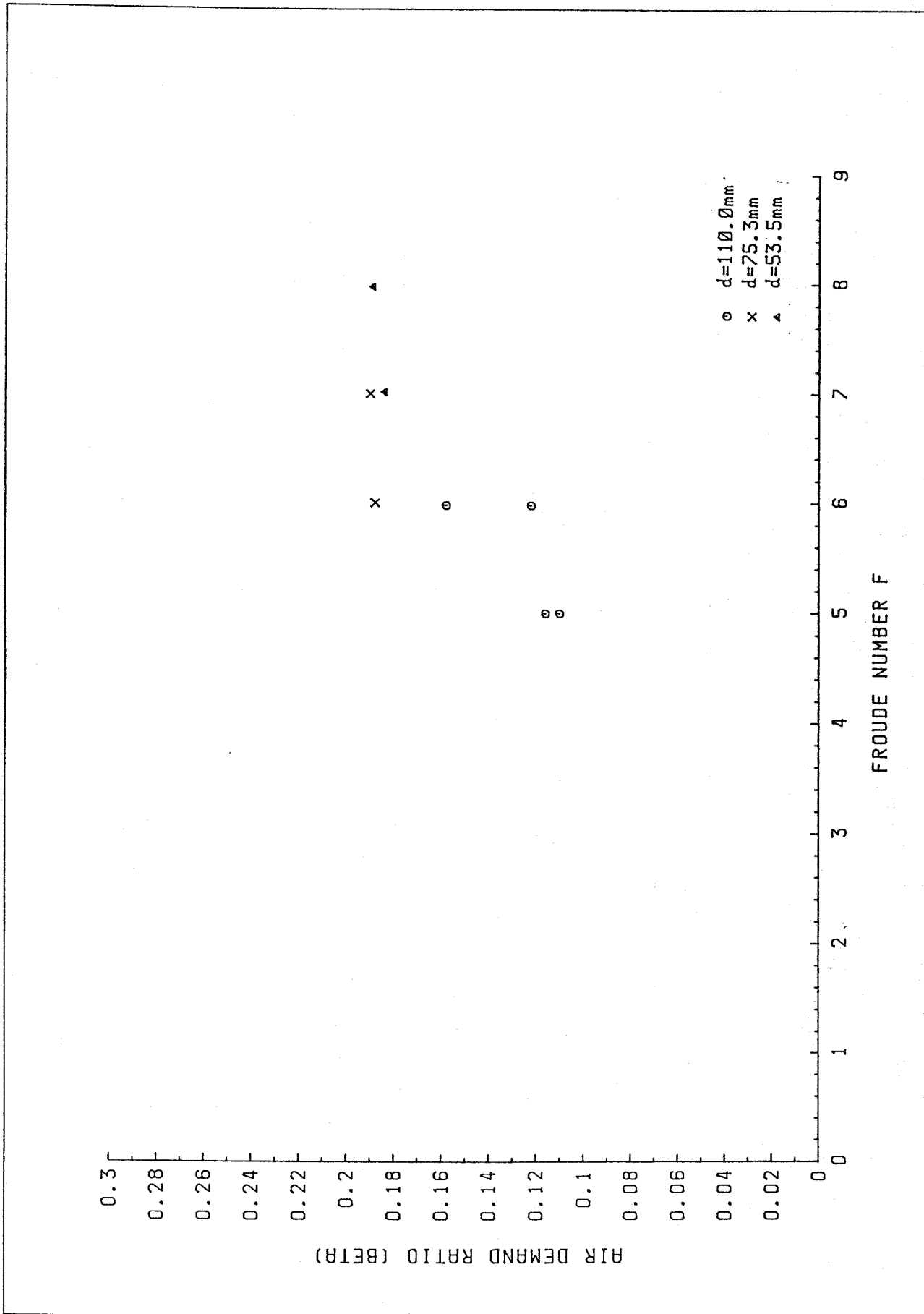


FIG 46 AIR DEMAND RATIO  $V$ 's FROUDE NUMBER  
 AERATOR 1; VALVE SETTING 3; FLUME SLOPE 45.3 DEGREES

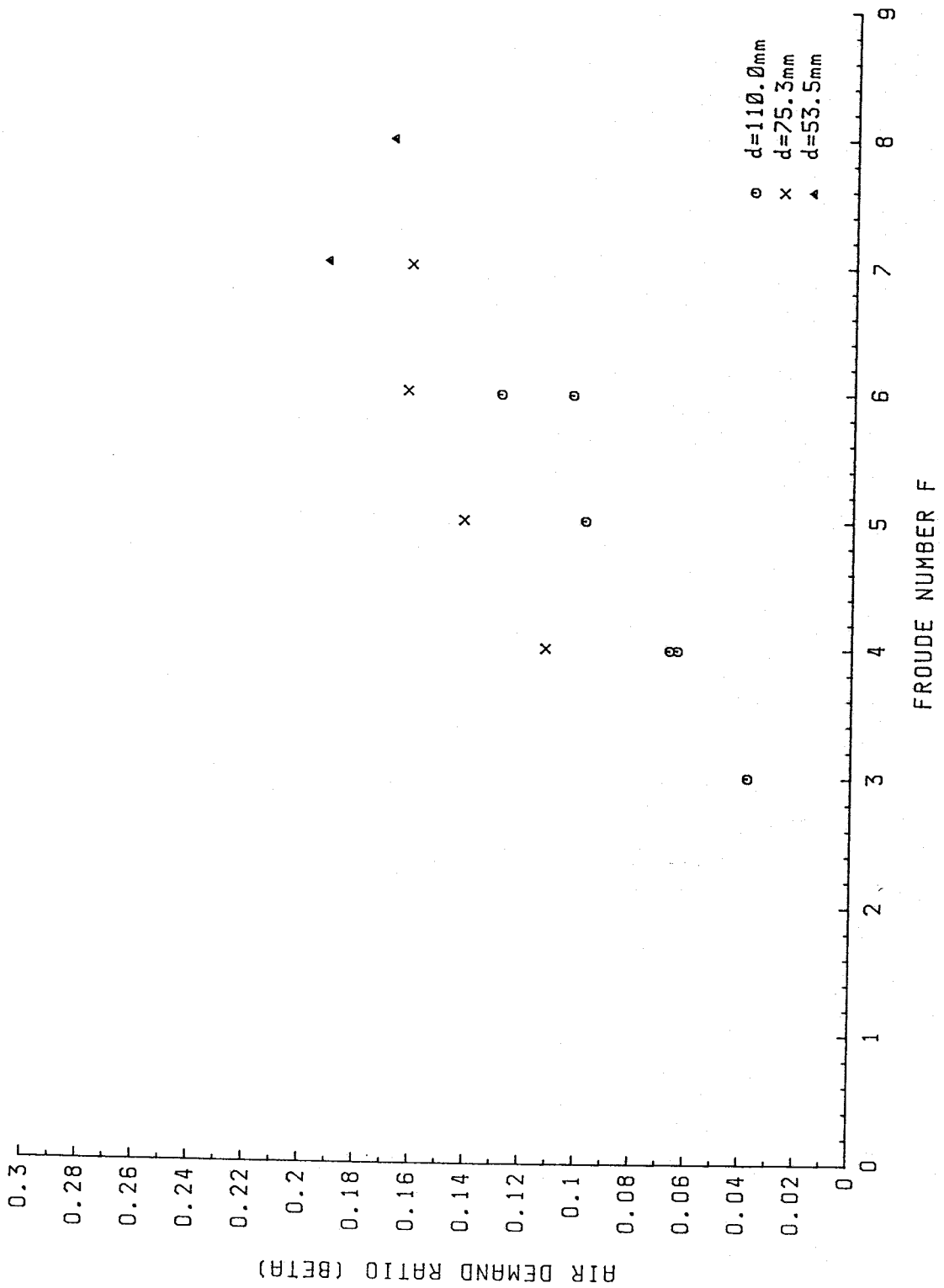


FIG 47 AIR DEMAND RATIO V's FROUDE NUMBER  
 AERATOR 1; VALVE SETTING 4; FLUME SLOPE 45.3 DEGREES

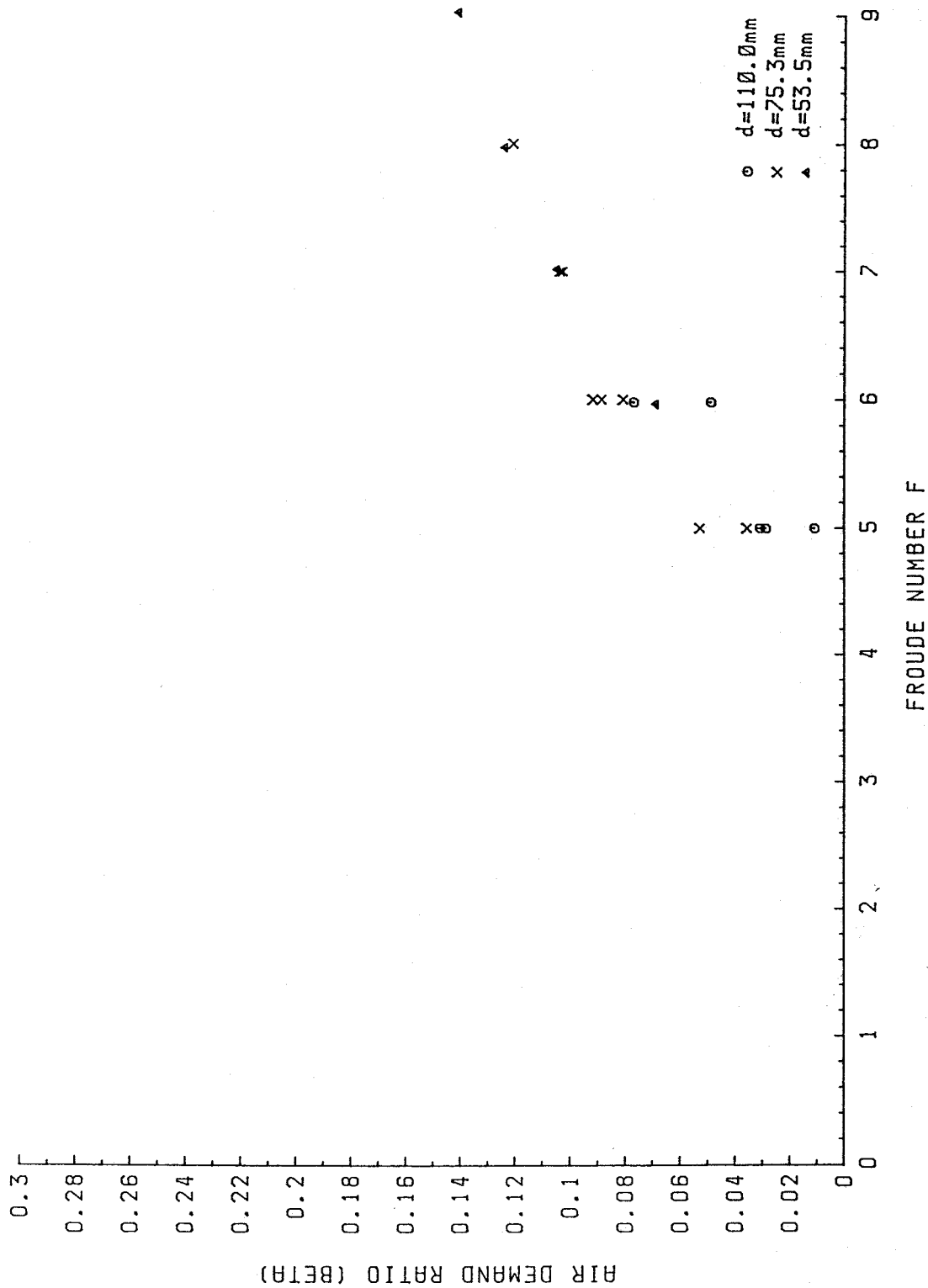


FIG 48 AIR DEMAND RATIO  $V'$  vs FROUDE NUMBER  
 AERATOR 3; VALVE SETTING 0; FLUME SLOPE 15.5 DEGREES

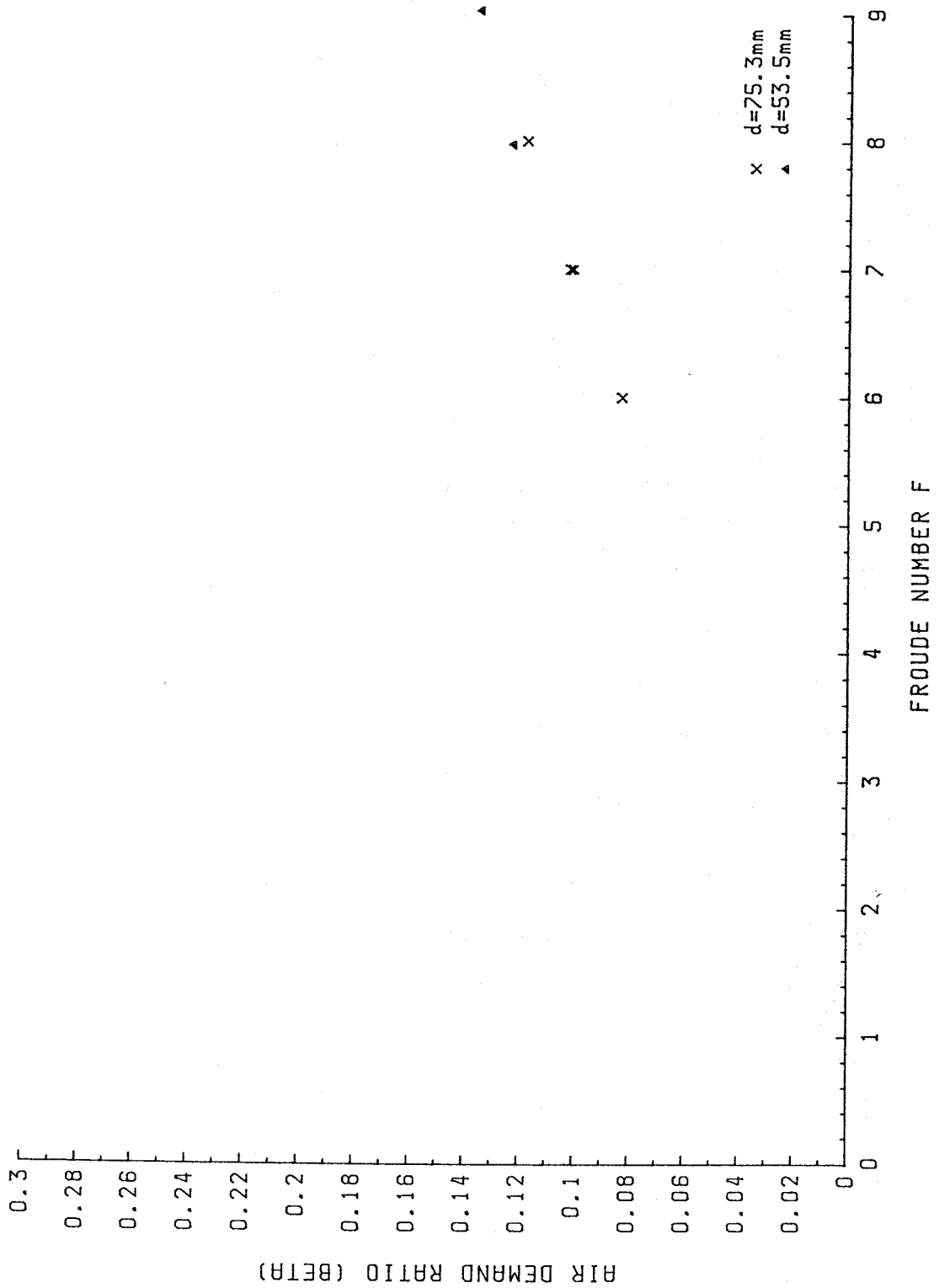


FIG 49 AIR DEMAND RATIO  $V'$ 's FROUDE NUMBER  
 REARTOR 3; VALVE SETTING 2; FLUME SLOPE 15.5 DEGREES

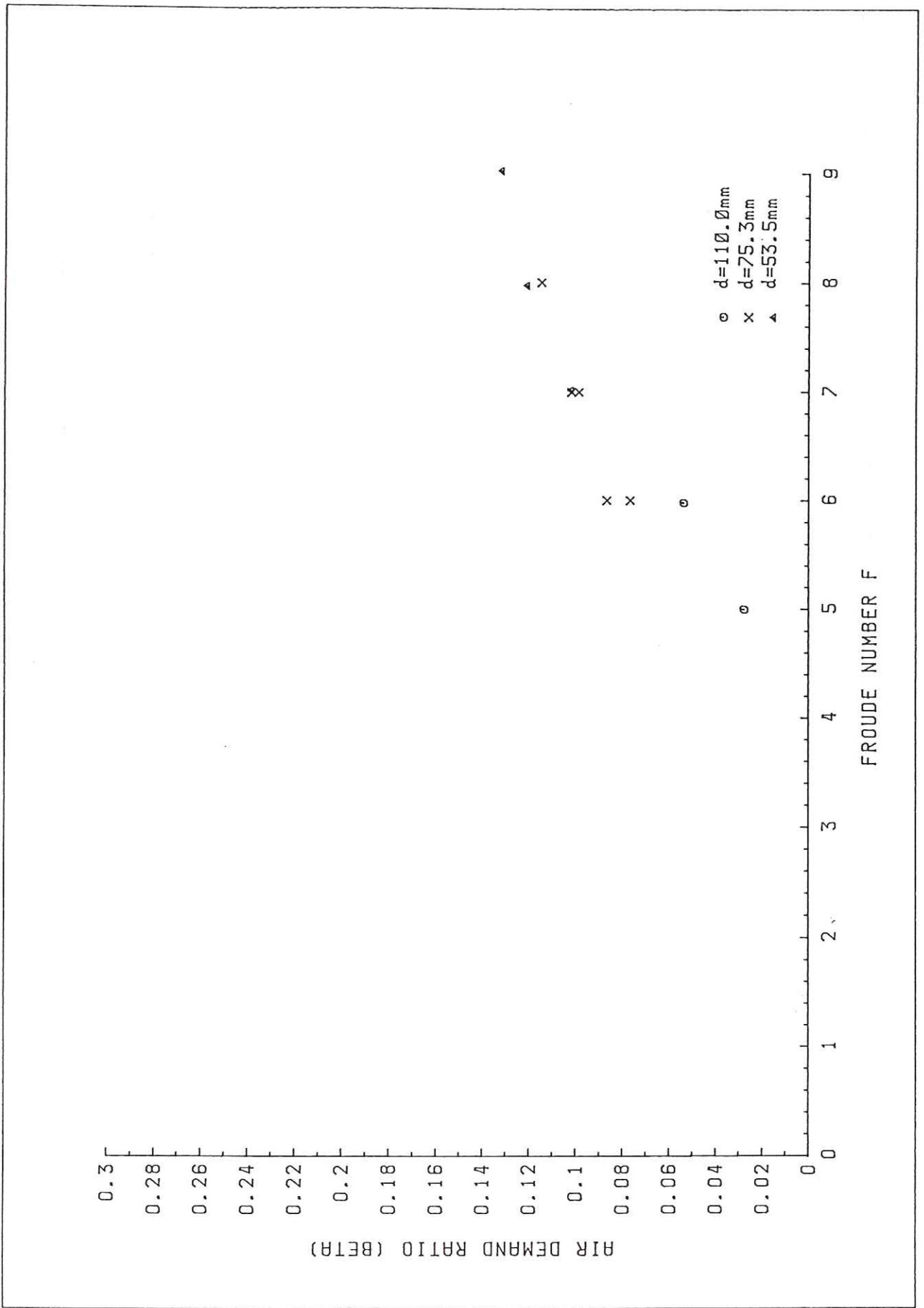


FIG 50 AIR DEMAND RATIO  $V'$ 's FROUDE NUMBER  
 AERATOR 3; VALVE SETTING 3; FLUME SLOPE 15.5 DEGREES

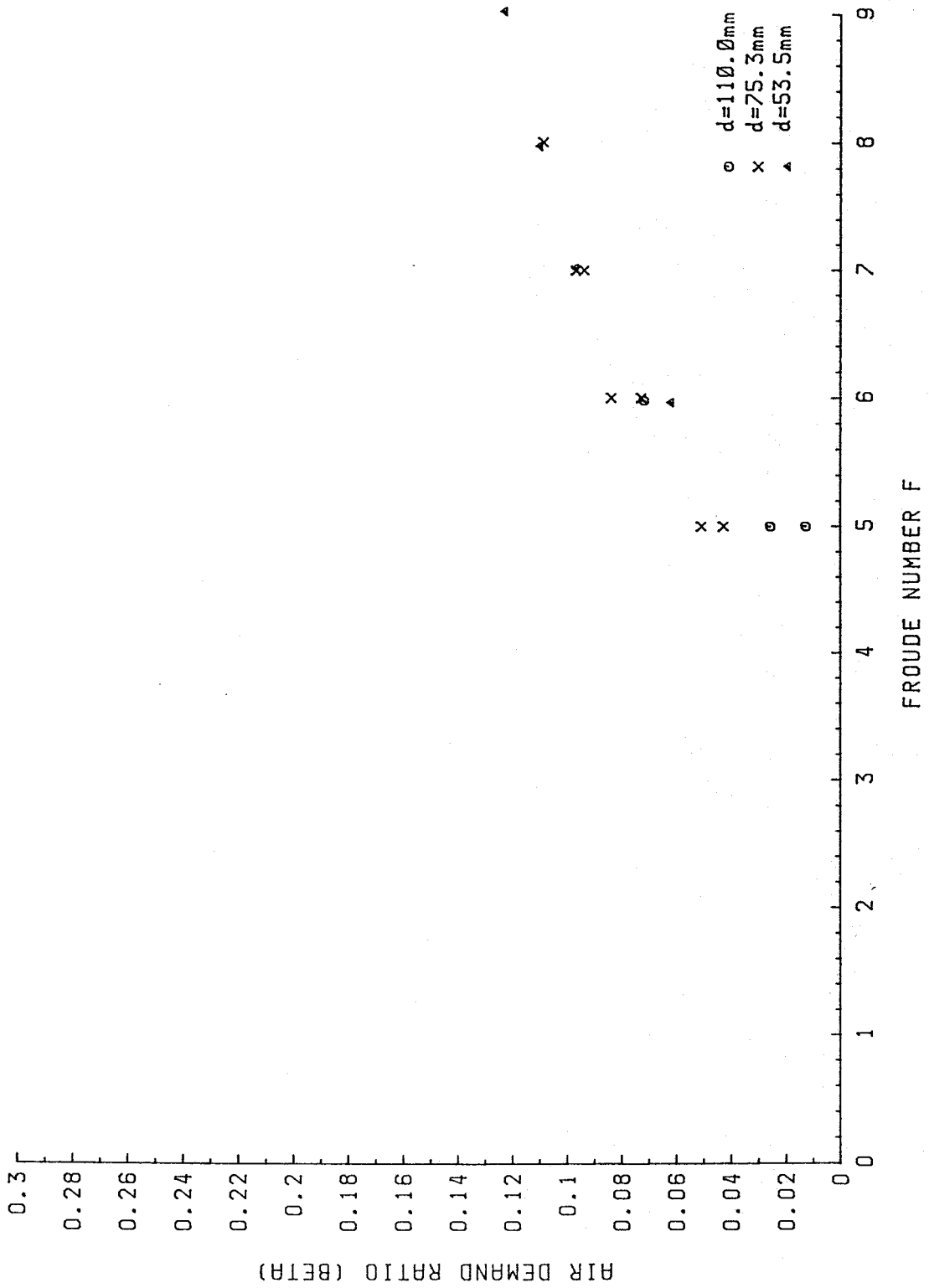


FIG 51 AIR DEMAND RATIO  $V$ 's FROUDE NUMBER  
 AERATOR 3; VALVE SETTING 4; FLUME SLOPE 15.5 DEGREES

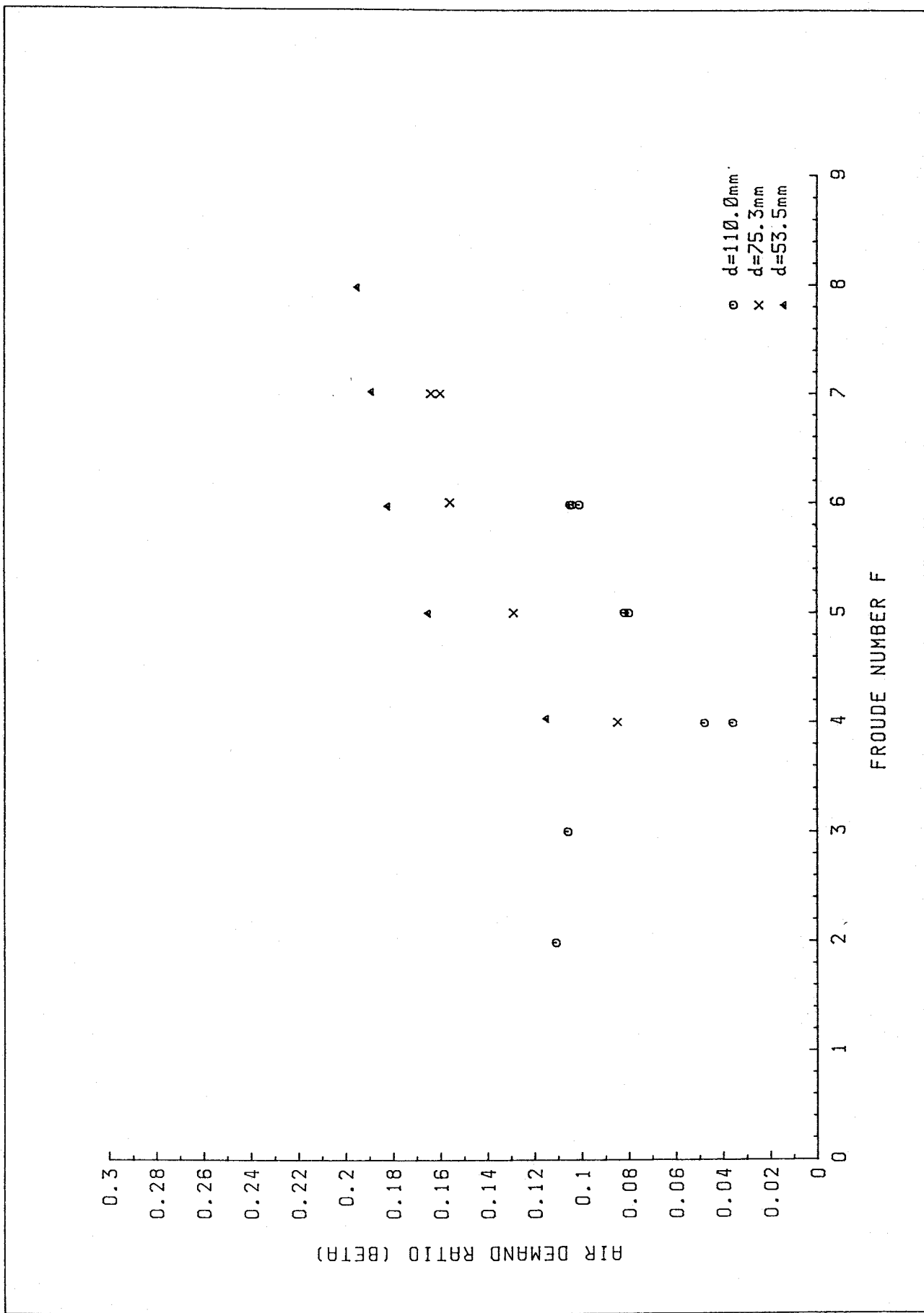


FIG 52 AIR DEMAND RATIO V's FROUDE NUMBER  
 AERATOR 3; VALVE SETTING 0; FLUME SLOPE 45.3 DEGREES

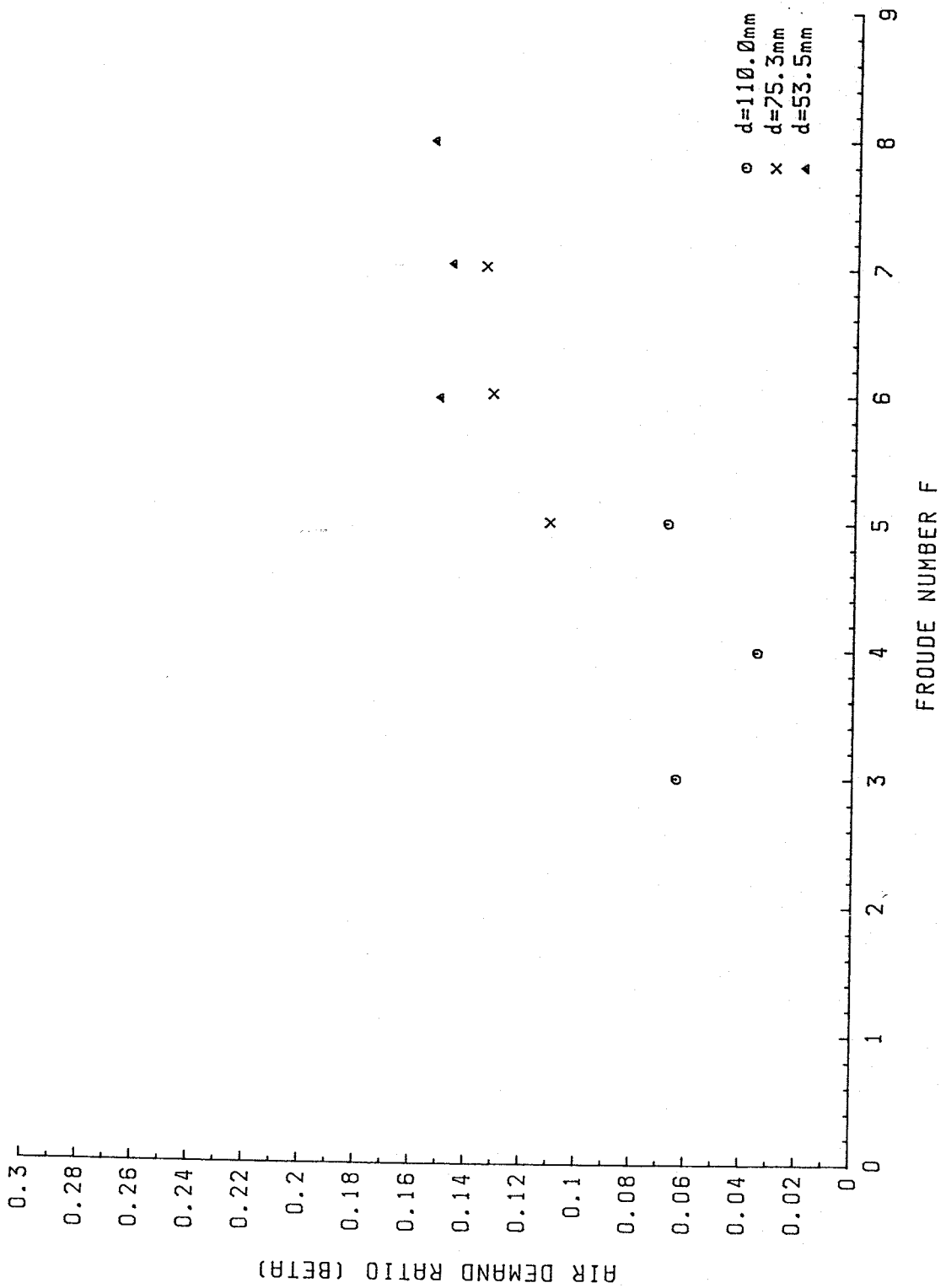


FIG 53 AIR DEMAND RATIO V's FROUDE NUMBER  
 AERATOR 3; VALVE SETTING 4; FLUME SLOPE 45.3 DEGREES

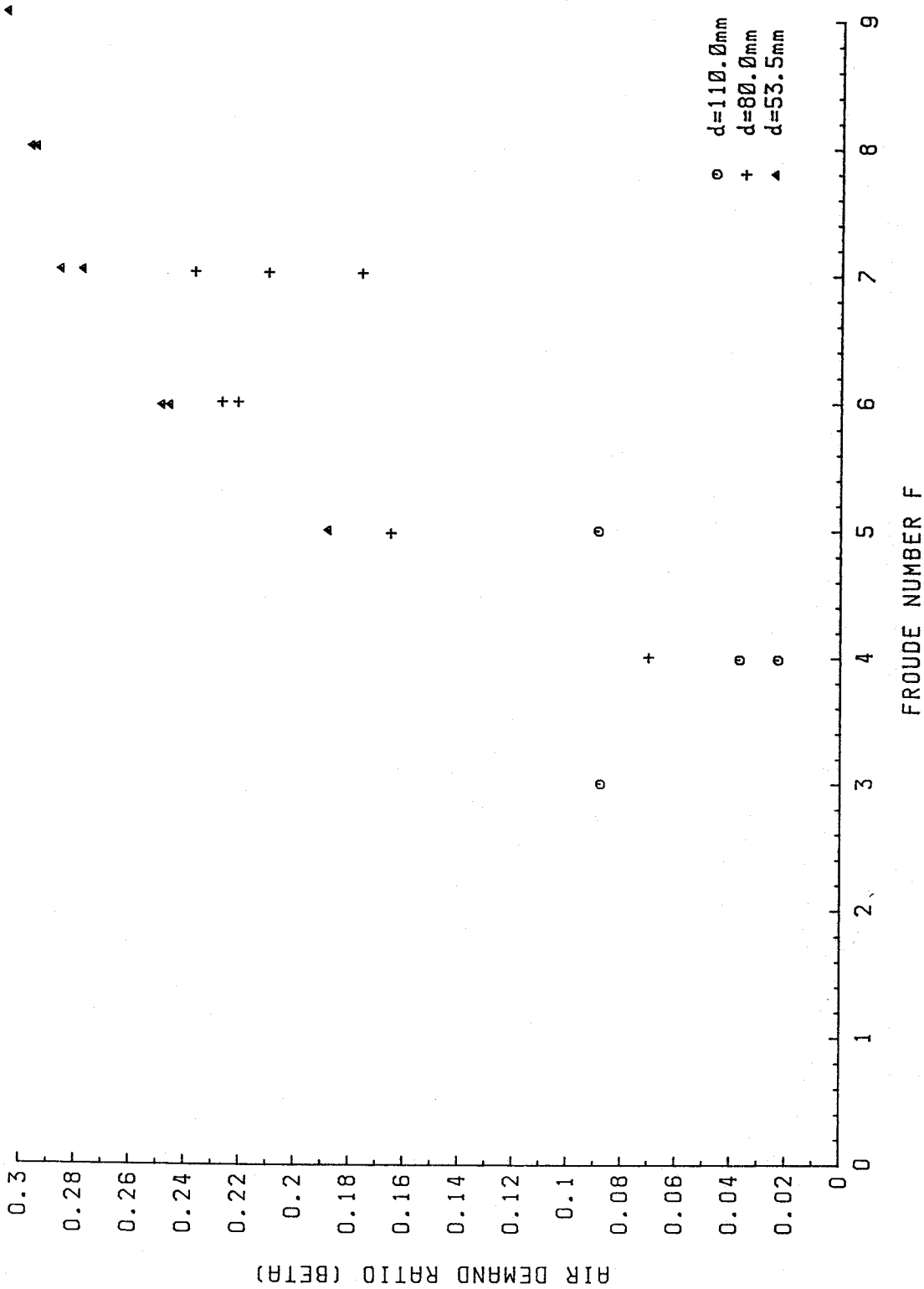


FIG 54 AIR DEMAND RATIO V's FROUDE NUMBER  
 AERATOR 7; VALVE SETTING  $\emptyset$ ; FLUME SLOPE 15.5 DEGREES

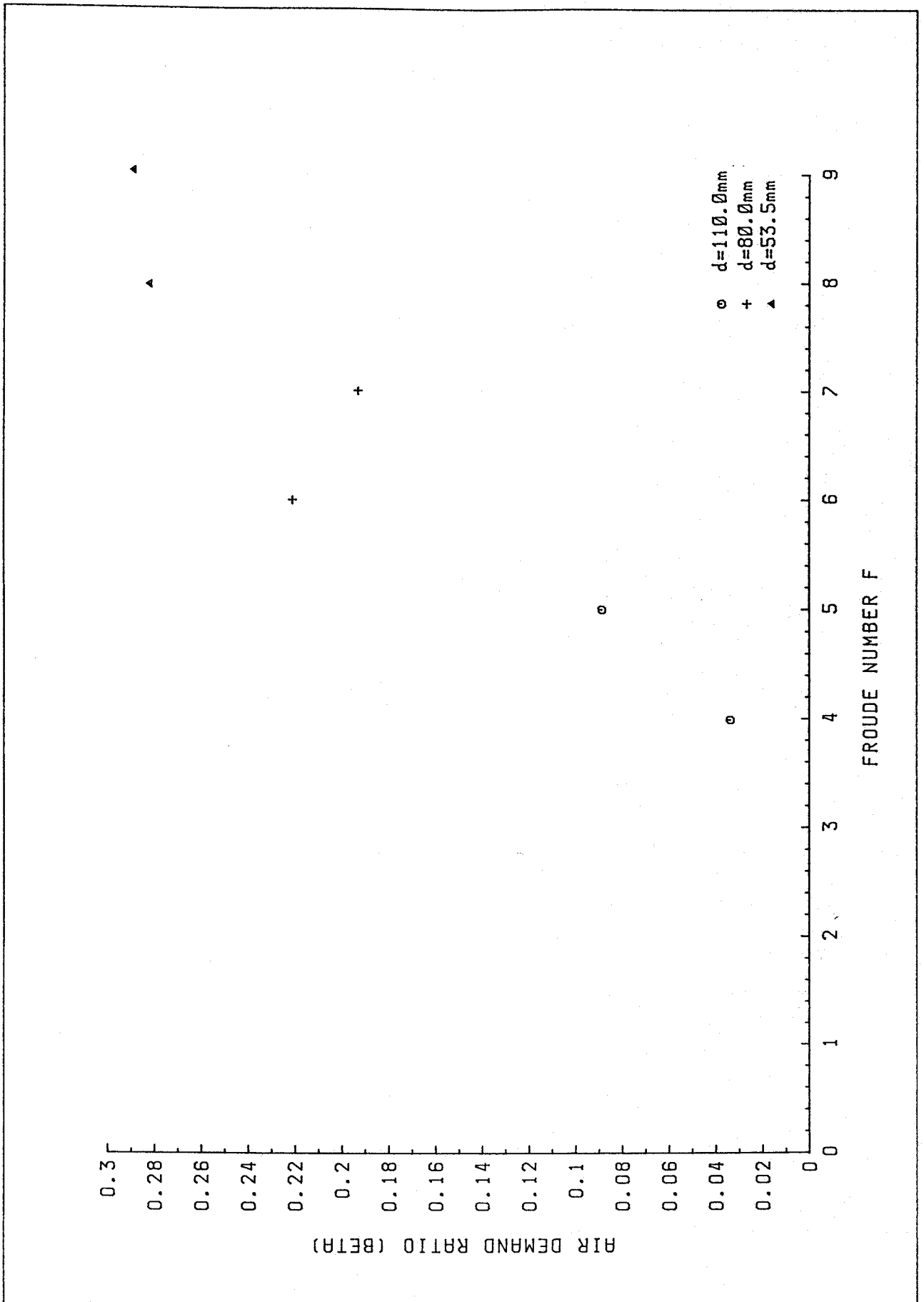


FIG 55 AIR DEMAND RATIO  $V$ 's FROUDE NUMBER  
 AERATOR 7; VALVE SETTING 2; FLUME SLOPE 15.5 DEGREES

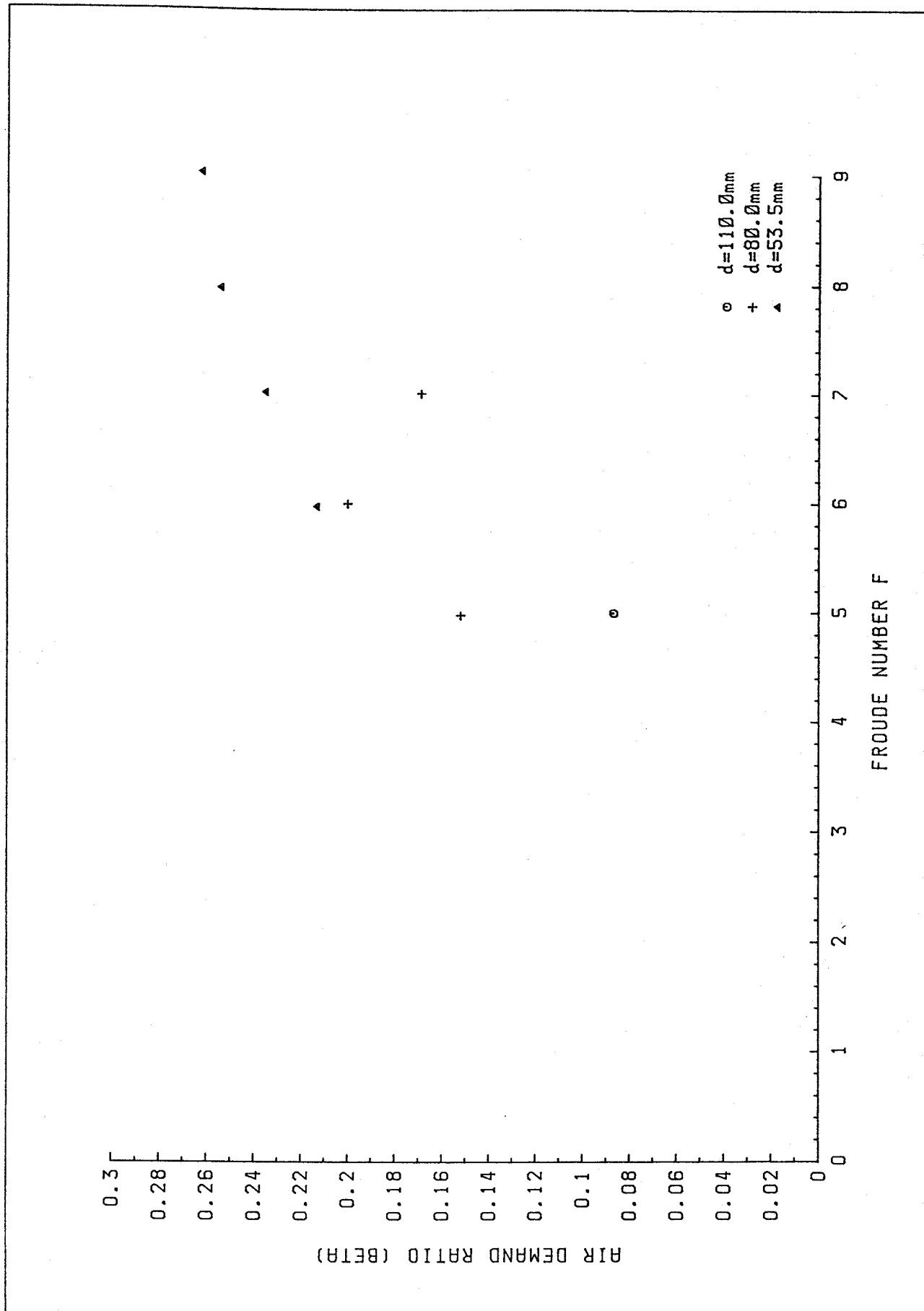


FIG 56 AIR DEMAND RATIO V's FROUDE NUMBER  
 AERATOR 7; VALVE SETTING 3; FLUME SLOPE 15.5 DEGREES

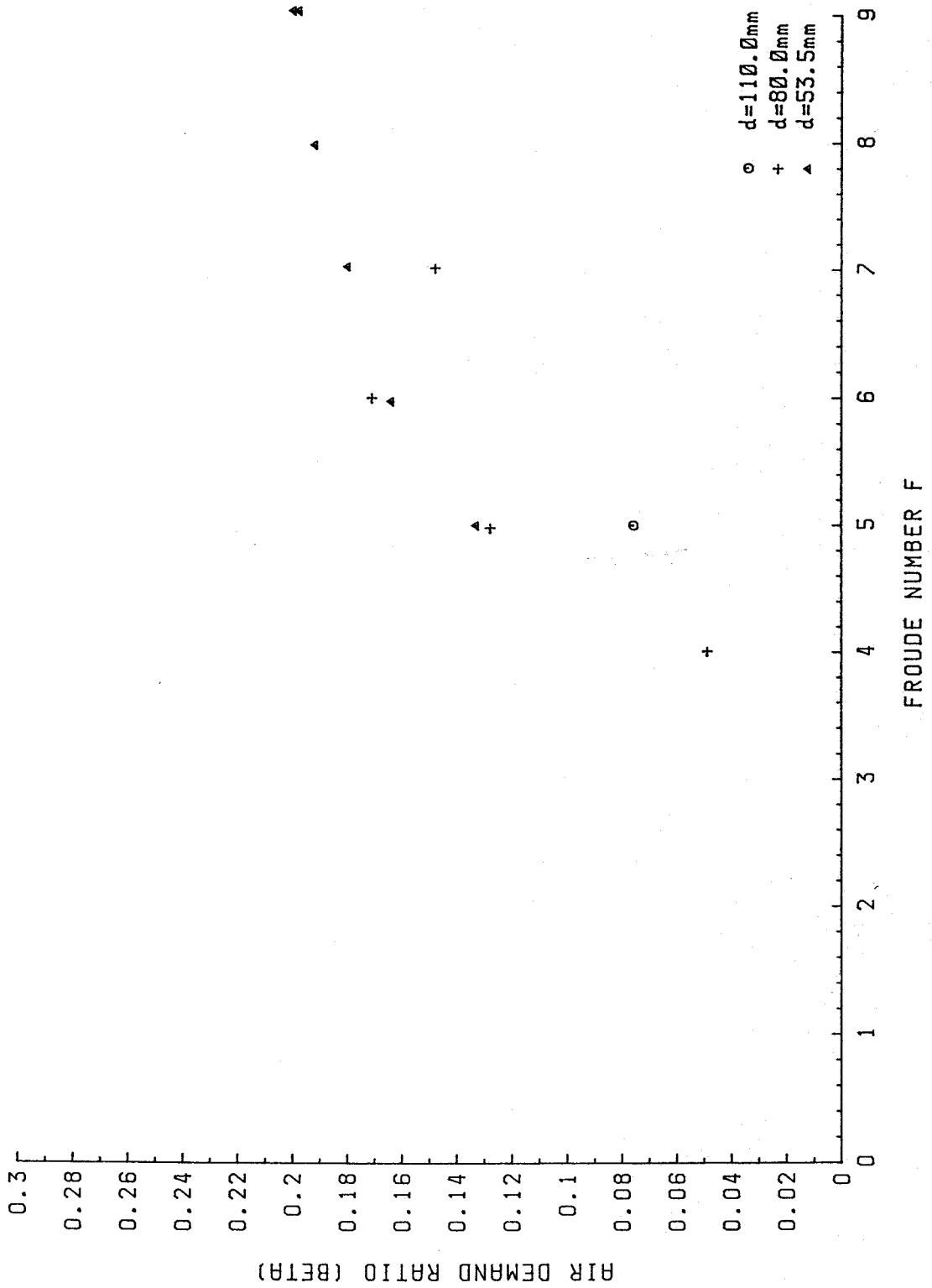


FIG 57 AIR DEMAND RATIO V's FROUDE NUMBER  
 AERATOR 7; VALVE SETTING 4; FLUME SLOPE 15.5 DEGREES

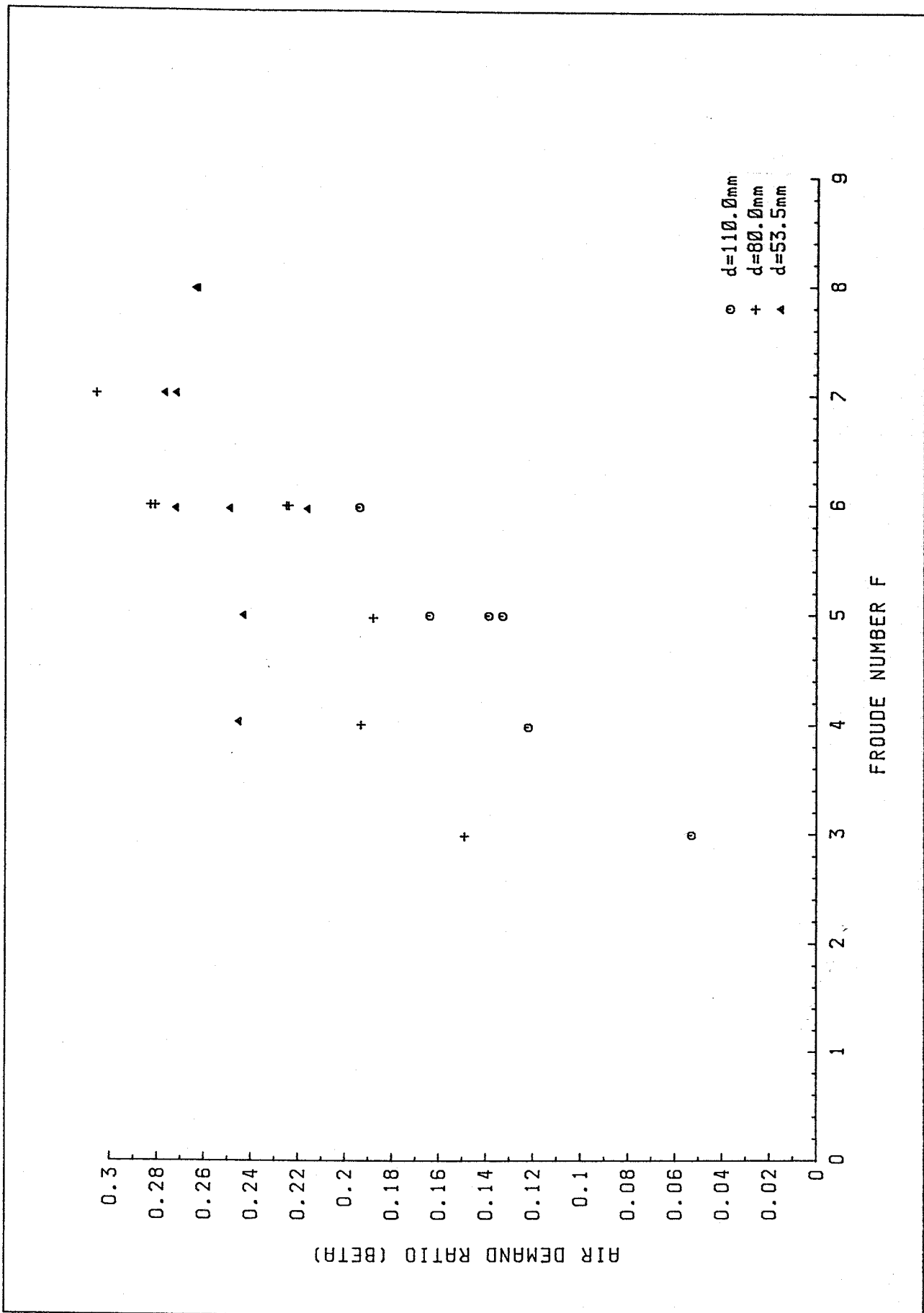


FIG 58 AIR DEMAND RATIO  $V'$ 's FROUDE NUMBER  
 AERATOR 7; VALVE SETTING  $\emptyset$ ; FLUME SLOPE 45.3 DEGREES

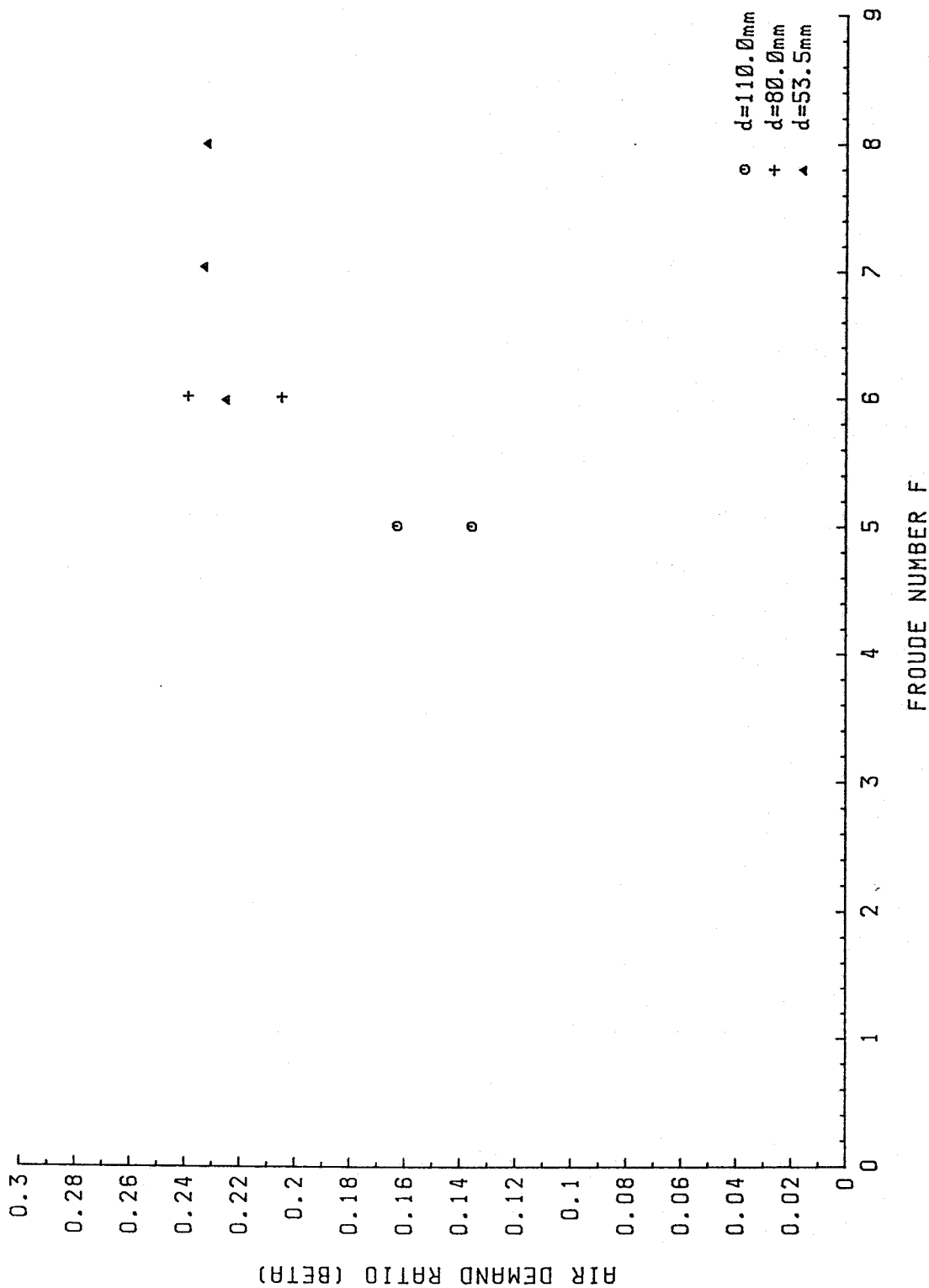


FIG 59 AIR DEMAND RATIO V's FROUDE NUMBER  
 AERATOR 7; VALVE SETTING 3; FLUME SLOPE 45.3 DEGREES

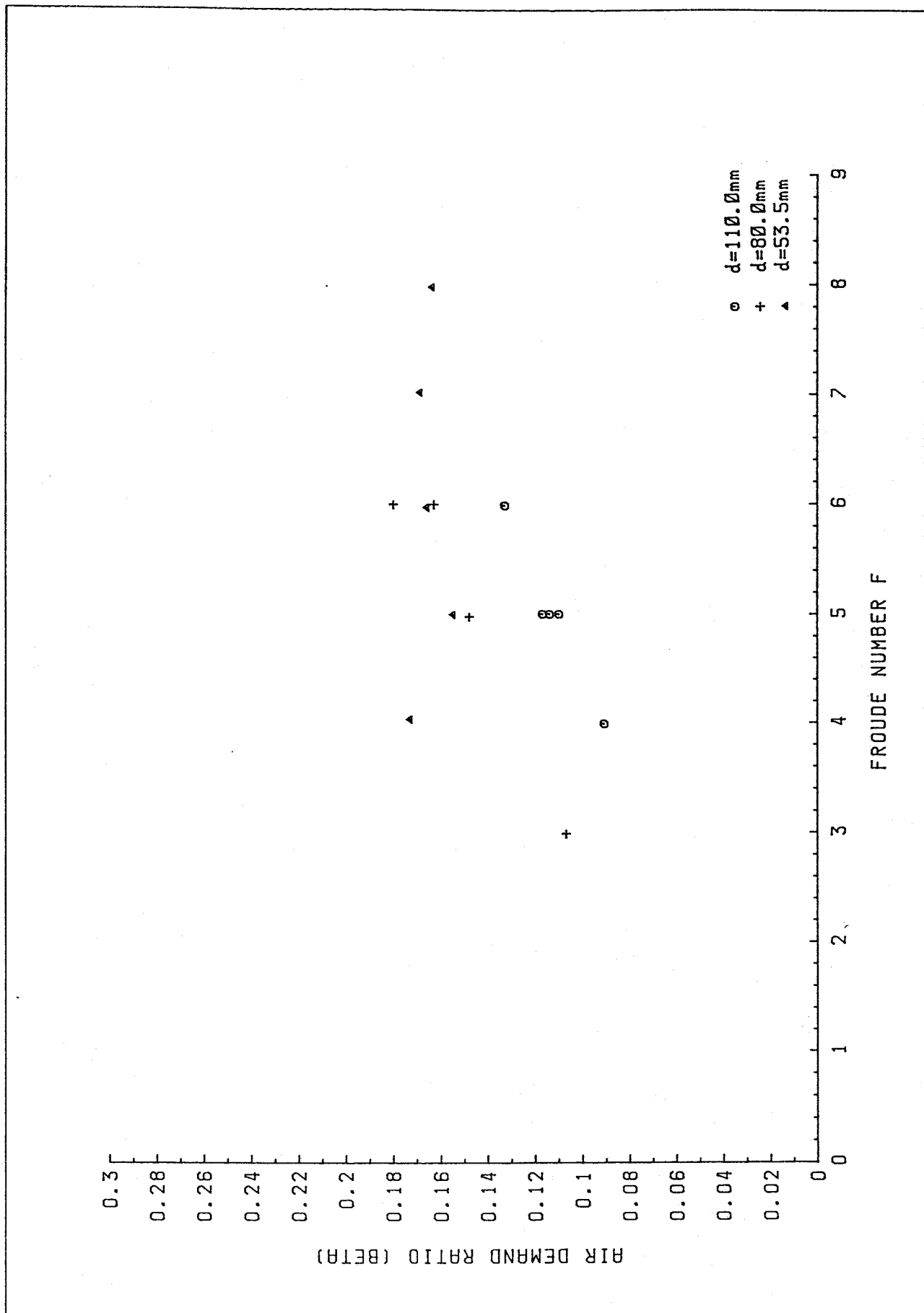


FIG 60 AIR DEMAND RATIO V's FROUDE NUMBER  
 AERATOR 7; VALVE SETTING 4; FLUME SLOPE 45.3 DEGREES

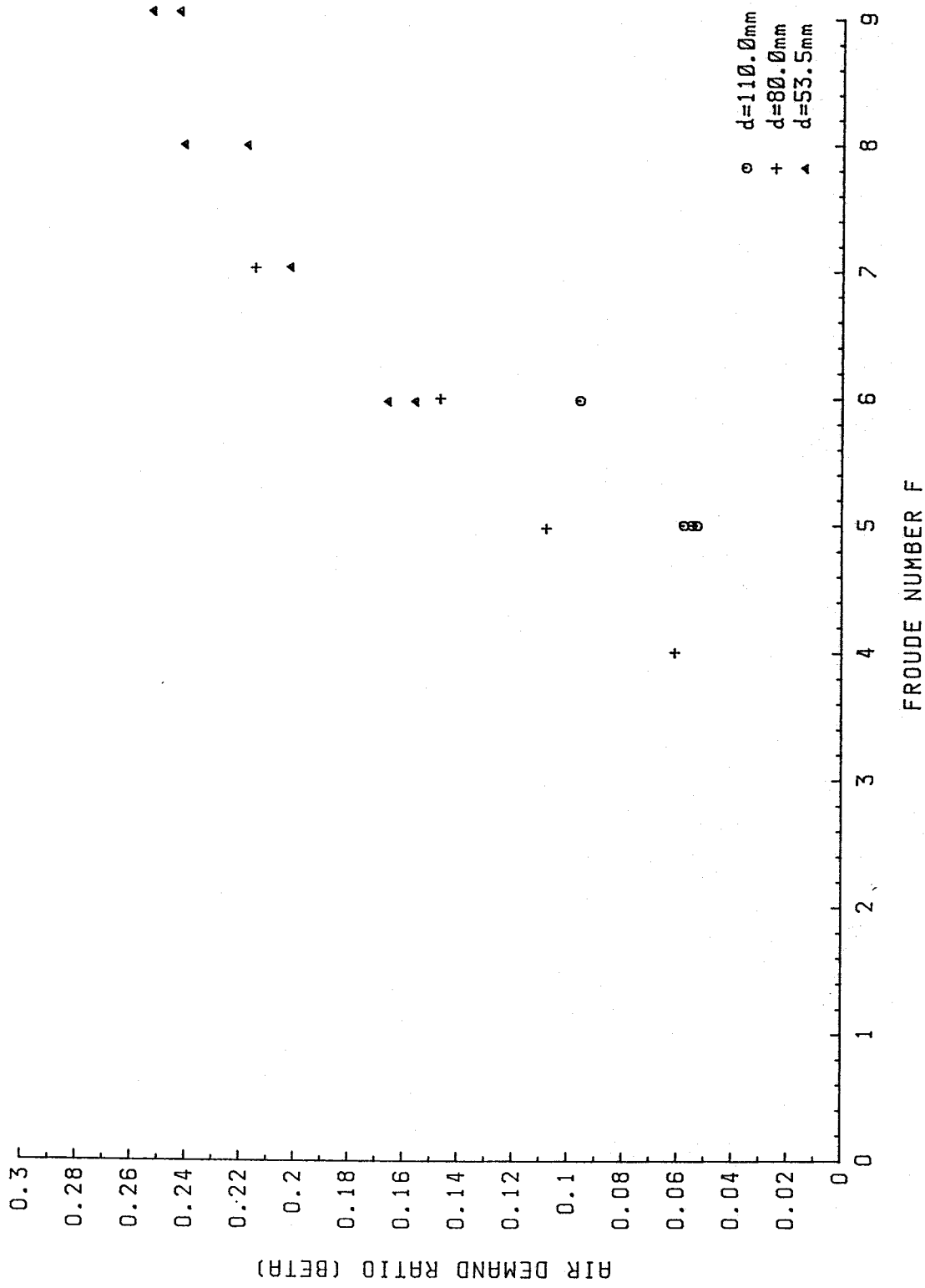


FIG 61 AIR DEMAND RATIO V's FROUDE NUMBER  
 AERATOR 9; VALVE SETTING Ø; FLUME SLOPE 15.5 DEGREES

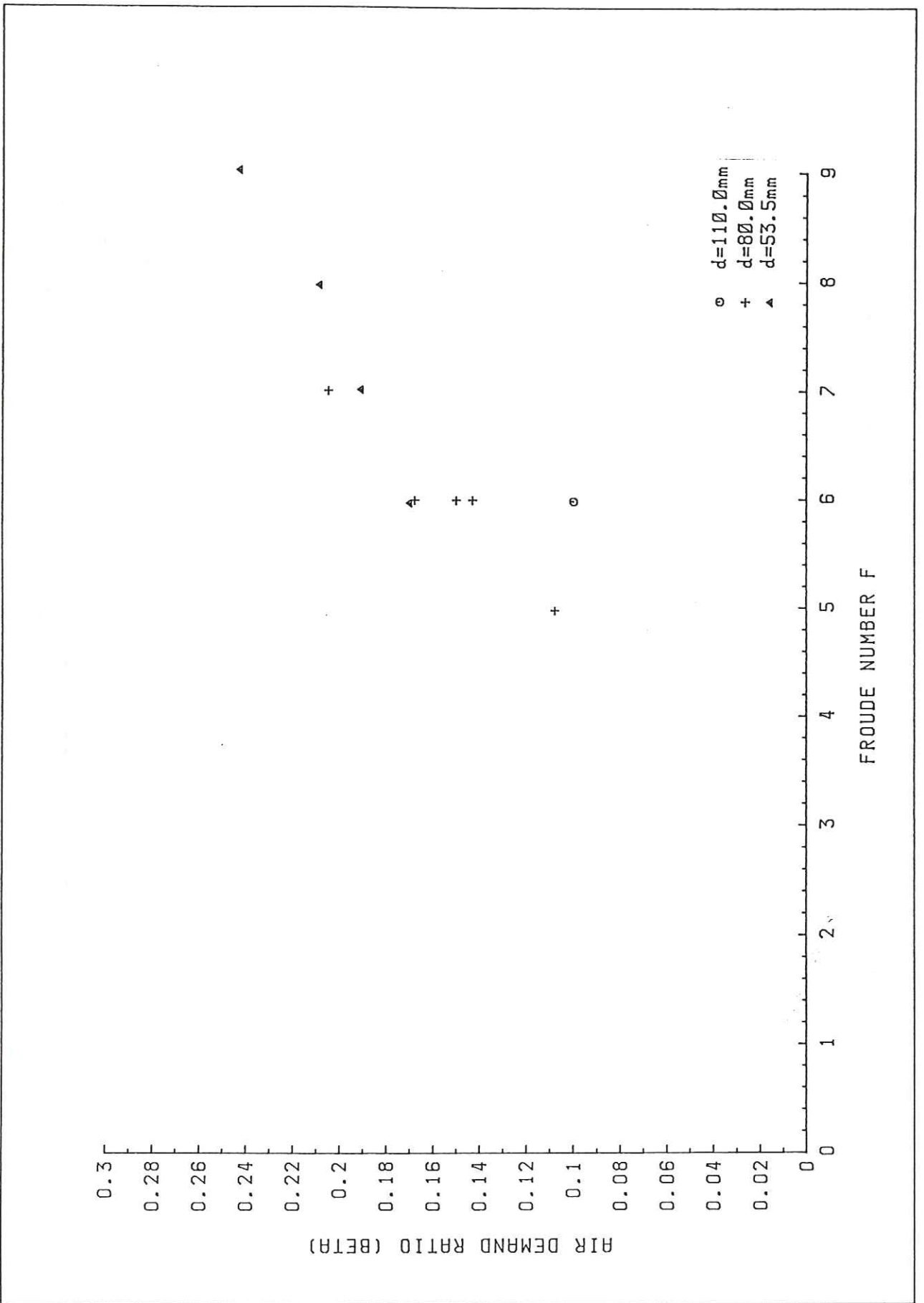


FIG 62 AIR DEMAND RATIO  $V'$ 's FROUDE NUMBER  
 AERATOR 9; VALVE SETTING 2; FLUME SLOPE 15.5 DEGREES

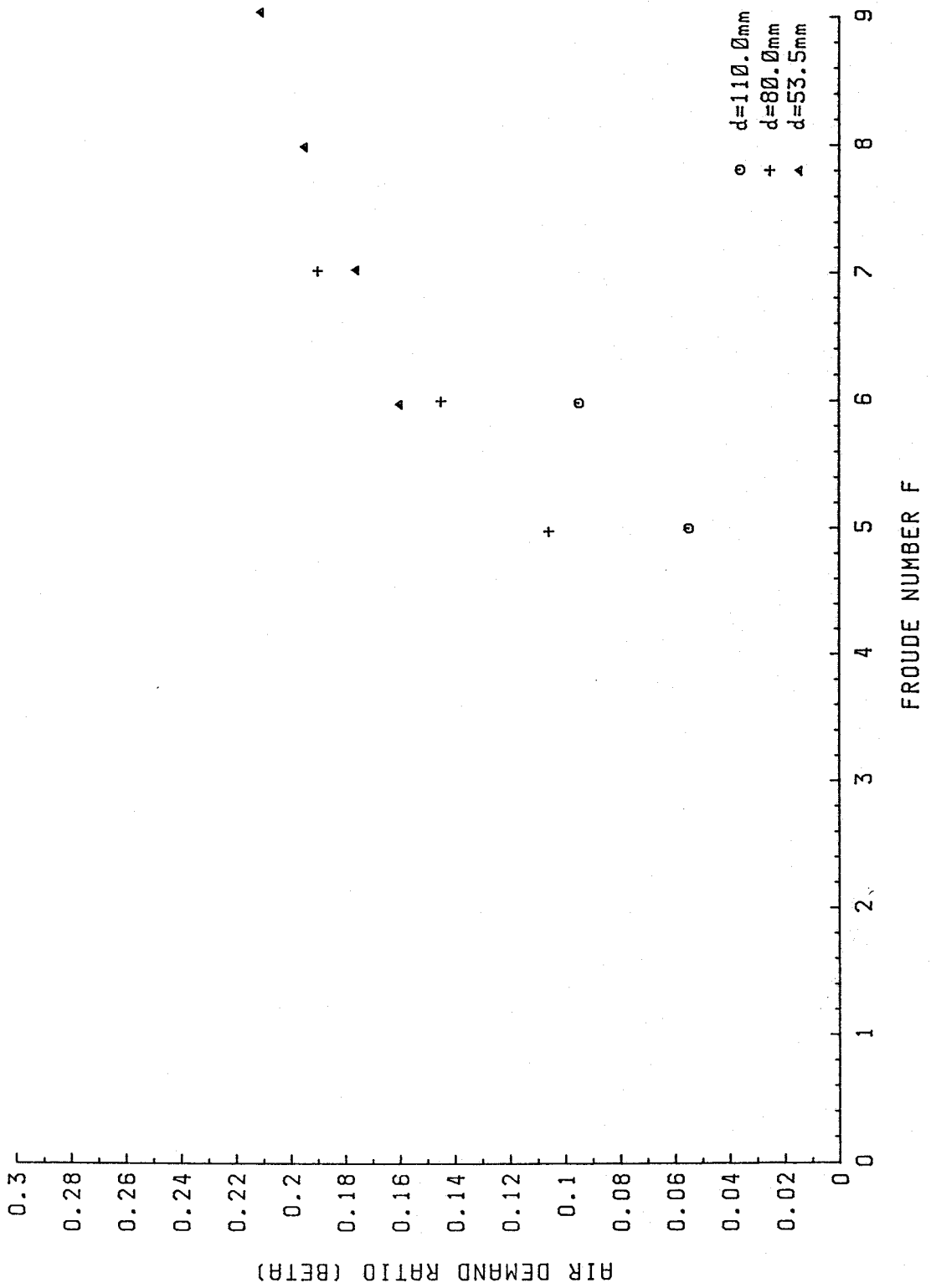


FIG 63 AIR DEMAND RATIO  $V$ 's FROUDE NUMBER  
 AERATOR 9; VALVE SETTING 3; FLUME SLOPE 15.5 DEGREES

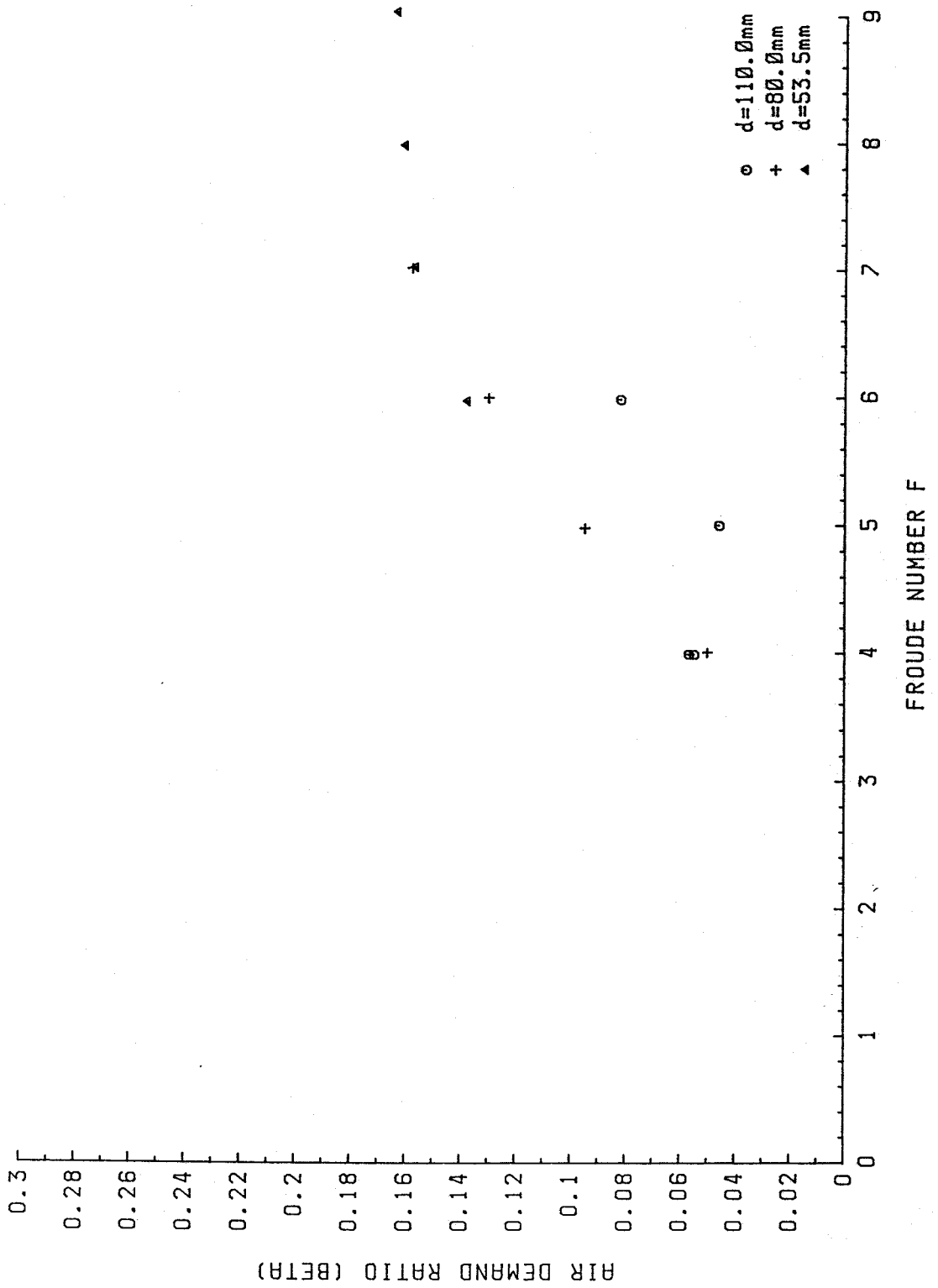


FIG 64 AIR DEMAND RATIO V's FROUDE NUMBER  
 AERATOR 9; VALVE SETTING 4; FLUME SLOPE 15.5 DEGREES

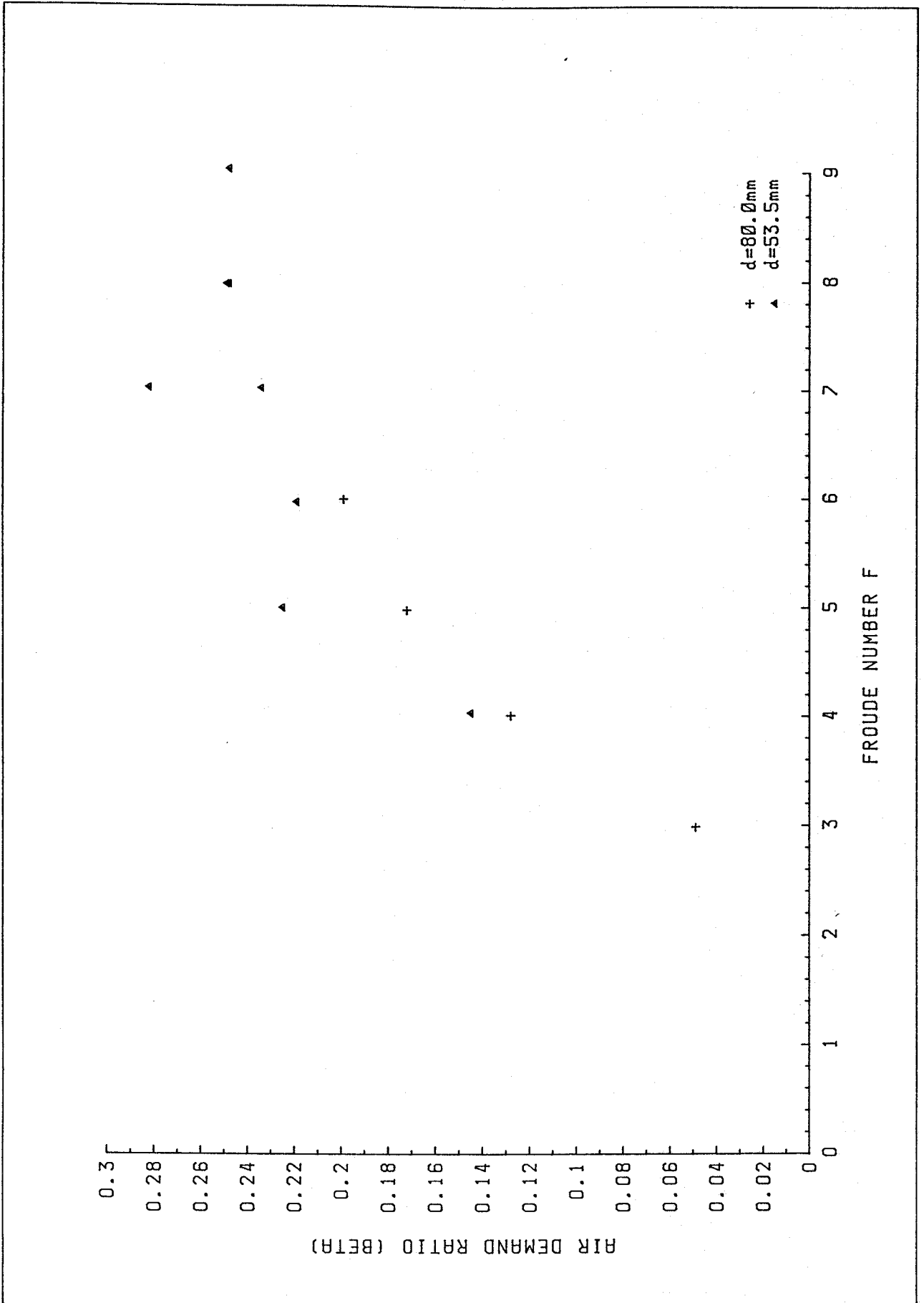


FIG 65 AIR DEMAND RATIO  $V'$ 's FROUDE NUMBER  
 AERATOR 9; VALVE SETTING  $\emptyset$ ; FLUME SLOPE 45.3 DEGREES

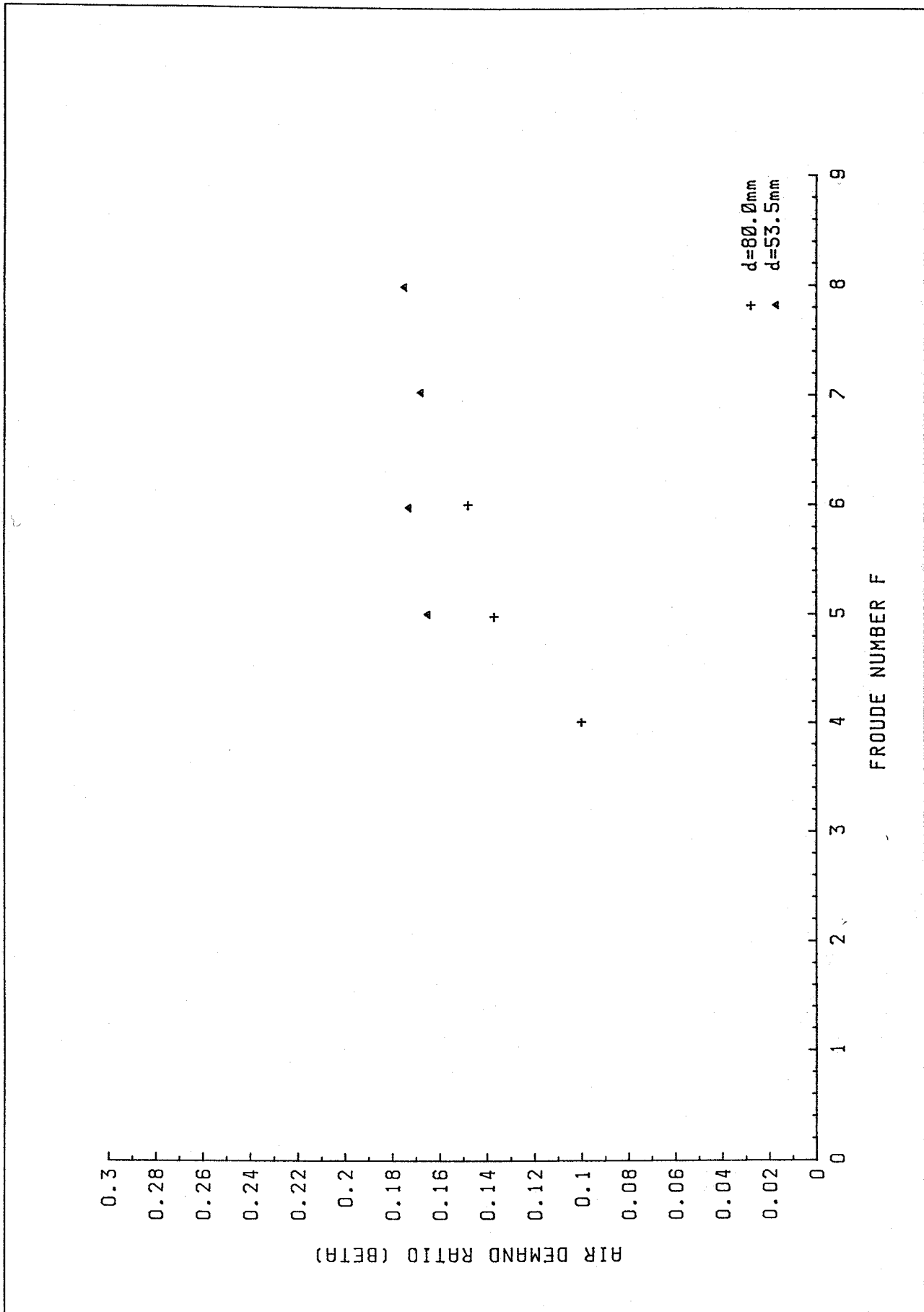


FIG 66 AIR DEMAND RATIO  $\beta$ 's FROUDE NUMBER  
 AERATOR 9; VALVE SETTING 4; FLUME SLOPE 45.3 DEGREES

**APPENDICES.**



## APPENDIX A

### Numerical convection-diffusion model

An important factor in the design of aeration systems for spillways is the spacing between aerators needed to maintain an air concentration at the channel boundaries that is sufficient to prevent cavitation damage. Air introduced by an aerator will be carried (or convected) downstream by the flow and will diffuse from regions of high air concentration to regions of low concentration as a result of fluid turbulence; air bubbles will also tend to rise vertically due to their buoyancy in water. The changes in air concentration profile downstream of an aerator can be measured in a physical model, but the results may not predict the prototype behaviour reliably because in a small-scale model it is difficult to reproduce correctly the rise velocity of the air bubbles and the effects of turbulent diffusion. Therefore, a numerical model based on a satisfactory mathematical description of turbulent diffusion potentially offers a better method of determining suitable spacings for spillway aerators.

The flow is assumed to be two-dimensional and rectangular co-ordinates, with an origin in the invert of the channel, are used:  $x$  is measured along the channel, positive in the direction of flow;  $y$  is measured normal to the invert, positive upwards. The slope of the channel makes an angle  $\theta$  with the horizontal. Consideration of the fluxes of air into and out of an elemental volume due to convection and diffusion leads to the following equation

$$\begin{aligned} (u - r \sin \theta) \frac{\partial C}{\partial x} + (v + r \cos \theta) \frac{\partial C}{\partial y} - \epsilon_x \frac{\partial^2 C}{\partial x^2} \\ - \epsilon_y \frac{\partial^2 C}{\partial y^2} = - \frac{\partial C}{\partial t} \end{aligned} \quad (\text{A.1})$$

where  $u$  and  $v$  are respectively the time-averaged flow velocities parallel to the  $x$  and  $y$  axes, and  $r$  is the vertical rise velocity of the bubbles due to their buoyancy;  $\epsilon_x$  and  $\epsilon_y$  are the coefficients of turbulent diffusion for air in water along the  $x$  and  $y$  axes. If the flow conditions averaged over time remain constant, the right-hand side is zero; this will be assumed to be the case in the following discussion.

Two boundary conditions are needed to solve Equation (A.1) which is parabolic in type. The first is the distribution of air concentration through the depth of flow at the upstream end, ie

$$C(0, y) = f(y) \quad (A.2)$$

where  $f$  is some function of  $y$ . The second boundary condition is provided by the fact that there can be no net flux of air through the invert of the channel so that

$$\epsilon_y \frac{\partial C}{\partial y} - (v + r \cos \theta) C = 0, \text{ for all } x \quad (A.3)$$

Cui (1985) obtained an analytical solution of Equation (A.1) in the reduced form

$$\epsilon_y \frac{\partial^2 C}{\partial y^2} = u \frac{\partial C}{\partial x} + r \frac{\partial C}{\partial y} \quad (A.4)$$

Note that the second-order differential of  $C$  has been omitted and that the slope of the channel is assumed to be small. Cui's solution was expressed in the form

$$C(x,y) = C_1(y) + C_2(x,y) \quad (\text{A.5})$$

where the variables of  $C_2$  are assumed to be separable so that

$$C_2 = X(x) Y(y) \quad (\text{A.6})$$

$C_1$ , therefore, represents the equilibrium vertical distribution of air that will be reached as  $x \rightarrow \infty$ . The  $C_2$  term represents the "transient" component resulting from the initial vertical distribution which is imposed as the upstream boundary condition at  $x = 0$  (ie Equation (A.2)). In Cui's method, this arbitrary vertical distribution was expressed in terms of an infinite Fourier series of harmonic functions. In order to obtain the analytical solution it was also necessary to assume that the horizontal flow velocity was independent of depth. Results were compared with measurements from a physical model of an aerator and showed fair agreement.

The usefulness of an analytical solution of the convection-diffusion equation is limited by the restrictions and assumptions that need to be applied. Some preparatory work was therefore carried out for a proposed computer model based on the steady-state form of Equation (A.1). A numerical solution based on finite differences is more flexible because it can include all the diffusion terms and can take account of a vertical velocity distribution such as occurs in a fully-developed boundary layer.

Alternative types of finite difference scheme were considered, and preliminary work carried out on a matrix solution for a centred-difference scheme. Since Equation (A.1) is of parabolic type, calculations need to start from the upstream vertical boundary (where the initial air concentration is

specified). Use is then made of the boundary condition given by Equation (A.3) to determine the concentrations at the next adjacent vertical in the solution grid; the solution can be continued in this way as far downstream as necessary.

Information on suitable values for the rise velocity  $r$  and the turbulent diffusion coefficients  $\epsilon_x$  and  $\epsilon_y$  in Equation (A.1) is very limited. Data on drag coefficients for spheres can be used to estimate the rise velocity if the size of the bubbles is known and they are assumed to be spherical; this latter may be reasonable in the case of small bubbles whose shape is dominated by surface tension effects. Values of diffusion coefficients for air-water mixtures are not known, and as a first step it would probably be necessary to assume that they were equal to the momentum diffusion coefficients for single phase flows. However, development of the proposed model would make it possible to analyse experimental measurements of air concentration profiles, and hence obtain more accurate estimates of the rise velocity and the diffusion coefficients.

## APPENDIX B

### Numerical model of cavitation and aeration

Aeration systems are usually installed in dam spillways either where cavitation damage has occurred or where experience or calculation indicates there is a risk of such damage. Most prototype aerators have been designed using data from physical models because the information needed to predict their performance was not available. This situation is changing as more laboratory studies are carried out and as more experience of operating prototype systems accumulates. It is therefore possible to envisage a numerical model that could assess the risk of cavitation and then, if necessary, design the aerators and their associated air supply systems. Initially, the model would probably be used in the preliminary design stages to compare alternative options and spillway layouts; physical model tests might still be needed to confirm and refine the performance of the chosen design. However, as more experience is gained with the numerical model, it should be possible to improve the accuracy of its predictions and eliminate the need for physical model tests.

A suitable basis for such a numerical model exists in the shape of the SWAN program developed by Binnie & Partners; a description of the underlying principles was given by Ackers & Priestly (1985). The program first determines the flow profile along the spillway, taking account of the growth of the bottom boundary layer downstream from its inception point at the crest. The point at which the boundary layer reaches the free surface of the water is taken to be the point at which self-aeration begins. Turbulence in the flow then causes air to be entrained downwards from the surface until, if the channel is sufficiently long, an

equilibrium air concentration profile is achieved. The program carries out simple checks to determine the maximum size of irregularity that can be allowed on the surface of the spillway if the risk of cavitation is to be avoided.

This program could be developed in two areas. Firstly, more detailed information about the cavitation potential of different types of surface irregularity could be provided, based on the conclusions from the Stage 1 literature review (see May (1987)). Secondly, data on the performance of aeration systems could be added, based on the results from the Stage 2 experiments described in this report and from other studies. Thus, if a risk of cavitation damage were identified, it would be possible to calculate the size and shape of the aerator and associated supply ducts needed to entrain the required quantity of air into the flow. It would also be necessary to predict the rate at which the air concentration at the invert of the channel decreased with distance downstream, because this would determine the required spacing between successive aerators. The numerical convection-diffusion model described in Appendix A could be developed to study this aspect of the problem.